UNIVERSITY OF NOVI SAD
FACULTY OF SCIENCES
DEPARTMENT OF
MATHEMATICS AND INFORMATICS

Jelena Stojanov

ANISOTROPIC FRAMEWORKS FOR DYNAMICAL SYSTEMS AND IMAGE PROCESSING

- PhD thesis -

Mentors:

Prof. dr. Vladimir Balan

Doc. dr. Sanja Konjik

Novi Sad, 2015.

Preface

This dissertation is the result of work carried out in the period May 2012 - November 2014, at University of Novi Sad and partly at Politehnica University of Bucharest Bucharest, Faculty of Applied Sciences, Romania. Many years of intensive study preceded this research.

Research topics

The research topics of this PhD thesis are:

- A comparative analysis of classical and specific geometric frameworks and their anisotropic extensions;
- The construction of Finsler frameworks, which are suitable for the analysis of dynamical systems;
- The development of anisotropic Beltrami framework theory with the derivation of the evolution flow equations corresponding to different classes of anisotropic metrics.

Main goals

The two main goals of this research are:

- The mathematical modelling of the real dynamical system of the evolution of cancer cell population, with the comprehensive description of its characteristics;
- The development of theoretical results which provide new techniques for image processing.

Motivation

The Garner mathematical model reflecting the dynamical system of the evolution of cancer cell population is presented in [53], while advantages of the Finsler framework in dynamical system analysis are presented in [3, 111]. The statistically determined Finsler norm modelling certain measurements in medical image analysis is defined in [10]. This inspired us to determine a Finsler framework for the Garner dynamical system.

Beltrami frameworks are extremely useful in image processing, since they present a digital image as a geometric active object, commonly a surface in a Riemannian (hence, isotropic) ambient [63, 103, 105, 114, 115]. On the other hand, [52] and [74] promote anisotropic extensions, which motivate the development of the general anisotropic Beltrami framework theory, applicable in image processing.

A comparative overview of metric structures of interest for the research is based on the theoretic background and general applicative aspects [34, 27, 35, 6, 42].

Structure

The PhD thesis has the following structure. The first chapter considers differentiable manifolds endowed with metrical structure - ranging from the Euclidean metric to the Generalized Lagrange one. The theory of differential equations on manifolds is concisely presented in accordance with the research topics. The importance of the Finsler framework for dynamical system analysis is emphasized.

The second chapter presents an original example of constructing certain Finsler norms, which are naturally related to the Garner dynamical system.

In the third chapter, an overview of the basic concepts for surface theory in Riemannian spaces is given, with special emphasis on the Beltrami framework. It also contains the new original anisotropic extension of the Beltrami framework, and the appropriate variational calculus, which provides the minimization of the embedded surfaces.

The fourth chapter presents original results of the variational calculus applied to the particular anisotropic Beltrami frameworks of Finsler-Randers and general Lagrange types and determines the evolution flow PDE for the embedded surfaces.

The last chapter presents several commonly used applications of the existing isotropic image processing techniques and the original tentative applications of the obtained anisotropic evolution flows.

Remarks

We will use the terms "isotropic" and "anisotropic" regarding the dependence on direction of the geometric objects constructed on a manifold and on its tangent bundle. "Isotropic" means that an object depends only on the points of the manifold, while "anisotropic" means the dependence both on the point and on tangent vectors belonging to the corresponding fibers of the tangent bundle.

We will use the Einstein convention of implicit summation on repeated indices throughout, in order to simplify formulas that usually contain components of tensors.

Acknowledgements

My Family merits much more than thanks!

Many people have given support and help to my work:

> Many Professors from University of Novi Sad, which have given generously their professional help in their respective areas.
>
> The thesis defend board members, who have supervised my work for a very long time (some of them were my teachers), and have given me permanent encouragement.
>
> My mentors, which have provided invaluable help and support during my research.

I am grateful to them all!

Contents

Chapter 1

Anisotropic extensions of the Euclidean framework

This chapter contains a brief overview of differentiable manifolds, their subspaces and tangent bundles, and metric spaces, from the Euclidean one to the general Lagrange space. The main metrical properties are presented and compared. The usage of certain metric spaces as frameworks for dynamical systems is further considered.

1.1 Preliminaries

Differentiable manifolds are essential in various areas of mathematics, and they are straightforward generalizations of finite-dimensional vector spaces. Roughly speaking, a differentiable manifold is a space locally behaving like the Euclidean one, but whose global structure is more complex.

Definition 1.1.1. Let M be a paracompact Hausdorff topological space, such that every open set $U \subset M$ is homeomorphic with an open set in $\mathbb{R}^n$, by a mapping $\phi : x \mapsto (x^1, \ldots, x^n)$. The pair (U, ϕ) is a *coordinate chart* on M, and the components of the n-tuple $\phi(x) = (x^i)$ are the *local coordinates* of the point x.

If the intersection of two chart domains is nonempty, the map $\phi_\beta \circ \phi_\alpha^{-1} : \phi_\alpha(U_\alpha \cap U_\beta) \to \phi_\beta(U_\alpha \cap U_\beta)$ from one coordinate mapping ϕ_α to another ϕ_β is called the *transition map*.

The maximal family of charts $\big\{(U_\alpha, \phi_\alpha)\big|\alpha \in A\big\}$ with smooth transition maps, is the *differentiable structure* on M, and M is said to be a *differentiable manifold* of dimension n.

Geometric objects on a manifold have also their local representations regarding a local chart, and transition maps indicates changes of corresponding local coordinates (e.g. vector fields, connections, tensors). The general basic notions and results on differentiable manifolds used in this text can be found in [34, 41, 42, 66, 70, 79, 90].

Definition 1.1.2. A *curve* on a differentiable manifold is a smooth mapping

$$c : I \to M,\ I \subset \mathbb{R}.$$

The curve c is said to be *regular* if $\frac{dc}{dt} \neq 0,\ \forall t \in I$.

A curve is often composed with a local chart and therefore the notation $c : t \mapsto x(t)$ is commonly used, and regularity condition can be written as $\frac{dx^i}{dt} \neq 0,\ i = \overline{1,n}, \forall t \in I$.

We shall introduce the notion of tangent space to a given manifold M at its point x as the collection of all tangent vectors to M at that point [35]. There are some other approaches that also lead to the same notion (cf. [34, 60, 70]).

Definition 1.1.3. The *tangent bundle* of an n-dimensional differentiable manifold M is the triple (TM, π, M), where

1. the total space TM is a $2n$-dimensional manifold
$$TM = \bigcup_{x \in M} T_x M,$$
whose elements are denoted by $u = (x, y)$, and $y \in T_x M$ is called the tangent vector on manifold M at the point x;

2. the surjection map $\pi : TM \to M$ given by $\pi(x, y) = x$ is called natural projection;

3. for every point $x \in M$ the fiber $\pi^{-1}(x) = T_x M$ is isomorphic with $\mathbb{R}^n$.

The tangent bundle is the $2n$-differentiable manifold with the structure induced by the differentiable structure of M, see [69, 76]. The elements of a fiber $T_x M$ can be viewed as tangent vectors of curves on M passing through x.

Definition 1.1.4. A *section of the tangent bundle* (TM, π, M) is a map $f : M \to TM$ with $\pi \circ f = id_M$.

A *frame* in the tangent bundle (TM, π, M) is a collection of smooth sections $s_1, s_2, \ldots, s_n$ of TM defining for each point $x \in M$ a basis $s_1(x), s_2(x), \ldots, s_n(x)$ for the fiber $\pi^{-1}(x)$.

The set of all smooth sections of the tangent bundle is a vector space over $\mathbb{R}$, but also a module over the ring $\mathcal{C}^\infty(M)$ of smooth functions on M. The canonical frame of the tangent bundle is $\left\{\frac{\partial}{\partial x^1}, \frac{\partial}{\partial x^2}, \ldots, \frac{\partial}{\partial x^n}\right\}$. It produces the decomposition of each tangent vector $y \in T_x M,\ \forall x \in M$
$$y = y^i \frac{\partial}{\partial x^i}\Big|_x .$$
Further, with the induced differentiable structure, the decomposition assigns coordinates to tangent vectors. The tangent bundle TM of M without the global zero section is called the *slit tangent bundle*,
$$\widetilde{TM} = TM \setminus \{0\} = TM \setminus \{(x, 0) \mid x \in M\}.$$
The collection $T^*M = \bigcup_{x \in M} T_x^* M$ of all dual vector spaces $T_x^* M = \{\omega_x \bigm| \omega_x : T_x M \to \mathbb{R}, \omega_x \text{ linear}\}$ provides the cotangent bundle (T^*M, π^*, M) of the differentiable manifold M. The canonical dual local frame of the cotangent bundle is $\{dx^1, \ldots, dx^n\}$ is related to the tangent frame by $dx^i\big|_x \left(\frac{\partial}{\partial x^j}\Big|_x\right) = \delta^i_j,\ \forall x \in M$.

Definition 1.1.5. A *vector field* on M is a smooth section of the tangent bundle $X : M \to TM$. The collection of all vector fields on M is denoted by $\chi(M)$. The Lie bracket is the operator from $\chi(M)$, given by
$$[X, Y](f) = X(Y(f)) - Y(X(f)), \quad \forall f \in \mathcal{C}^\infty(M).$$

A smooth curve $c : I \to M$ is said to be an *integral curve* of a vector field $X \in \chi(M)$, if

$$\frac{dc}{dt} = X \circ c, \text{ i.e., } \left.\frac{dc}{dt}\right|_t = X_{c(t)}, \ \forall t \in I.$$

The vector field X smoothly assigns one tangent vector to every point of M, i.e.,

$$X : M \to TM, \quad X(x) = X_x \in T_xM.$$

Definition 1.1.6. An *1-form* on M is a smooth section of the cotangent bundle, which smoothly assigns one tangent covector to every point of M, i.e.,

$$\omega : M \to T^*M, \quad \omega(x) = \omega_x \in T_x^*M.$$

The collection of all 1-forms on M is denoted by $\Lambda^1(M)$.

Vector fields and 1-forms are examples of tensors - smooth collections, over M, of scalar linear maps acting on the elements of the corresponding fibres in the tangent and cotangent bundles.

Definition 1.1.7. A *tensor of* (p, s)*-type* in a vector space V over the field $\mathbb{R}$, is a scalar $\mathbb{R}$-multilinear function on $\underbrace{V^* \times \ldots \times V^*}_{p} \times \underbrace{V \times \ldots \times V}_{s}$, i.e., an element of

$$T_s^p(V) = L^{p+s}(\underbrace{V^*, \ldots, V^*}_{s}, \underbrace{V, \ldots, V}_{p}; \mathbb{R}).$$

The element $T_s^p \in T_s^p(V)$ is called p *times contravariant* and s *times covariant* tensor.

A *tensor field* of (p, s)-type on the manifold M is T, a section of the product bundle

$$\underbrace{TM \otimes \ldots \otimes TM}_{p} \otimes \underbrace{T^*M \otimes \ldots \otimes T^*M}_{s}$$

whose fibres are $T_s^p(T_xM) = L^{p+s}(\underbrace{T_x^*M, \ldots, T_x^*M}_{s}, \underbrace{T_xM, \ldots, T_xM}_{p}; \mathbb{R})$.

Submanifolds

A map between two C^∞-manifolds $f : M \to N$ is called smooth if it is continuous and for each point $x \in M$ there exist charts (U, ϕ) around x, and (V, ψ) around $f(x)$, such that $\psi \circ f \circ \phi^{-1}$ is smooth. The map $\psi \circ f \circ \phi^{-1} : \phi(U \cap f^{-1}(V)) \to \psi(V)$ is called the local representation of f. If f is bijective, smooth and f^{-1} is also smooth, then f is said to be a diffeomorphism, and the corresponding Jacobian matrix of the local representation $D(\psi \circ f \circ \phi^{-1})$ is regular and invertible.

Definition 1.1.8. Let $f : M \to N$ be a smooth map between two differentiable manifolds, and let $x \in M$ be an arbitrary point. The tangent map of f at x maps the tangent space at x to the tangent space at $f(x)$, $T_xf : T_xM \to T_{f(x)}N$, in the following way:

$$T_xf(y) = \frac{d}{dt}(f \circ c)|_{t=0},$$

where $y \in T_xM$ and $c = c(t)$ is a curve on M such that $c(0) = x$ and $\frac{dc}{dt}|_{t=0} = y$.

The corresponding map between the tangent bundles $Tf : TM \to TN$ is called the *tangent map of* f and is defined by

$$Tf(x, y) = (f(x), T_xf(y)).$$

According to the induced charts on TM and the basis elements of T_xM, one can write the local representation of Tf. Let (U, ϕ) and (V, ψ) be the local charts around x and $f(x)$, respectively. Then, one can write

$$Tf(x, y) = \left(f(x), D(\psi \circ f \circ \phi^{-1})(x)y\right).$$

Therefore, the tangent map Tf is also called the *derivative map*, and sometimes it is also denoted by df or f_*.

Definition 1.1.9. A smooth map $f : M \to N$ between two C^∞-manifolds is called *immersion* if the derivative map of f at x, $f_{*,x} : T_xM \to T_{f(x)}N$ is injective for all $x \in M$. Moreover, if f is a homeomorphism, then $f(M)$ is said to be a *submanifold* of N.

A smooth map $f : M \to N$ between two C^∞-manifolds is called the *embedding* (or the imbedding) if it is an immersion which is a homeomorphism onto the submanifold $f(M)$. Then, $f(M)$ is an embedded (or a regular) submanifold of N, and has the induced topology as a subspace in N.

An immersion $f : M \to N$ is a local embedding, i.e., each point $x \in M$ of the domain has a neighborhood $U \subset M$ such that $f|_U : U \to N$ is an embedding.

More details on the subject can be found in [2, 34, 66, 70].

Distributions

Another generalization of vector spaces and 1-forms can be defined by assigning to each point $x \in M$ a linear subspace of the fiber $\pi^{-1}(x)$ or $(\pi^*)^{-1}(x)$, rather then a vector or an 1-form, respectively.

Definition 1.1.10. A *smooth and regular m-distribution* on the n-dimensional differentiable manifold M is a smooth mapping $\mathcal{D} : M \to TM$ that assigns to every point $x \in M$ an m-dimensional linear subspace $(m < n)$ of the fiber $\pi^{-1}(x)$, $\mathcal{D}(x) \subset T_xM$.

Remark. A notion which generalizes the previous one, is the distribution, a family $\{\mathcal{D}(x)\big|x \in M\}$ of linear subspaces $\mathcal{D}(x) \subset T_xM$, which smoothly depends on the point $x \in M$, but where the subspaces of the family need not necessarily be of the same dimension.

A smooth and regular m-distribution $\mathcal{D}$ of TM is locally spanned by smooth vector fields $X_1, \ldots, X_m$, such that for each point $x \in M$ it holds $\mathcal{D}(x) = \mathit{span}\,\{X_1(x), \ldots, X_m(x)\}$[1]. The regularity of the distribution ensures that vectors $X_1(x), \ldots, X_m(x)$ are linearly independent.

Definition 1.1.11. A distribution $\mathcal{D}$ on M is *integrable* if for every point $p \in M$ there is a submanifold $S(p) \subset M$ around p, such that $\mathcal{D}(x) = T_xS(p), \quad \forall x \in S(p)$. $S(p)$ is called an *integral submanifold* of the distribution $\mathcal{D}$.

[1] *span* denotes the collection of all linear combinations of the considered vectors or - more generally - fields of the same type over $\mathbb{R}$.

The notion of integral submanifold of a distribution generalizes the one of integral curve of a vector field.

Metric structures

To turn a differentiable manifold M into a metric space (M, g), one can equip each fiber T_xM with a scalar product $g_x : T_xM \times T_xM \to \mathbb{R}$. It is of particular interest to consider the case when the scalar product varies smoothly from point to point. The trivial case when the scalar product $g_x(y, v)$ does not depend on $x \in M$ leads to a Eucledean space, and we denote the family of all Euclidean spaces as $\mathcal{E}^n$. Otherwise, M is said to have a Riemannian structure, and (M, g) is an element of the family $\mathcal{R}^n$ of all Riemannian spaces.

If each tangent space is endowed with a whole family of scalar products, that depend smoothly not only on the point, but also on tangent vectors in T_xM, one obtains Finsler, Lagrange or generalized Lagrange manifold, that belongs to the corresponding family of metric spaces, $\mathcal{F}^n$, $\mathcal{L}^n$ or $\mathcal{GL}^n$ (cf. [76]). It other words, the field of scalar products is given over the tangent space of the manifold as

$$g : TM \to B(\mathbb{R}^n), \quad g : (x, y) \mapsto g_{(x,y)}, \quad g_{(x,y)} : \mathbb{R}^n \times \mathbb{R}^n \to \mathbb{R},$$

where $B(\mathbb{R}^n)$ denotes the set of all bilinear maps. Thus, the characteristics of the scalar product field considered as a function over TM, determine the nature of the space structure, and place it into one of the classes related as follows, [76]:

$$\mathcal{E}^n \subset \mathcal{R}^n \subset \mathcal{F}^n \subset \mathcal{L}^n \subset \mathcal{GL}^n.$$

The linearity of the scalar product $g_{(x,y)}$ yields the following coordinate expression:

$$g_{(x,y)}(u, v) = g_{ij}(x, y)u^iv^j, \quad u = (u^1, \ldots, u^n), v = (v^1, \ldots, v^n) \in T_xM.$$

Hence, the definition of the scalar product field is equivalent with a globally defined symmetric, nondegenerate two times covariant tensor field on TM, $g(x, y) = g_{ij}(x, y)dx^i \otimes dx^j$, called *metric* or *fundamental tensor*. Each scalar product $g_{(x,y)}$ in the fiber T_xM of the tangent bundle (for the particularly chosen flagpole $y \in T_xM$) produces in a natural way, the quadratic form $Q_{(x,y)}(u) = g_{(x,y)}(u, u)$ of a vector $u \in T_xM$, and the norm function $|u|_{g_{(x,y)}} = \sqrt{g_{ij}(x, y)u^iu^j}$. The norm of a vector coincides with its length, and can be used to calculate angles and areas. In other words, the metric tensor field on a differentiable manifold enables measuring the length of a curve on the manifold and other related notions.

The existence of isotropic vector fields for the quadratic forms over TM which is induced by the metric tensor, will lead to assigning to the structure the prefix "pseudo" (e.g., pseudo-Riemann structure). If the metric tensor ceases to be non-degenerate, then the added prefix will be "sub" (e.g., sub-Riemannian structure).

A vector space is flat, which means that parallel transport of its elements is achieved simply by translation. On a differentiable manifold, there is no canonical isomorphism between tangent vector spaces at different points. Hence, a parallel transport that relates a tangent vector at one point with precisely one tangent vector at another point, can not be defined in a natural way. A parallel transport is achieved along curves on the manifold and is defined by the notions of connection and covariant derivative. They further introduce geometric objects of the manifold (autoparallel curves, torsion and curvature as the most important ones).

1.2 Euclidean and Riemannian structures

A constant metric tensor field $g_{ij}(x,y) = \text{const}, i,j = \overline{1,n}$ over the tangent space TM of a differentiable manifold M leads to the same measure of distances and angles in all tangent spaces over the differentiable manifold M. The *Euclidean structure* on the manifold M is given by the constant scalar product field, $g : (x,y) \mapsto g$, i.e., by a nondegenerate symmetric bilinear form g,

$$g(u,v) \in \mathbb{R}, \ \ \forall u,v \in T_xM, \ \ \forall x \in M,$$

i.e., by a two times covariant nondegenerate symmetric tensor. The local chart can be chosen in such a way that components of the corresponding metric tensor is locally provided by the identity matrix, i.e.,

$$g(u,v) = g_{ij}u^iv^j = u^1v^1 + u^2v^2 + \ldots + u^nv^n, \ \ \forall u,v \in T_xM, \ \ \forall x \in M.$$

Moreover, the norm

$$\|u\| = \sqrt{(u^1)^2 + (u^2)^2 + \ldots + (u^n)^2}, \ \ \forall u \in T_xM, \ \ \forall x \in M$$

is the same in each fiber of the tangent bundle.

Locally, the Euclidean space is flat, which means that the parallel transport of a tangent vector does not depend on the curve along which the transport is made. That property is globally present only in Euclidean spaces and it is described by the vanishing curvature.

The length of an arc of the regular curve c is locally approximated by the length (norm) of the tangent vector $\|(\frac{dx^i}{dt})\|$. Globally, the curve length is defined by the integration $\ell(c) = \int \|(\frac{dx^i}{dt})\|\, dt$, hence, in the Euclidean space

$$\ell(c) = \int_I \sqrt{\left(\frac{dx^1}{dt}\right)^2 + \ldots + \left(\frac{dx^n}{dt}\right)^2}\, dt.$$

The notion of a straight line in the Euclidean space means a curve of the minimal length between two given points, but also a curve whose tangent vector field is parallel along the curve. This notion is generalized in non-Euclidean spaces by geodesics and autoparallel curves.

In the Riemannian geometry, it is necessary to consider at the same time a differentiable manifold and its associated tangent bundle.

Definition 1.2.1. A *Riemannian manifold* $V^n = (M,g)$ is an n-dimensional differentiable manifold M with a positive definite scalar product g on tangent spaces. g is called a *Riemannian metric* and can be written as $g = g_{ij}dx^i \otimes dx^j$, where g is a smooth two times covariant tensor field over M, with components

$$g_{ij}(x), \quad x \in M, \quad i,j = \overline{1,n} \tag{1.1}$$

satisfying the following conditions

1. symmetric: $\quad g_{ij}(x) = g_{ji}(x)$,

2. regular (nondegenerate): $\quad \text{rank}(g_{ij}) = n$,

3. positive definite: $\quad g_{ij}(x)X^iX^j > 0, \quad \forall X \in T_xM\backslash\{0\}, \quad \forall x \in M.$

Without the condition of positive definiteness in Definition 1.2.1, (M, g) is a pseudo-Riemannian manifold, and if g is degenerate, the space is of sub-Riemannian type.

The regularity of matrices $(g_{ij}(x)), \forall x \in M$ ensures the existence of the dual metric tensor $g^{ij}\frac{\partial}{\partial x^i} \otimes \frac{\partial}{\partial x^j}$. Contractions with both metric tensors are used to change the character of a tensor. Namely, the tensor g_{ij} is used for lowering the indices of tensors, and its inverse g^{ij} is used for raising the indices.

The existence of a Riemannian metric on an arbitrary differentiable manifold is not mandatory (para-compacity of M is a sufficient condition), and a constructive proof can be found in [39, 42, 79]. A Riemannian space can be embedded in the Euclidean space of high enough dimension [81].

The metric tensor field of a Riemannian manifold depends on the point x, and produces in each tangent space T_xM the unique scalar product defined by the total contraction,

$$g_x(u, v) = g_{ij}(x)u^iv^j, \ u, v \in T_xM.$$

The length of a regular curve $x = x(t), t \in I$ in the Riemannian space (M, g) can be expressed in terms of the metric tensor g. An infinitesimal displacement along the curve can be approximated by the infinitesimal tangent vector $\frac{dx}{dt}$ in the corresponding tangent space, so the arc length differential $d\ell$ can be expressed by the scalar invariant determined by the Riemannian metric and the curve itself

$$d\ell = \sqrt{g_{ij}(x)dx^idx^j}.$$

The length of the regular curve $c : I \to M$ is given by

$$\ell(c) = \int_I \sqrt{g_{ij}(x(t))\frac{dx^i}{dt}\frac{dx^j}{dt}}\, dt. \tag{1.2}$$

The notion of connection is necessary in non-Euclidean structures as a tool for locally analyzing vector fields. The connection is a mapping that further defines the parallel transport of vector fields along curves and the covariant derivatives operator ∇, that expresses the infinitesimal variation of a tensor field.

Definition 1.2.2. In the Riemannian manifold (M, g) the *connection* ∇ is defined as the mapping

$$\nabla : \chi(M) \times \chi(M) \to \chi(M), \quad \nabla(X, Y) \mapsto \nabla_X Y,$$

that is linear in the first argument over the module $C^\infty(M)$, linear in the second argument over the field $\mathbb{R}$ and satisfies the product rule

$$\nabla_X(fY) = f\nabla_X Y + X(f)Y, \ f \in C^\infty(M).$$

Remark. Due to the linearity in the first argument, it is natural to call ∇ linear connection. It should be emphasized that a connection in a manifold may be defined regardless of the existence of a metric.

Any linear connection ∇ is determined by its coefficients

$$\nabla_{\frac{\partial}{\partial x^i}}\frac{\partial}{\partial x^j} = \Gamma^k_{ij}\frac{\partial}{\partial x^k}.$$

The main geometric objects that characterize a connection are its torsion and curvature.

Definition 1.2.3. Let M be a differentiable manifold endowed with the connection ∇. The *torsion* of the connection is the mapping

$$T : \chi(M) \times \chi(M) \to \chi(M), \quad T(X,Y) = \nabla_X Y - \nabla_Y X - [X,Y],$$

while the *curvature* of the connection is

$$R : \chi(M) \times \chi(M) \times \chi(M) \to \chi(M), \quad R(X,Y)Z = \nabla_X \nabla_Y Z - \nabla_Y \nabla_X Z - \nabla_{[X,Y]} Z.$$

Both the torsion and the curvature associated to the linear connection can be locally expressed by their components [35, 75, 76]:

$$T\left(\frac{\partial}{\partial x^i}, \frac{\partial}{\partial x^j}\right) = T^k_{ji}\frac{\partial}{\partial x^k}, \qquad R\left(\frac{\partial}{\partial x^i}, \frac{\partial}{\partial x^j}\right)\frac{\partial}{\partial x^k} = R^h_{k,ji}\frac{\partial}{\partial x^h}.$$

The torsion tensor field measures the symmetricity of the connection ∇ and has the following components

$$T^k_{ji} = \Gamma^k_{ij} - \Gamma^k_{ji}.$$

The deviation of a vector $X \in T_xM$ parallelly transported along a closed contour is described by the Riemannian curvature tensor field with components

$$\left(\nabla_{\frac{\partial}{\partial x^i}} \nabla_{\frac{\partial}{\partial x^j}} - \nabla_{\frac{\partial}{\partial x^j}} \nabla_{\frac{\partial}{\partial x^i}}\right) X^h = R^h_{k,ji} X^k,$$

where

$$R^h_{k,ji} = \frac{\partial \Gamma^h_{jk}}{\partial x^i} - \frac{\partial \Gamma^h_{ik}}{\partial x^j} + \Gamma^h_{ip}\Gamma^p_{jk} - \Gamma^h_{jp}\Gamma^p_{ik}.$$

In a Riemannian manifold (M,g) there is only one torsion free connection ($T \equiv 0$) that preserves scalar product of two vectors transported parallel along a curve. That is the *Riemannian connection* or the *Levi-Civita connection* Γ^i_{jk}, which is symmetric ($\Gamma^i_{jk} = \Gamma^i_{kj}$) metric-compatible, and whose coefficients are given by:

$$\Gamma^i_{jk} = \frac{1}{2} g^{ih}\left(\frac{\partial g_{jh}}{\partial x^k} + \frac{\partial g_{kh}}{\partial x^j} - \frac{\partial g_{jk}}{\partial y^h}\right). \tag{1.3}$$

The coefficients of the Levi-Civita connection are called the Cristoffel symbols (of 2-nd kind).

The associated covariant curvature tensor $R_{ij,kl} = g_{ih}R^h_{j,kl}$ is symmetric in the pairs of indices, but it is antisymmetric within each pair. Its contraction with the contravariant metric tensor g^{il} produces the *Ricci tensor* with components $R_{jk} = R^h_{j,kh}$, and a second contraction with g^{jk} produces the *scalar curvature* $S = g^{jk}R_{jk}$. The Riemannian curvature tensor vanishes (and consequently, the Ricci tensor and scalar curvature) if and only if the metric tensor field is constant and the space is of locally Euclidean type.

A curve $c : I \to M$ in a Riemannian manifold (M,g) with the Levi-Civita connection ∇ is said to be a *geodesic* if its tangent vector filed $\dot{c} = \frac{dx}{dt}$ is parallel along the curve,

$$\nabla_{\dot{c}}\dot{c} = 0. \tag{1.4}$$

Remark. Actually, if the relation (1.4) is considered for an arbitrary (possibly different from the Levi-Civita) connection, then the corresponding curves are called autoparallel curves of the connection, and are not generally related to the metric structure of the manifold.

A geodesic curve is the trajectory of the following system of second order differential equations (called the geodesic equations)

$$\frac{d^2x^i}{dt^2} + \Gamma^i_{jk}\frac{dx^j}{dt}\frac{dx^k}{dt} = 0. \tag{1.5}$$

There exists a unique geodesic passing through a given point and having a given vector as emerging given tangent vector. At the same time, a minimal geodesic is the shortest curve connecting two given close points, and is an extremal curve for the variation of the length functional (and of the energy functional, too).

More details on the Riemannian geometry can be found in, e.g., [37, 41].

1.3 Anisotropic structures

Further extensions of Euclidean spaces include anisotropic structures, i.e., metrics that depend on points and tangent vectors. Since the metric tensor field will be defined over the tangent space, it is necessary to consider the second order tangent bundle of a differentiable manifold.

1.3.1 The second order tangent bundle

The second order tangent bundle of a differentiable manifold M is the tangent bundle of TM, (TTM, π_*, TM) with π_* denoting the derivative map of $\pi : TM \to M$, given by $\pi_*(x, y, X, Y) = (x, X)$. The elements of TTM are $(u, Z) \in TTM$, where $u = (x, y) \in TM$, and $Z \in T_{(x,y)}TM$. The fibers are $2n$-dimensional vector spaces with the natural basis

$$T_{(x,y)}TM = span\left\{ \frac{\partial}{\partial x^i}\Big|_{(x,y)}, \frac{\partial}{\partial y^i}\Big|_{(x,y)} \;\Big|\; i = \overline{1, n} \right\},$$

which provides the decomposition of a tangent vector as

$$Z(x, y) = X^i(x, y)\frac{\partial}{\partial x^i}\Big|_{(x,y)} + Y^i(x, y)\frac{\partial}{\partial y^i}\Big|_{(x,y)}.$$

Some of tensorial objects defined in the tangent space TTM change their coordinates like the tensors which are defined on the base manifold, i.e., in the bundle TM. They are particularly important and are called *distinguished*, or *d*-tensors.

The natural submersion $\pi : TM \to M$ induces on TTM a regular and integrable n-dimensional distribution $V : TM \to TTM$ called the vertical distribution. In fact, the kernel of the derivative map π_* restricted to some point $u = (x, y) \in TM$ is a subspace of T_uTM, called the vertical subspace, and

$$VTM = \bigcup_{u \in TM} \mathrm{Ker}(\pi_{*,u}),$$

where $\pi_{*,u}$ is the restriction of π_* on the fiber $\pi_*^{-1}(u)$. The triple (VTM, τ, TM) is called the vertical bundle with τ its canonical projection induced by π_*. Since $\pi_*\left(\frac{\partial}{\partial y^i}\right) = 0$, it is straightforward to see that

$$V_uTM = span\left\{ \frac{\partial}{\partial y^i}\Big|_u \Big| i = \overline{1, n} \right\}.$$

The vector fields $\dfrac{\partial}{\partial y^i}$, $i=\overline{1,n}$, are local $d-$tensors on TM.

A complementary distribution to the vertical one VTM will be denoted as HTM and will be called horizontal distribution. It determines a Whitney decomposition of the second order tangent bundle

$$TTM = HTM \oplus VTM. \tag{1.6}$$

A fiber $\pi_*^{-1}(u)$ of TTM is a direct sum of the vertical subspaces V_uTM and the complementary to it, horizontal subspace H_uTM, $\pi_*^{-1}(u) = H_uTM \oplus V_uTM$. Hence,

$$HTM = \bigcup_{u\in TM} H_uTM$$

defines a subbundle of TTM, also with the canonical projection (HTM, τ, TM). The horizontal distribution is not unique, it is related with a kernel of a linear submersion of TTM into VTM and with the notion of nonlinear connection (see [35, 76]).

Definition 1.3.1. A linear submersion $N : TTM \to VTM$ is called a nonlinear connection if $N \circ \iota = id|_{VTM}$, where $\iota : VTM \to TTM$ is the canonical inclusion.

A nonlinear connection is determined by a connection form, that is a vector 1-form defined on $\widetilde{TM}$ by a smooth mapping $N = N^i_j(x,y)$,

$$N : (x, y, X^i, Y^i) \to (x, y, 0, X^i N^j_i + Y^j). \tag{1.7}$$

The zero section is an invariant of the nonlinear connection map.

The horizontal distribution providing the decomposition (1.6) is a mapping $H : TM \to TTM$, that assigns to each point $u \in TM$ the subspace of T_uTM defined by

$$H_uTM = H(u) = \mathrm{Ker}(N\big|_{T_uTM}).$$

The horizontal bundle $HTM := \bigcup_u H_uTM$ is spanned by the local frame elements

$$\frac{\delta}{\delta x^i} = \frac{\partial}{\partial x^i} - N^j_i \frac{\partial}{\partial y^j}.$$

At any point $u \in TM$, the subspaces H_uTM and V_uTM are complementary. The frames adjusted to the Whitney decomposition (1.6) contain $d-$vector fields

$$\frac{\delta}{\delta x^i} = \frac{\partial}{\partial x^i} - N^j_i \frac{\partial}{\partial y^j} \in \Gamma(HTM), \quad \frac{\partial}{\partial y^j} \in \Gamma(VTM), \tag{1.8}$$

and the local basis of T_uTM is called *Berwald basis*. By means of the Whitney decomposition (1.6) and (1.8), the nonlinear connection introduces on (TTM, π_*, TM) a structure with structural group $GL(n,\mathbb{R}) \times GL(n,\mathbb{R})$.

The main purpose of the nonlinear connection is to connect tangent spaces at two separate points on the base manifold M, T_pM and T_qM. The vectors from spaces T_pM and T_qM can be related by a parallel transport along some curve, such that the transport depends only on the curve direction and not on the curve itself. So, a nonlinear connection yields a covariant derivative $\nabla : \chi(M) \times \chi(M) \to \chi(M)$, where $\nabla_X Y = \nabla(X,Y)$ provides the resulting vector obtained by a parallel transport of Y in the direction of X. The covariant derivative still has to be linear over $\mathbb{R}$ and to satisfy the Leibniz rule in the second argument. But the linearity in the first argument is not postulated. The covariant derivative is defined as

$$\nabla_X Y = \left\{ X(Y^j) + N_i^j(x, X)Y^i \right\} \frac{\partial}{\partial x^j}, \quad \text{where} \quad Y = Y^i \frac{\partial}{\partial x^i},$$

and $X, Y \in T_x M$. Hence (x, X) is an element of $\widetilde{TM}$ where the connection coefficients N_i^j are defined.

If the connection coefficients are linear also in the second argument $N_j^i(x, y) = \gamma_{jk}^i y^k$, then the connection N is called linear connection. In that case, the covariant derivative ∇ becomes linear in the first argument too, and γ_{jk}^i are coefficients uniquely determined by the spanning relations

$$\nabla_{\frac{\partial}{\partial x^i}} \frac{\partial}{\partial x^j} = \gamma_{ij}^k \frac{\partial}{\partial x^k}.$$

A curve c on M is called autoparallel with respect to the nonlinear connection ∇ if the tangent vector field $\dot{c}$ on c remains tangent during the parallel transport along c. Necessary and sufficient condition for the latter is (like in the Riemannian case)

$$\nabla_{\dot{c}} \dot{c} = 0.$$

The second order differential equation of an autoparallel curve is

$$\frac{d^2 x^i}{dt^2} + N_j^i \left(x, \frac{dx}{dt} \right) \frac{dx^j}{dt} = 0. \tag{1.9}$$

The nonlinear connection N is said to be integrable if the corresponding horizontal distribution is integrable or, equivalently, involutive. The verification consists of checking whether the Lie bracket of two horizontal vectors remains horizontal. The calculation gives

$$\left[\frac{\delta}{\delta x^i}, \frac{\delta}{\delta x^j} \right] = R_{ij}^k \frac{\partial}{\partial y^k},$$

where

$$R_{ij}^k = \frac{\delta N_i^k}{\delta x^j} - \frac{\delta N_j^k}{\delta x^i} \tag{1.10}$$

are the components of the *curvature tensor of the nonlinear connection* , $R = \frac{1}{2} R_{ij}^k dx^j \wedge dx^i \otimes \frac{\partial}{\partial y^k}$ measuring the (non)integrability of the horizontal distribution. The vanishing of the curvature components R_{ij}^k is a necessary and sufficient condition for the integrability of the horizontal distribution. Due to the skew symmetry in the low indices, R_{ij}^k is also interpreted as the $hhv-$torsion tensor (see eg. [111]).

The nonlinear connection is said to be *symmetric* if $t_{jk}^i = 0$, where

$$t_{jk}^i = \frac{\partial N_j^i}{\partial y^k} - \frac{\partial N_k^i}{\partial y^j},$$

are the components of the so called *weak torsion* tensor of the nonlinear connection.

Let us consider a linear connection

$$D : \chi(TM) \times \chi(TM) \to \chi(TM).$$

If D preserves the Whitney decomposition (1.6) induced by a given nonlinear connection N, then D is called *N-linear connection.* It transports horizontal vectors into horizontal ones and vertical vectors into vertical ones. The compatibility of the linear connection D with the nonlinear connection N yields two types of connection coefficients, $D(N) = (F^i_{jk}, C^i_{jk})$. The coefficients F^i_{jk} describe the transport in horizontal direction, and the coefficients C^i_{jk} describe the transport in vertical direction. The covariant derivative of $D(N)$ uniquely provides the coefficients, by means of

$$\begin{array}{ll} D_{\frac{\delta}{\delta x^j}} \dfrac{\delta}{\delta x^k} = F^i_{jk} \dfrac{\delta}{\delta x^i}, & D_{\frac{\delta}{\delta x^j}} \dfrac{\partial}{\partial y^k} = F^i_{jk} \dfrac{\partial}{\partial y^i}, \\ D_{\frac{\partial}{\partial y^j}} \dfrac{\delta}{\delta x^k} = C^i_{jk} \dfrac{\delta}{\delta x^i}, & D_{\frac{\partial}{\partial y^j}} \dfrac{\partial}{\partial y^k} = C^i_{jk} \dfrac{\partial}{\partial y^i}. \end{array} \tag{1.11}$$

The vertical coefficients C^i_{jk} are components of a $d-$tensor, and the horizontal ones F^i_{jk} transform like the local coefficients of an affine connection on the base manifold.

Consequently, the covariant derivative can be decomposed into two parts: horizontal and vertical covariant derivatives. Further, the notions of metricity and symmetry will be independently addressed.

A regular curve $c : I \to TM, \quad c(t) = (x^i(t), y^i(t))$ is a *horizontal* curve if the tangent vector field $\dot{c}$ along c is in HTM. The curve c is said to be an *autoparallel curve of the N-linear connection D* if

$$D_{\dot{c}}\dot{c} = 0.$$

The necessary and sufficient condition for a curve c to be horizontal is

$$\frac{d^2x^i}{dt^2} + F^i_{jk} \frac{dx^j}{dt} \frac{dx^k}{dt} = 0. \tag{1.12}$$

A regular curve on the base manifold $c : I \to M, \quad c(t) = (x^i(t))$ is an autoparallel curve of an N-linear connection, if its natural lift to TM, $\widehat{c}(t) = (x^i(t), \frac{dx^i}{dt}(t))$ is a horizontal curve.

Remark. Though the equations (1.9) and (1.12) are analogous, the curves are differently named. The reason is an ability to relate the N-linear connection with a metric structure, and further to consider curves by their length minimality.

The properties of a N-linear connection D are described by the components of the torsion tensor and of the curvature tensor.

The *torsion tensor* of the N-linear connection $D(N) = (F^i_{jk}, C^i_{jk})$ is defined as

$$T(X, Y) = D_X Y - D_Y X - [X, Y], \quad \forall X, Y \in \chi(TM)$$

and can be expressed by five d-tensors defined in the following way:

$$\begin{array}{rcl} T\left(\dfrac{\delta}{\delta x^i}, \dfrac{\delta}{\delta x^j}\right) & = & T^k_{ji} \dfrac{\delta}{\delta x^k} + R^k_{ji} \dfrac{\partial}{\partial y^k}, \\ T\left(\dfrac{\partial}{\partial y^i}, \dfrac{\delta}{\delta x^j}\right) & = & C^k_{ji} \dfrac{\delta}{\delta x^k} + P^k_{ji} \dfrac{\partial}{\partial y^k}, \\ T\left(\dfrac{\partial}{\partial y^i}, \dfrac{\partial}{\partial y^j}\right) & = & S^k_{ji} \dfrac{\partial}{\partial y^k}; \end{array} \tag{1.13}$$

where the components of the d-tensors are explicitly given by

$$T^k_{ji} = F^k_{ji} - F^k_{ij}, \qquad R^k_{ji} = \frac{\delta N^k_j}{\delta x^i} - \frac{\delta N^k_i}{\delta x^j}, \qquad P^k_{ji} = \frac{\partial N^k_j}{\partial y^i} - F^k_{ij}, \qquad S^k_{ji} = C^k_{ji} - C^k_{ij}. \quad (1.14)$$

The curvature of the N-linear connection $D(N) = (F^i_{jk}, C^i_{jk})$ defined as

$$R(X,Y)Z = D_X D_Y Z - D_Y D_X Z - D_{[X,Y]}Z, \quad \forall X,Y,Z \in \chi(TM),$$

has only three sets of components defined by (cf. [35, 76])

$$\begin{aligned} R\left(\frac{\delta}{\delta x^i}, \frac{\delta}{\delta x^j}\right)\frac{\delta}{\delta x^h} &= R^k_{hji}\frac{\delta}{\delta x^k}, \\ R\left(\frac{\partial}{\partial y^i}, \frac{\delta}{\delta x^j}\right)\frac{\delta}{\delta x^h} &= P^k_{hji}\frac{\delta}{\delta x^k}, \\ R\left(\frac{\partial}{\partial y^i}, \frac{\partial}{\partial y^j}\right)\frac{\delta}{\delta x^h} &= S^k_{hji}\frac{\delta}{\delta x^k}; \end{aligned} \quad (1.15)$$

where

$$\begin{aligned} R^k_{hji} &= \frac{\delta F^k_{hj}}{\delta x^i} - \frac{\delta F^k_{hi}}{\delta x^j} + F^m_{hj}F^k_{mi} - F^m_{hi}F^k_{mj} + C^k_{hm}R^m_{jk}, \\ P^k_{hji} &= \frac{\partial F^k_{hj}}{\partial y^i} - \frac{\delta C^k_{hi}}{\delta x^j} - C^m_{hi}F^k_{mj} + C^k_{mi}F^m_{hj} + C^k_{hm}F^m_{ij} + C^k_{hm}P^m_{ji}, \\ S^k_{hji} &= \frac{\partial C^k_{hj}}{\partial y^i} - \frac{\partial C^k_{hi}}{\partial y^j} + C^m_{hj}C^k_{mi} - C^m_{hi}C^k_{mj}. \end{aligned} \quad (1.16)$$

There are three more expressions of vertical type defining the curvature tensor; these can be obtained by changing the third argument in (1.15) to be from the vertical local basis. Then, the righthand sides will be changed in the same manner, but the components of the curvature tensor remain the same as in (1.16).

The nonlinear connection N on M produces some special N-linear connections on TM. One of them is the Berwald connection $B\Gamma = D(N)$, whose local coefficients are:

$$B\Gamma(N^i_j) = \left(F^i_{jk} = \frac{\partial N^i_j}{\partial y^k}, C^i_{jk} = 0\right). \quad (1.17)$$

The relations (1.11) show that the vertical connection coefficients vanish.

Considering the torsion of the Berwald connection described by (1.13) and (1.14), one can see that the only nonvanishing set of components of the torsion is of type $hh - v$, and the $hh - v$ torsion of the Berwald connection coincides with the already mentioned invariant, the curvature tensor of the nonlinear connection (1.10).

Analogously, the curvature tensor of the Berwald connection has only two nonvanishing sets of components: the horizontal and the mixed one:

$$R^k_{hji} = \frac{\delta F^k_{hj}}{\delta x^i} - \frac{\delta F^k_{hi}}{\delta x^j} + F^m_{hj}F^k_{mi} - F^m_{hi}F^k_{mj}, \quad P^k_{hji} = \frac{\partial F^k_{hj}}{\partial y^i} = \frac{\partial^2 N^k_h}{\partial y^j \partial y^i}. \quad (1.18)$$

The curvature of the nonlinear connection and the horizontal curvature of the induced Berwald connection are related by

$$R^k_{hji} = \frac{\partial R^k_{ji}}{\partial y^h}. \quad (1.19)$$

Some more mappings and geometric objects existing in TTM will be further described.

The *tangent structure* J is the submersion $J : TTM \to VTM$, that is nilpotent of the second order, and its kernel and image coincide

$$J^2 = 0, \quad \mathrm{Im}J = \mathrm{Ker}J = VTM.$$

It can be considered as a globally defined $(1,1)$-type tensor field on TM, $J = \delta^i_j \frac{\partial}{\partial y^i} \otimes dx^j$. The action of J on the canonical frame of $\chi(TTM)$ is the following:

$$J\left(\frac{\partial}{\partial x^i}\right) = \frac{\partial}{\partial y^i}, \quad J\left(\frac{\partial}{\partial y^i}\right) = 0.$$

Definition 1.3.2. The canonical vertical vector field $C = y^i \frac{\partial}{\partial y^i}$, globally defined on the slit tangent bundle, is called the *Liouville vector field*. A vector field $S \in \chi(TM)$ is called a *semispray* (or a *second order vector field*) if and only if $JS = C$.

The second order tangent bundle provides by duality the cotangent bundle with total space T^*TM and dual coframe $\{dx^i, dy^i\}$. Analogously, there exists the dual decomposition $T^*TM = H^*TM \oplus V^*TM$ induced by the nonlinear connection N, and the adjusted dual coframe $\left\{dx^i, \delta y^i = dy^i + N^i_j dx^j\right\} \subset \Gamma(T^*TM)$.

For more details on d-connection theory we refer to [35].

1.3.2 Finsler structures

The theory of Finsler spaces has been systematically and comprehensively considered by many authors, see [27, 35, 40, 94, 101]. Here, we give a concise introduction to the basic notions and results from the Finsler geometry.

Finsler geometry has its physical motivation in the variational calculus of the following integral

$$\int_a^b F\left(x^1, \ldots, x^n, \frac{dx^1}{dt}, \ldots, \frac{dx^n}{dt}\right) dt, \tag{1.20}$$

where $F(x^1, \ldots, x^n, y^1, \ldots, y^n)$ is nonnegative real function (cf.[27]). Some additional constrains for the dependency F on y^i will be given in Definition 1.3.3.

1.3.1. Examples

1. When interpreting t as the time, x as the physical position and y as the velocity of a particle, then F describes the motion speed of the particle, and the above integral measures the distance between the positions $x(a)$ and $x(b)$.

2. If x stands for the position inside a vector field action, then a force $F(x, y)$ depends on the direction too, and the integral (1.20) represents the work done by the force F.

3. If x stands for the position inside an anisotropic medium (e.g. crystal structure), the speed of light propagation $F(x, y)$ depends on its direction. The integral (1.20) represents the total time that light needs to traverse the given path.

4. One can find examples from biology and ecology in [4, 6, 7, 27].

A Finsler manifold is a pair (M, F), where M is a differentiable manifold equipped with a Finsler fundamental function F, that can arise from two different approaches: from differential geometry, by defining a metric tensor field on the tangent space TM (see e.g. [27, 94]), or from functional analysis, by defining a family of inner products in every fiber T_xM of the tangent bundle (cf. [35, 100]). The Finsler structure is globally defined on the tangent space of M by allowing F to act on the total tangent space TM of the manifold.

Definition 1.3.3. A function $F : TM \to [0, \infty)$ is the *Finsler fundamental function* on an n-dimensional differentiable manifold M if it satisfies the following conditions:

1. *(regularity)* $F(x, y)$ is C^∞-differentiable on the slit tangent bundle $\widetilde{TM}$ and only continuous on the null section;

2. *(positive homogeneity)* $F(x, y)$ is positively homogeneous of the first order with respect to the fiber coordinates,
$$F(x, \lambda y) = \lambda F(x, y), \quad \forall \lambda > 0;$$

3. *(strong convexity)* the Hessian matrix of F^2 with respect to the fiber coordinates
$$(g_{ij}(x, y)) = \left(\frac{\partial^2}{\partial y^i \partial y^j} \left[\frac{1}{2} F^2(x, y) \right] \bigg|_{(x,y)} \right)_{i,j=\overline{1,n}} \tag{1.21}$$
is positive definite on the slit tangent bundle.

The fundamental function defines a Finsler structure on M and turns M into a Finsler manifold (M, F). The collection of scalar functions $g_{ij}(x, y)$, $i, j = \overline{1, n}$, represent the components of the so-called *fundamental tensor* $g = g_{ij}(x, y)dx^i \otimes dx^j$.

The fundamental tensor field on M, $g = g_{ij}(x, y)dx^i \otimes dx^j$ is well defined. Actually, it is a tensor field on $\widetilde{TM}$, but the properties of the fundamental function ensures it being a d-tensor field. More, the corresponding inverse tensor field with components $(g^{ij}(x, y))$ is also a d-tensor field on $\widetilde{TM}$.

The strong convexity condition is well defined, i.e., it does not depend on the choice of fiber coordinates and implies that the symmetric bilinear form
$$g_{(x,y)}(u, v) = \frac{1}{2} \frac{\partial^2}{\partial s \partial t} \left[F^2(x, y + su + tv) \right] \big|_{s=t=0}, \quad (x, y) \in TM, u, v \in T_xM,$$
is positive definite at every point of the slit tangent bundle.

The restriction of F to a specific tangent space $F_x = F(x, \cdot) : T_xM \to [0, \infty)$ satisfies all the needed conditions to be a *Minkowski norm* in the vector space T_xM ([40, 100]). The direction of the zero-tangent vector is trivial, so there is no interest of existence of partial derivatives of F at $y = 0$. This explains the absence of the differentiability request at the zero section of TM. But homogeneity and strong convexity of the fundamental function guarantee the continuity at the null section of the tangent bundle.

Remark. Some authors, see [35], allow the third condition in Definition 1.3.3 to be weaker, namely that the Hessian matrix and the corresponding bilinear form be nondegenerate and of constant signature. In order to avoid the ambiguity such a structure will be called pseudo-Finsler structure.

Remark. One may also consider a generalized Finsler structure (M, F), whose fundamental function F is not defined on the whole tangent space, but only on certain distributions of TM, or has its smoothness domain strictly included in the slit tangent space. Some classical illustrative examples in this respect are the Kropina metric, the m-th root pseudo-Finsler metrics, including the Berwald-Moor metric, etc (see [86, 87]).

Remark. Any Riemannian manifold (M, g) is also Finslerian. The scalar product $g_x(u, v) = g_{ij}(x)u^i v^j, \quad \forall u, v \in T_xM$ is induced by the following norm

$$F(x, y) = \sqrt{g_{ij}(x)y^i y^j}, \quad \forall y \in T_xM.$$

Then F defines a fundamental function of the Finsler manifold of Riemann type.

The problem of existence of a Finsler structure on a differentiable manifold is considered in [35]. In this matter, we have the following result:

1.3.2. Theorem *([35]) Let M be a paracompact manifold with a differentiable structure and the tangent bundle TM. Then there exists a function $F : TM \to \mathbb{R}$, which satisfies the axioms of a Finsler fundamental function on M, and hence endows M with a Finsler structure.*

The necessary and sufficient condition for (M, F) to be reducible to a Riemannian manifold is the parallelogram equality

$$F^2(x, y + z) + F^2(x, y - z) = 2F^2(x, y) + 2F^2(x, z), \quad \forall y, z \in T_xM.$$

There is another geometric object specific for Finsler manifolds, which describes the dependency on direction (fiber coordinates) of the fundamental tensor.

Definition 1.3.4. The Cartan tensor is the $(0, 3)$-type tensor field on $\widetilde{TM}$ defined as

$$C_{ijk}(x, y) := \frac{1}{2} \frac{\partial g_{ij}(x, y)}{\partial y^k}\Big|_{(x,y)} = \frac{1}{4} \frac{\partial^3 F^2(x, y)}{\partial y^i \partial y^j \partial y^k}\Big|_{(x,y)}.$$

The vanishing of the components of the Cartan tensor field is a necessary and sufficient condition for the Finsler manifold to be Riemannian. The Cartan tensor is totaly symmetric, due to the smoothness of the fundamental function. The partial contraction of the contravariant metric with the Cartan tensor gives the *mean Cartan tensor*

$$I_i = g^{jk} C_{ijk},$$

which is simpler, but with analogous properties and similar importance as C_{ijk}. By Deicke's theorem ([44]), one has the following equivalences (cf. [27]):

1.3.3. Theorem *Let (M, F) be a Finsler manifold. Then the following conditions are equivalent:*

1. *M is Riemannian manifold.*
2. *The Cartan tensor C_{ijk} vanishes.*
3. *The mean Cartan tensor I_i vanishes.*

Both Cartan tensors C_{ijk} and I_i are d-tensors on $\widetilde{TM}$. Their main properties arise from the homogeneity of F and will be presented in Proposition 1.3.4.

The homogeneity of the fundamental function is the necessary and sufficient condition for the existence of an extremal for the integral (1.20), see [94]. Euler's theorem for homogeneous functions gives an equivalent condition for the positive 1-homogeneity of the Finsler fundamental function ([27]):

$$\frac{\partial F(x,y)}{\partial y^i} y^i = F(x,y). \tag{1.22}$$

1.3.4. Proposition *The following properties hold true in a Finsler space (M,F):*

1. *The Finsler fundamental function satisfies*

$$\frac{\partial^2 F(x,y)}{\partial y^i \partial y^j} y^i = 0; \tag{1.23}$$

$$\frac{\partial^2 F^2(x,y)}{\partial y^i \partial y^j} y^i = 2F(x,y)\frac{\partial F}{\partial y^j};$$

$$F^2(x,y) = g_{ij}(x,y) y^i y^j, \quad \text{or equivalently} \quad g_{ij}(x,y)\frac{y^i}{F(x,y)}\frac{y^j}{F(x,y)} = 1; \tag{1.24}$$

$$g_{ij}(x,\lambda y) = g_{ij}(x,y). \tag{1.25}$$

2. *The Cartan tensor and the mean Cartan tensor are positively homogeneous of degree -1:*

$$C_{ijk}(x,\lambda y) = \lambda^{-1} C_{ijk}(x,y), \quad \text{and} \quad C_{ijk} y^k = 0,$$
$$I_i(x,\lambda y) = \lambda^{-1} I_i(x,y), \quad \text{and} \quad I_i y^i = 0.$$

3. *The Finsler norm $F_x = F(x,\cdot)$ in T_xM is equivalent with any other norm of Finsler type $\|\cdot\|_F$, including the Euclidean one.*

Proof. These relations are consequences of Euler's theorem, precisely of the relation (1.22). □

The property (1.23) shows that the Hessian matrix of the fundamental function F is singular. The equality (1.25) shows that the fundamental tensor is positively homogeneous of order 0. Inside any fiber $T_xM\backslash\{0\}$, the function $g_{ij}(x,\cdot)$ is constant on each subset $\{\lambda y \big| \lambda > 0\}$, so one can say that the fundamental tensor is constant in the direction of the tangent vector $y \in T_xM \setminus \{0\}$. Precisely, the fundamental tensor is constant only on the positive semi-ray determined by y. The first relation in (1.24) can be interpreted as $F(x,y) = \sqrt{g_{ij}(x,y) y^i y^j}$, hence it makes sense to call $F(x,y)$ the *length* (or *norm*), of the tangent vector y at the point x. The unit length vector $l(x,y) \in T_xM$ associated to a tangent vector $y \in T_xM \setminus \{0\}$ is called a supporting element at the point x in the direction of y, and the second relation at (1.24) provides its explicit form:

$$l(x,y) = \frac{y}{F(x,y)} = \left(\frac{y^1}{F(x,y)}, \dots, \frac{y^n}{F(x,y)}\right).$$

The set of all unit tangent vectors at point x of a Finsler manifold is a hypersurface in T_xM, called the *indicatrix* at x,

$$I_x = \left\{ y \in T_xM \big| F(x,y) = 1 \right\}.$$

The theory of these hypersurfaces is developed in [31, 62, 94] and widely applicable, especially in the wavefront representation and propagation, cf. [12, 54, 45, 112].

Without loss of generality, we can assume that the further considered regular curves in the Finsler manifold (M, F), given by $c : I \to M,\ c : t \mapsto \left(x^i(t)\right)$, are parameterized by arclength, which means $F\left(c(t), \frac{dc}{dt}(t)\right) = 1, \quad \forall t \in I$.

The *length* and the *energy* of the curve c in the Finsler manifold are defined by the restriction of the fundamental function and its square to the curve extension $\hat{c} : I \to \widetilde{TM}, \quad \hat{c}(t) = \left(c(t), \frac{dc}{dt}\Big|_t\right)$, as follows

$$\ell(c) = \int_I F(\hat{c}(t))\, dt, \qquad E(c) = \int_I F^2(\hat{c}(t))\, dt.$$

Both integrals do not depend on parameterization, due to the homogeneity of F, and they achieve extremal values on the same curve assuming that the endpoints are fixed.

Definition 1.3.5. A *variation of a curve* c is a smooth mapping $c_\varepsilon : (-\epsilon, \epsilon) \times [0, 1] \to M \quad (\epsilon > 0)$, where the following holds:

1. $c_0(t) = c(t), \quad t \in [a, b]$, ($\varepsilon = 0$ provides the initial curve);
2. $c_\varepsilon(0) = c(0), \quad c_\varepsilon(1) = c(1), \quad \forall \varepsilon \in (-\epsilon, \epsilon)$, (the endpoints are fixed).

Definition 1.3.6. A curve c in Finsler manifold is called a *geodesic* if its length $\ell(c)$ is stationary with respect to the variations of c, i.e.,

$$\frac{d\ell(c_\varepsilon)}{d\varepsilon}\bigg|_{\varepsilon=0} = 0.$$

The classical Euler-Lagrange equation for the variational problem of curve length in the Finsler manifold aims to minimize the length $\ell(c)$ and produces the local condition for a curve to be geodesic (see [35]). This is described by the following proposition.

1.3.5. Proposition *(The geodesic equation, [35]) A curve $c : I \to M$ with arclength parameterization is a geodesic in the Finsler manifold (M, F) if and only if its local coordinates satisfy the following second-order system of differential equations*

$$\frac{d^2 c^i}{ds^2} + 2G_F^i\left(c(s), \frac{dc}{ds}\right) = 0, \quad i = \overline{1, n}, \tag{1.26}$$

where

$$2G_F^i(x, y) = \frac{1}{2} g^{ij}\left[\frac{\partial^2 F^2}{\partial x^k \partial y^j}(x, y) y^k - \frac{\partial F^2}{\partial x^j}(x, y)\right], \quad y = \frac{dx}{ds}. \tag{1.27}$$

The meaning of this proposition is that an arclength parameterized curve on M is geodesic if and only if its canonical lift is an integral curve of the corresponding semispray vector field on $\widetilde{TM}$,

$$S_F(x, y) = y^i \frac{\partial}{\partial x^i}\bigg|_{(x,y)} - 2G_F^i(x, y) \frac{\partial}{\partial y^i}\bigg|_{(x,y)}. \tag{1.28}$$

The functions $G_F^i(x, y)$ are called the *geodesic coefficients*, and further computation based on their homogeneity gives another, equivalent form of (1.27):

$$G_F^i(x, y) = \frac{1}{2}\gamma_{jk}^i(x, y) y^i y^j,$$

where $\gamma^i_{jk}(x,y)$ are the formal Cristoffel symbols of the fundamental tensor (similar to (1.3)),

$$\gamma^i_{jk}(x,y) = \frac{1}{2}g^{ir}(x,y)\left(\frac{\partial g_{rk}}{\partial x^j}(x,y) + \frac{\partial g_{jr}}{\partial x^k}(x,y) - \frac{\partial g_{jk}}{\partial x^r}(x,y)\right).$$

The homogeneity property holds for the geodesic coefficients too. The vector field (1.28) is said to be the *geodesic spray* of the Finsler manifold.

Further, through the geodesic coefficients, the Finsler structure uniquely determines the *Cartan nonlinear connection*

$$N^i_j(x,y) = \frac{\partial G^i}{\partial y^j}\bigg|_{(x,y)}.$$

There are four special N-linear connections canonically associated to the Finsler space (M,F): Berwald, Cartan, Chern-Rund and Hashiguchi, but none of them has the two important properties of metricity and symmetry of the Levi-Civita connection associated to a Riemannian structure. Various choices of the horizontal and vertical connection coefficients (in the four cases) provide vanishing torsion and compatibility with the Finsler metric but separately considered in horizontal and vertical distribution, but not simultaneously.

The Berwald N-linear connection is h-metrical and h-symmetric and has the following coefficients

$$F^i_{jk} = \frac{\partial N^i_j}{\partial y^k}, \quad C^i_{jk} = 0.$$

The Cartan N-linear connection is metrical and symmetric in both distributions and has the following generalized Cristoffel symbols

$$F^i_{jk} = \frac{1}{2}g^{ih}\left(\frac{\delta g_{hk}}{\delta x^j} + \frac{\delta g_{hj}}{\delta x^k} - \frac{\delta g_{jk}}{\delta x^h}\right), \quad C^i_{jk} = \frac{1}{2}g^{ih}\left(\frac{\partial g_{hk}}{\partial y^j} + \frac{\partial g_{hj}}{\partial y^k} - \frac{\partial g_{jk}}{\partial y^h}\right).$$

The Chern-Rund N-linear connection is h-metrical and h-symmetric and has the following coefficients

$$F^i_{jk} = \frac{1}{2}g^{ih}\left(\frac{\delta g_{hk}}{\delta x^j} + \frac{\delta g_{hj}}{\delta x^k} - \frac{\delta g_{jk}}{\delta x^h}\right), \quad C^i_{jk} = 0.$$

The Hashiguchi N-linear connection is h-symmetric, v-metrical and v-symmetric and has the following coefficients

$$F^i_{jk} = \frac{\partial N^i_j}{\partial y^k}, \quad C^i_{jk} = \frac{1}{2}g^{ih}\left(\frac{\partial g_{hk}}{\partial y^j} + \frac{\partial g_{hj}}{\partial y^k} - \frac{\partial g_{jk}}{\partial y^h}\right).$$

More details on this subject can be found in [35].

The theory of submanifolds in Finsler spaces is presented in [99]. Particularly, minimality of a surface in Finsler spaces of different types is considered in [15, 16, 17].

1.3.3 Finsler structures of Randers type

Randers spaces are the simplest non-Riemannian examples of Finsler structures. A Randers fundamental function can be considered as a linearly deformed Riemannian norm. More precisely, a Randers structure on a differentiable manifold M is given by a Finsler fundamental function of the form:

$$F(x,y) = \sqrt{a_{ij}(x)y^i y^j} + b_i(x)y^i, \tag{1.29}$$

where $a = a_{ij}dx^i \otimes dx^j$ is a Riemannian metric on M and $b = b_i dx^i$ is a 1-form on M. These naturally produce the following scalar functions on the tangent space TM,

$$\alpha(x,y) = \sqrt{a_{ij}(x)y^i y^j}, \quad \beta(x,y) = b_i(x)y^i, \qquad \forall y \in T_xM, x \in M.$$

Since $\beta(x,\cdot)$ does not have a fixed sign and F has to be positive on $\widetilde{TM}$, the following function which is globally defined on M has to be bounded,

$$||b|| = \sqrt{a^{ij}b_ib_j} < 1.$$

The absolute homogeneity of the Riemannian norm α and the linearity of β ensure that F is positively homogeneous.

1.3.6. Theorem *Let (M,F) be the Finsler space with Randers type fundamental function (1.29). The metric tensor field defined by (1.21) has the following form*

$$g_{ij} = \frac{F}{\alpha}a_{ij} - \frac{F}{\alpha^2}y_iy_j + \left(b_i + \frac{y_i}{\alpha}\right)\left(b_i + \frac{y_i}{\alpha}\right), \tag{1.30}$$

the corresponding inverse metric is given by

$$g^{ij} = \frac{\alpha}{F}a^{ij} + \frac{\beta + \alpha||b||^2}{F^3}y^iy^j - \frac{\alpha}{F^2}a^{ik}b_ky^j - \frac{\alpha}{F^2}a^{jk}b_ky^i, \tag{1.31}$$

and the fundamental determinant $g = \det(g_{ij})$ has the following expression

$$g = \left(\frac{F}{\alpha}\right)^{n+1}\det(a_{ij}). \tag{1.32}$$

The proof of this theorem can be found in [27], and is based on the following algebraic fact:

1.3.7. Lemma *Let (Q_{ij}) be a nonsingular real square matrix of order n with the inverse matrix (Q^{ij}), and let (C_i) be an $n \times 1$ real matrix. Then, denoting $c^2 = Q^{ij}C_iC_j$, the following holds true:*

$$\det(Q_{ij} + C_iC_j) = (1 + c^2)\det(Q_{ij}).$$

If $1 + c^2 \neq 0$ then the matrix $(Q_{ij} + C_iC_j)$ is nonsingular and has its inverse defined by

$$(Q_{ij} + C_iC_j)^{-1} = \left(Q^{ij} - \frac{1}{1+c^2}C^iC^j\right),$$

where $C^i = Q^{ij}C_j$.

Further details about Randers spaces, including examples, can be found in [6, 38, 73].

1.3.4 Ingarden structures

On a Randers space $(M, F = \alpha + \beta)$, the Finslerian nonlinear connection can be constructed in many ways, in accordance with Definition 1.3.1. The choice of the connection coefficients

N^i_j provides through the mapping (1.7) the horizontal sections for the Whitney decomposition (1.6). Besides of the Cartan nonlinear connection (1.27), one can chose

$$N^i_j = \gamma^i_{jk} y^k - \frac{1}{2} a^{ih} \left(\frac{\partial b_h}{\partial x^j} - \frac{\partial b_j}{\partial x^h} \right), \quad \text{or} \quad N^i_j = \gamma^i_{jk} y^k - \frac{1}{2} a^{ih} b_k y^k \left(\frac{\partial b_h}{\partial x^j} - \frac{\partial b_j}{\partial x^h} \right), \tag{1.33}$$

where γ^i_{jk} are the Cristoffel symbols of the Riemannian metric a. The coefficients (1.33) define variants of the Lorenz nonlinear connection, which are nonhomogeneous or homogeneous, respectively.

Ingarden spaces are Finsler spaces with Randers structure and Lorenz type nonlinear connection. An important property of these spaces is their having a simple Berwald connection (1.17), whose horizontal coefficients coincide with the coefficients of the Levi-Civita connection associated to the Riemannian structure a.

In the case of nonhomogeneous Lorentz connection, Ingarden spaces can be regarded as Lagrange spaces. The theory of Ingarden spaces is presented in [77, 78].

1.3.5 Other special Finsler structures

$(\alpha, \beta)-$structures

The previously considered Randers structures belong to the class of $(\alpha, \beta)-$structures, whose fundamental function F is given by a Riemannian norm α and an 1-form β, as

$$F = \alpha \phi \left(\frac{\beta}{\alpha} \right),$$

where ϕ is a smooth real function defined on a symmetric open interval $I \subset \mathbb{R}$. In [40] one can find the proof that the same condition $||b|| < 1$ is sufficient for F to be a Finsler fundamental function.

Another particular case of $(\alpha, \beta)-$structure is the Kropina structure, with the fundamental function given by

$$F(x, y) = \frac{\alpha^2}{\beta} = \frac{a_{ij}(x) y^i y^j}{b}.$$

This type of metric is used for modelling dissipative mechanical systems and the corresponding theory is presented in [9]. Global properties of Randers-Kropina metrics are considered in [21].

m-th root Finsler structures

An m-th root Finsler space is a differentiable manifold endowed with a fundamental function of the form

$$F(x, y) = \sqrt[m]{a_{i_1 i_2 \ldots i_m}(x) y^{i_1} y^{i_2} \ldots y^{i_m}}, \tag{1.34}$$

where $a_{i_1 i_2 \ldots i_m}$ are components of a totaly symmetric covariant tensor field on M, and $m > 2$. Generally, an m-th root Finsler fundamental function does not produce necessarily a positive definite metric tensor (1.21), hence it is a pseudo-Finsler structure.

The fundamental metric tensor of an m-th root structure has the components

$$g_{ij} = (m - 1) a_{ij} - (m - 2) a_i a_j,$$

where

$$a_{ij} = a_{iji_3 i_4 \dots i_m}(x) y^{i_3} y^{i_4} \dots y^{i_m}, \quad \text{and} \quad a_i = a_{ii_2 i_3 \dots i_m}(x) y^{i_2} y^{i_3} \dots y^{i_m}.$$

In the cases when a_{ij} is a regular tensor, the metric is regular too, and its dual components are

$$g^{ij} = \frac{1}{m-1}\left(a^{ij} + (m-2)a^i a^j\right),$$

where $a^i = a^{ij} a_j$. Properties of these Finsler spaces are considered in [18], where explicit expressions for the representative geometric objects are given. Some particular cases are:

1. The firstly considered Finsler fundamental function, proposed by Riemann, see [18]:

$$F(x,y) = \sqrt[4]{(y^1)^4 + (y^2)^4 \dots + (y^n)^4}.$$

2. The cubic (3-rd root) Finsler metric, which canonically possesses a Wagner type N-linear connection, was studied in [71, 73, 84, 85].

3. The Berwald-Moor structure with the fundamental function

$$F(x,y) = \sqrt[n]{y^1 y^2 \dots y^n}$$

is pseudo-Finslerian. Its metric tensor has the signature $(+, -, -, \dots, -)$, hence it is commonly used in Relativity models. Other significant properties are presented in [14]. More details on the subject, from different approaches, can be found in [9, 11, 72].

1.4 Generalized Lagrange structures

Weaker conditions in Definition 1.3.3 produce a generalization of Finsler spaces, the Lagrange spaces. An (x,y)-dependent metric tensor field provides a Generalized Lagrange structure. The notion of generalized Lagrange structure was motivated by the fact that many properties of Lagrange spaces refer only to the metric tensor instead of considering *ab initio* a Lagrangian. The theory of generalized Lagrange structures was introduced by Miron, and details of the theory can be found in [35, 75]. Here, we present basic facts that are of the interest for our work.

Definition 1.4.1. A *generalized Lagrange space*, or shortly GL-space is the pair (M,g), where M is a differentiable manifold and $g = g_{ij}(x,y)dx^i \otimes dy^j$ is d-tensor field on the tangent space TM, satisfying the following properties:

1. g is symmetric, $g_{ij}(x,y) = g_{ji}(x,y), \quad \forall (x,y) \in TM$,
2. g is regular, $\det(g_{ij}(x,y)) \neq 0, \quad \forall (x,y) \in TM$,
3. the quadratic form $g(x,y) : \mathbb{R}^n \to \mathbb{R}$ given by $g_{ij}(x,y)v^i v^j$ has constant signature.

The tensor g is said to be the *GL-metric* on the space.

Obviously, any Finsler space is also a GL-space. Conversely, the restriction of a GL-metric $g_{ij}(x,y)$ to the slit tangent bundle $\widetilde{TM}$ is reducible to a Finslerian metric if there exists a function $F : TM \to [0, \infty)$, of C^∞-class on $\widetilde{TM}$ and only continuous on the zero section, which is positively homogeneous of order 1 in the second argument, and satisfies

$$g_{ij}(x, y) = \frac{1}{2} \frac{\partial^2 F^2}{\partial y^i \partial y^j}(x, y).$$

The Cartan tensor, which is a d-tensor specific for Finsler geometry, can be extended to the GL-framework as follows:

Definition 1.4.2. The Cartan tensor of a GL-metric g is the (0,3)-type d-tensor

$$C_{ijk} = \frac{1}{2} \left(\frac{\partial g_{ik}}{\partial y^j} + \frac{\partial g_{ij}}{\partial y^k} - \frac{\partial g_{jk}}{\partial y^i} \right).$$

This generalization is well defined while in the case of Finsler spaces, only the first term remains. The Cartan tensor of a GL-space is symmetric in the last two indices.

1.4.1. Proposition *A GL-metric g_{ij} is reducible to a Finsler metric if and only if*

$$C_{ijk} y^j = 0.$$

A GL-metric g is said to be reducible to a Riemannian metric if it does not depend on tangent vectors, i.e., $g_{ij}(x, y) = g_{ij}(x)$. A necessary and sufficient condition for a GL-metric to be reducible to a Riemannian metric is the vanishing of the Cartan tensor.

A GL-space (M, g) does not have a canonical nonlinear connection. Hence, it is usual to establish a nonlinear connection N induced by a semispray S defined on M. Further, the compatibility of the two geometries (M, g) and (S, N) can be considered.

The variational problem of a GL-space (M, g) can be considered if the GL-metric is zero homogeneous and if it canonically defines a nonlinear connection. Then, it becomes a variational problem of the Finsler space with $F(x, y) = \sqrt{g_{ij}(x, y) y^i y^j}$.

1.4.1 The Lagrange structure

Definition 1.4.3. [35] A *Lagrange space* is a couple (M, L), where M is a differentiable manifold and the Lagrangian $L : TM \to \mathbb{R}$ is a scalar function, which is C^∞-differentiable on the slit tangent bundle $\widetilde{TM}$, only continuous on the null section, and regular, meaning that the halved Hessian of $L(x, y)$ with respect to the fiber coordinates y^i,

$$g_{ij}(x, y) = \frac{1}{2} \frac{\partial^2 L}{\partial y^i \partial y^j}(x, y) \tag{1.35}$$

is regular (of maximal rank) and of constant signature over the slit tangent bundle $\widetilde{TM}$.

A Lagrange space (M, L) is said to be reducible to a Finsler space if there is a Finsler fundamental function defined on TM, such that $L(x, y) = F^2(x, y)$.

Remark. Lagrange spaces represent a generalization of the Riemannian and Finslerian ones. In the first case, the Lagrangian is exactly the square of the Riemannian norm $L_R(x, y) = g_{ij}(x) y^i y^j$ and in the second one, it is the square of the Finsler norm $L_F(x, y) = F^2(x, y)$.

An example of a Lagrange space that is not reducible to a Finsler space is given by the following Lagrangian

$$L(x,y) = F^2(x,y) + A_i(x)y^i + U(x),$$

where F is a Finsler fundamental function, A_i are the components of a covector field on M, and U is a smooth scalar function on M.

The Cartan tensor of a Lagrange space (M,L) is defined in an analogous way,

$$C_{ijk} = \frac{1}{2}\frac{\partial g_{ij}}{\partial y^k} = \frac{1}{4}\frac{\partial^3 L}{\partial y^i \partial y^j \partial y^k},$$

and it is a totaly symmetric d-tensor field.

1.4.2. Proposition *A GL-space (M,g) is reducible to a Lagrange space if and only if its Cartan tensor given in Definition 1.4.2 is totally symmetric.*

Definition 1.4.4. The *energy* of the Lagrange space (M,L) is defined by the Lagrangian in the following way

$$E_L = y^i \frac{\partial L}{\partial y^i} - L. \tag{1.36}$$

In the particular case of Finslerian (and Riemannian) spaces, the energy (1.36) coincides with the Lagrangian itself, since the 2-homogeneity of corresponding Lagrangian L produces the relation $y^i \dfrac{\partial L}{\partial y^i} = 2L$.

Similarly as before, the geodesics of a Lagrange space are curves which minimize the action of the Lagrangian

$$I(c) = \int_c L\left(x, \frac{dx}{dt}\right) dt, \quad c : [0,1] \mapsto x^i(t) \in M.$$

Hence, they are determined from the Euler-Lagrange equations

$$\frac{\partial L}{\partial x^i} - \frac{d}{dt}\frac{\partial L}{\partial y^i} = 0, \quad y^i = \frac{dx^i}{dt}.$$

The Lagrange structure canonically defines a semispray vector field with the coefficients [61]

$$2G^i(x,y) = \frac{1}{2} g^{ij}\left(\frac{\partial^2 L}{\partial x^k \partial y^j} y^k - \frac{\partial L}{\partial x^j}\right),$$

and the nonlinear connection $N^i_j = \frac{\partial G^i}{\partial y^j}$. An N-linear connection compatible with the Lagrange metric can be defined analogously as for the Cartan N-linear connection of a Finsler structure.

1.4.2 The Synge-Beil structure

Due to the relation between classes of Finsler and GL structures, a whole class of GL-metrics can be obtained by deformations of Finsler metrics. One particular type of GL-metric, called the Beil metric, will be of the interest in the sequel. Beil proposed a metric applicable in unified field theory [29, 30], with the following components:

$$\widetilde{g}_{ij}(x,y) = g_{ij}(x,y) + c(x,y)B_i(x,y)B_j(x,y), \tag{1.37}$$

where g_{ij} is a Finslerian metric on a differentiable manifold, c is a smooth scalar function over the tangent space, and $B_i = g_{ik}B^k$ for B^k being a given d-vector field over the tangent space, see [35]. $\widetilde{g}_{ij}$ are components of a symmetric d-tensor field. For $c > 0$ the Beil metric is positive definite. By using the algebraic Lemma 1.3.7, one obtains the dual metric in an analogous form,

$$\widetilde{g}^{ij}(x,y) = g^{ij}(x,y) - \frac{c}{1+cB^2}B^i(x,y)B^j(x,y), \qquad B^2 = B_iB^i = g_{ij}B^iB^j, \tag{1.38}$$

and the determinant value

$$\det(\widetilde{g}_{ij}) = (1+cB^2)\det(g_{ij}). \tag{1.39}$$

The deformation (1.37) of a Riemannian metric $g_{ij}(x,y) = g_{ij}(x)$ produces the *Synge-Beil metric*, which is significant in geometric theory of relativistic optics ([13, 75]). The reducibility of Synge-Beil metrics is considered in [35] and depends on the function c and the tensor field (B^i). The simplest example of a Beil-type metric is obtained for the canonical vector field $B^i = y^i$,

$$\widetilde{g}_{ij}(x,y) = g_{ij}(x) + c(x,y)y_iy_j, \tag{1.40}$$

where $y_i = g_{ik}y^k$.

For a constant $a \in \mathbb{R}$ and $c(x,y) = a\left(||y||_g^2\right)^{-1} = a\left(g_{kh}y^ky^h\right)^{-1}$, one obtains the so called *normalized Miron metric*, or shortly *NM-metric*,

$$\widetilde{g}_{ij}(x,y) = g_{ij}(x) + \frac{a}{g_{kh}y^ky^h}y_iy_j. \tag{1.41}$$

The metric (1.41) on a 2-dimensional manifold is directionally homogeneous and nonreducible to Lagrange case. For the sake of completeness, we also provide the proof based on a more general theorem, see [35, 75].

1.4.3. Proposition *The metric structure (1.41) given on a 2-dimensional differentiable manifold is directionally 0-homogeneous and nonreducible to a Lagrange metric.*

Proof. The straightforward calculation verifies the homogeneity,

$$\widetilde{g}_{ij}(x,\lambda y) = g_{ij}(x) + \frac{a}{\lambda^2 g_{kh}y^ky^h}\lambda^2 y_iy_j = \widetilde{g}_{ij}(x,y).$$

Next, the total symmetry of the Cartan tensor has to be checked. The symmetry in the last two indices holds by the Definition 1.4.2, so $C_{ijk} = C_{kji}$ will be considered. But this is equivalent with

$$\frac{\partial\widetilde{g}_{ij}}{\partial y^k} = \frac{\partial\widetilde{g}_{kj}}{\partial y^i}.$$

Taking partial derivatives of (1.41), the total symmetry condition becomes

$$y^p g_{ip}g_{jk} = y^p g_{kp}g_{ji}.$$

Checking all 8 possibilities for the indices, one concludes that this equality holds if and only if $g_{12}g_{12} = g_{11}g_{22}$, which is in contradiction with the regularity of the Riemannian metric g. $\square$

In case that the metric d-tensor field is 0-homogeneous, we say that it is of generalized Finslerian type. An example is given by the normalized Miron metric (1.41).

1.5 Differential equations on differentiable manifolds

The theory of differential equations considered on differentiable manifolds has some constrains but also some specific properties. We present a concise description of the ODE and PDE theory on manifolds. The ODE theory is exposed in accordance with [32, 34, 65, 88, 109], while the particular case of the second order ODE follows [3, 35]. For the PDE theory approached by the geometrical point of view, we refer to [55, 95].

1.5.1 ODEs on manifolds

An autonomous ODE (a dynamical system) on an n-dimensional differentiable manifold M is given by a vector field $X \in \chi(M)$ (see Definition 1.1.5),

$$\dot{x} = X(x). \tag{1.42}$$

The solution of the Cauchy problem which consists of the differential equation (1.42) and the initial condition $x(0) = x_0$, is the integral curve c_{x_0} of the vector field X. The existence and the uniqueness of the solution of the Cauchy problem are basic issues of the ODE theory, (e.g. [32, 88, 109]). The integral curves are local solutions of (1.42). The following theorem ([65]) includes the essential facts on the integral curves ([34, 109]) and provides the global solution through the notion of flow.

1.5.1. Theorem *Let M be an n-dimensional manifold and X a vector field, $X \in \chi(M)$. Then:*

(1) Any point $x \in M$ is contained in a unique maximal integral curve of X, i.e.,

$$\exists!\; c_x : I_x = (t_1(x), t_2(x)) \to M,\; c_x(0) = x,$$

where $I_x \ni 0$ is the maximal domain of c_x.

(2) If $t_2(x) < \infty$ then the integral curve $c_x(t), t \to t_2(x)$, leaves every compact subset of M. (Similarly for $t_1(x) > -\infty$.)

(3) The set $W = \bigcup_{x \in M} I_x \times \{x\}$ is an open subset in $\mathbb{R} \times M$. The mapping

$$\varphi : W \to M, \qquad (t, x) \mapsto \varphi(t, x) = c_x(t) \tag{1.43}$$

is smooth and has the following properties:

(i) $\varphi_x(t) = \varphi(\cdot, x) : I_x \to M$ is the maximal integral curve at x, i.e., $\varphi_x(t) = c_x(t)$;

(ii) $\varphi(0, x) = x$, but also

$$\frac{d}{dt}\varphi(t, x)\Big|_{t=0} = X(x), \tag{1.44}$$

which means that the maximal integral curve $\varphi_x(t)$ passes through the point x in direction $X(x)$;

(iii) $\varphi_t(x) = \varphi(t, \cdot)$ is a local diffeomorphism on M and satisfies the semigroup property:

$$\varphi_t \circ \varphi_s = \varphi_{t+s}, \quad \forall s, t \in I_x \text{ such that } t + s \in I_x.$$

Definition 1.5.1. The *flow* of the vector field $X \in \chi(M)$ and of the corresponding differential equation (1.42) is the smooth map (1.43)

$$\varphi : W \to M, \qquad (t,x) \mapsto \varphi(t,x) = c_x(t), \qquad W = \bigcup_{x \in M} I_x \times \{x\} \subseteq \mathbb{R} \times M,$$

satisfying the properties $(i), (ii)$ and (iii) from Theorem 1.5.1.

The family of diffeomorphisms $\{\varphi_t\}$ is called one-parameter group of transformations induced by X. The image $\varphi\left(I_x \times \{x\}\right)$ is the orbit of x.

Theorem 1.5.1 shows that any vector field produces a flow. Conversely, one has that a given function $\varphi : W \to M, \quad \varphi = (\varphi^1, \ldots, \varphi^n)$, induces a vector field whose flow is the function itself, in the following way:

$$X(x) = f^i(x) \frac{\partial}{\partial x^i}\bigg|_x, \qquad f^i(x) = \frac{d\varphi_x^i}{dt}\bigg|_{t=0}. \tag{1.45}$$

The vector field X defined by (1.45) is called the infinitesimal generator of the flow φ.

From geometrical point of view the main benefit of considering ODE on manifolds is the following: the theory of existence and uniqueness of the solution for an autonomous ODE can be reconsidered over the whole manifold, emerging from local to global, by using concepts of vector fields, integral curves and flows.

In the sequel we shall consider second order ODEs, for which we refer to [35].

A system of second order ODE, denoted by SODE, given on a manifold M by

$$\frac{d^2 x^i}{dt^2} + 2G^i\left(x, \frac{dx}{dt}\right) = 0, \quad i = \overline{1,n}, \tag{1.46}$$

is defined over a local chart on the tangent bundle TM. The system (1.46) has to be compatible on the intersections of two local charts on the base manifold. More precisely, the left hand side of the above equation must be a d-tensor on TM, which is equivalent with the following transformation rule for the functions G^i under the coordinate change $x^i \mapsto \widetilde{x}^i(x^i)$ (see [35]):

$$2\widetilde{G^i} = \frac{\partial \widetilde{x}^i}{\partial x^j} 2G^j - \frac{\partial \widetilde{y}^i}{\partial x^j} y^j. \tag{1.47}$$

The functions G^i are assumed to be smooth enough on the slit tangent bundle $\widetilde{TM}$ and only continuous on the null section.

1.5.2 KCC theory and semispray geometry

The Kosambi-Cartan-Chern (KCC) theory of a SODE (1.46) deals with the geometric characteristics of the solutions - associated trajectories of the system. The KCC theory studies the deviation of closed trajectories, their stability, robustness and chaotic behavior. The aim is to find the geometric objects - called the invariants of the system (1.46) - which remain invariant under the regular coordinate transformation

$$\begin{cases} \widetilde{x}^i = & \widetilde{x}^i\left(x^1, \ldots, x^n\right), \quad i = \overline{1,n} \\ \widetilde{y}^i = & \dfrac{\partial \widetilde{x}^i}{\partial x^j} y^j, \quad i = \overline{1,n} \end{cases} \tag{1.48}$$

which is actually the transition map on TM. The invariants will be called the *KCC-invariants*. These are five d-tensors on the slit tangent bundle $\widetilde{TM}$, which describe the geometry of the SODE. More precisely, if two systems of type (1.46) have the same KCC-invariants, they can be locally transformed one into another. Particularly, if all five KCC-invariants vanish, there exist local coordinates where the trajectories of the system (1.46) are described by affine equations of first degree.

KCC theory is applicable in analyzing dynamical systems (see, e.g., [1, 33, 112]).

In order to find the KCC-invariants, one can define the covariant differential corresponding to the SODE (1.46) as follows ([3, 33, 18]): For a vector field $\xi = \xi^i(x)\frac{\partial}{\partial x^i} \in T_xM$, the KCC-covariant differential is defined on the open subset of $\mathbb{R}^n \times \mathbb{R}^n$ by

$$\frac{D\xi^i}{dt} = \frac{d\xi^i}{dt} + \frac{\partial G^i}{\partial y^j}\xi^j.$$

The KCC-covariant differential of y^i produces the invariant form of the system (1.46):

$$\frac{Dy^i}{dt} = -\varepsilon^i, \quad \text{where} \quad \varepsilon^i = 2G^i - \frac{\partial G^i}{\partial y^j}y^j. \tag{1.49}$$

We note that ε^i is a contravariant vector field on M (a d-tensor on $\widetilde{TM}$), called the *first KCC-invariant*, and representing an external force.

A variation of a solution of the SODE $c(t) = (x^i(t))$ can be given by

$$\overline{x}^i(t) = x^i(t) + \eta\xi^i(t), \quad 0 < \eta << 1. \tag{1.50}$$

Remark. Definition 1.3.5 gives a more general concept of curve variation, regardless of vector fields, but (1.50) is more appropriate to what follows.

By inserting (1.50) into (1.46), and letting $\eta \to 0$, we generate a local perturbation of the solution. Its infinitesimal change is described by a Jacobi vector field $\xi^i(t)$ satisfying the variational equation:

$$\frac{d^2\xi^i}{dt^2} + 2\frac{\partial G^i}{\partial y^j}\frac{d\xi^j}{dt} + \frac{\partial G^i}{\partial x^j}\xi^j = 0. \tag{1.51}$$

The following d-tensor field, called also Jacobi endomorphism,

$$B^i_j = 2\frac{\partial G^i}{\partial x^j} + 2G^l\frac{\partial^2 G^i}{\partial y^j \partial y^l} - \frac{\partial^2 G^i}{\partial y^j \partial x^l}y^l - \frac{\partial G^i}{\partial y^l}\frac{\partial G^l}{\partial y^j} \tag{1.52}$$

related to the KCC-covariant differential, enables to provide an invariant form of the variational equation (1.51):

$$\frac{D^2\xi^i}{dt^2} = B^i_j\xi^j. \tag{1.53}$$

The d-tensor B^i_j is the *second KCC-invariant* and it is related with the stability of solutions.

The *third KCC-invariant* is defined as follows:

$$B^i_{jk} = \frac{1}{3}\left(\frac{\partial B^i_j}{\partial y^k} - \frac{\partial B^i_k}{\partial y^j}\right), \tag{1.54}$$

and represents the field strength. An inflection of the field strength is also an invariant, the *fourth KCC-invariant*

$$B^i_{jkl} = \frac{\partial B^i_{jk}}{\partial y^l}. \tag{1.55}$$

The last invariant, the *fifth KCC-invariant* is related with the interaction in the system (it gives account of the chaotic behavior), and has the form

$$D^i_{jkl} = \frac{\partial^3 G^i}{\partial y^j \partial y^k \partial y^l}. \tag{1.56}$$

The KCC-theory in full detail can be found in [3].

1.5.2. Theorem *Two SODEs of form (1.46) defined on the same domain can locally be transformed one into another by a transition map, if and only if their five invariants ε^i, B^i_j, B^i_{jk}, B^i_{jkl} and D^i_{jkl} are equivalent tensors. In particular, there are local coordinates for which $G^i(x,\dot{x}) = 0$ if and only if all five KCC-tensors vanish.*

The functions G^i which change via (1.47) under (1.48), globally define semispray vector field ([35]):

1.5.3. Proposition *Let the functions $G^i(x,y)$ be defined on domains of all induced local charts on TM, and let $S \in \chi(TM)$ be a vector field of the form*

$$S = y^i \frac{\partial}{\partial x^i} - 2G^i(x,y)\frac{\partial}{\partial y^i}. \tag{1.57}$$

Then S is a semispray, $JS = C$, and the following two statements are equivalent:

(a) The vector field S is globally defined.

(b) Under the coordinate change (1.48), the functions G^i transform by the rule (1.47).

The functions $G^i(x,y)$ are called the *local coefficients of the semispray*.

A smooth curve on the base manifold, $c : I \to M, \quad t \mapsto c(t) = (x^i(t))$, which is a solution of (1.46) is called a *path of the semispray* (1.57), while its complete lift $\widehat{c} : I \to TM, \quad t \mapsto \widehat{c}(t) = \left(x^i(t), \frac{dx^i}{dt}\right)$ is an integral curve of the corresponding semispray vector field given by (1.57).

If the semispray is determined by a SODE, then global properties of the SODE are related to the semispray geometry: the nonlinear connection induced by the semispray can be assigned to the SODE (1.46) in such a way that the corresponding autoparallel curves of the connection and the solutions of the SODE coincide. Furthermore, the nonlinear connection produces five invariants of the semispray. More details on the subject can be found in [35].

A nonlinear connection (1.7) induced by the semispray has the following local coefficients

$$N^i_j = \frac{\partial G^i}{\partial y^j}. \tag{1.58}$$

Remark. Conversely, any symmetric nonlinear connection N^i_j induces a semispray with local coefficients $2G^i(x,y) = N^i_j(x,y)y^j$. This correspondence is one-to-one only under the additional conditions of homogeneity of the local coefficients.

With respect to the induced nonlinear connection N^i_j (1.58) and to the adjusted Berwald basis (1.8), the semispray can be expressed as

$$S = y^i \frac{\delta}{\delta x^i} - \varepsilon^i \frac{\partial}{\partial y^i}, \tag{1.59}$$

where

$$\varepsilon^i(x,y) = 2G^i(x,y) - N^i_j(x,y)y^j. \tag{1.60}$$

The scalar functions ε^i are components of a contravariant $d-$vector field called the *deviation tensor* of the semispray. It coincides with the first KCC-invariant (1.49).

A semispray determines through the induced nonlinear connection a

$$\nabla X^i = S(X^i) + N^i_j X^j, \tag{1.61}$$

and it maps vertical d-vector fields[2] of $\widetilde{TM}$, $\nabla : \chi^v(TM) \to \chi^v(TM)$,

$$\nabla\left(X^i(x,y)\frac{\partial}{\partial y^i}\right) = \nabla X^i \frac{\partial}{\partial y^i}; \qquad \nabla X^i = \frac{\partial X^i}{\partial x^j}y^j - \frac{\partial X^i}{\partial y^j}N^j_k y^k + N^i_j X^j. \tag{1.62}$$

Further, by the composition with the vertical lift $\chi(M) \to \chi^v(TM)$, $X^i\frac{\partial}{\partial x^i} \mapsto X^i\frac{\partial}{\partial y^i}$, the dynamical covariant derivative defines a map (also called the dynamical derivative) $\nabla : \chi(M) \to \chi^v(TM)$, given by

$$\nabla\left(X^i\frac{\partial}{\partial x^i}\right) = \nabla X^i \frac{\partial}{\partial y^i}$$

.

The dynamical covariant derivative provides the equivalent invariant form of the SODE,

$$\nabla\left(\frac{dx^i}{dt}\right) = -\varepsilon^i\left(x, \frac{dx^i}{dt}\right), \tag{1.63}$$

the same as the (1.49), expressed by the KCC-covariant differential and using the same ε^i.

1.5.4. Theorem *The variational equations of a path of the semispray (1.57) can be expressed by means of the dynamical covariant derivative as*

$$\nabla^2\xi^i + P^i_j\xi^j = 0. \tag{1.64}$$

The equation (1.64) is also a necessary and sufficient condition for a vector field $(\xi^i(t))$ given along the path of the semispray to be a Jacobi vector field.

Proof. ([35]) Since the path is also the solution of SODE, its variation is (1.50). The substitution of the varying solution (1.50) into (1.46), by considering $\eta \to 0$ yields

$$\frac{d\xi^2}{dt^2} + 2\frac{\partial G^i}{\partial y^j}\frac{d\xi^j}{dt} + 2\frac{\partial G^i}{\partial x^j}\xi^j = 0.$$

By the use of the dynamical covariant derivative (1.62) in order to calculate $\nabla^2\xi^i$ and denoting

$$P^i_j = R^i_{jk}y^k + \frac{\delta\varepsilon^i}{\delta x^j} + \frac{\partial^2 G^i}{\partial y^j \partial y^k}\varepsilon^k, \tag{1.65}$$

the variational equation gets the expected form (1.51). □

A vector field ξ^i which gives a variational equation is called a *Jacobi* vector field and (1.51) its defining condition, hence it is called *Jacobi equation.* The $(1,1)$-type tensor field

[2] We denote by $\chi^v(TM)$ the set of all vertical vector fields on TM.

P^i_j defined by (1.65) is called the *deviation curvature tensor*, it is the second invariant of the semispray and coincides with the second KCC-invariant (1.53).

The geometric object R^i_{jk} appearing in the above formula is called the third semispray invariant, but it actually is just the curvature (1.10) of the nonlinear connection N_S induced by the semispray (1.58).

The two remaining invariants of the SODE are provided by the Berwald N_S-linear connection, which now has its components arising from the nonlinear connection induced by the semispray,

$$B\Gamma_S = \left(F^i_{jk} = \frac{\partial^2 G^i}{\partial y^j \partial y^k},\ C^i_{jk} = 0 \right). \tag{1.66}$$

The curvature tensor of the Berwald connection yields the last two semispray invariants throughout its nonvanishing components, namely

$$R^i_{hjk} = \frac{\delta F^i_{hj}}{\delta x^k} - \frac{\delta F^i_{hk}}{\delta x^j} + F^m_{hj} F^i_{mk} - F^m_{hk} F^i_{mj}; \qquad P^i_{hjk} = \frac{\partial F^i_{hj}}{\partial y^k}.$$

The fourth semispray invariant is R^i_{hjk}, *the Riemann-Cristoffel curvature* of the Berwald linear connection and the fifth one is P^i_{hjk}, the *hv-curvature* of the Berwald linear connection, which coincides with the so called the *Douglas tensor* of the nonlinear connection,

$$D^i_{hjk} = \frac{\partial^2 N^i_h}{\partial y^j \partial y^k},$$

and obviously is the same as the fifth KCC-invariant (1.56).

It is proved in [3, 35] that all the five invariants of the semispray coincide with the corresponding KCC-ones.

1.5.3 PDEs on manifolds

A partial differential equation (PDE) in $\mathbb{R}^n$ of order k has the following general form:

$$\phi \left(x, u, \frac{\partial u}{\partial x^i}, \frac{\partial^2 u}{\partial x^i \partial x^j}, \ldots, \frac{\partial^k u}{\partial x^{i_1} \ldots \partial x^{i_k}} \right) = 0,$$

where $x = (x^1, \ldots, x^n)$ is a point of an open domain in $\mathbb{R}^n$. This PDE implicitly defines a scalar function $u = u(x)$. It is not always possible to solve PDE explicitly, i.e., to find a classical solution, but rather a weak (or distributional) solution. The questions of the existence and of the uniqueness of solutions are among the main problems in the theory of PDEs (cf. [49, 50]).

The theory of PDEs on manifolds means additional complexity. A PDE on a manifold must have its solutions on the manifold, too. In other words, the PDE should be defined in a coordinate independent way. It is possible to consider PDEs in a jet bundle [11, 96], analogously as a SODE (1.46) in TTM. In that way, the PDE on the manifold is related with a distribution over the manifold (in the corresponding jet bundle), and the solvability of the PDE is reflected by the integrability of the distribution, and further by its involutivity [66].

Our interest will be in PDEs derived from the variational problem that minimizes the energy E. Generally, a PDE is formulated as

$$\operatorname{argmin}_{\Sigma}\{E(X)\}, \tag{1.67}$$

where Σ is a submanifold - the image of a mapping X from an open domain in $\mathbb{R}^n$ to a differentiable manifold, E is a global scalar feature on Σ (usually an energy), and *argmin* gives a submanifold at which E is minimized. The integral of the PDE given by (1.67) will be a submanifold where the energy is extremal ($E' = 0$). In general, the solutions are not analytic, and cannot be obtained directly. One of the nonvariational techniques, useful in image processing, is the descent flow technique. This is a minimization process that evolves the geometric active object related to a digital image [55, 95].

One can consider the PDE

$$\frac{\partial X}{\partial t} = -E'(X) \tag{1.68}$$

with the unknown function $X = X(x,t)$, coupled with the initial condition $X(x,0) = X(x) =: X_0$. With respect to the parameter t, (1.68) is an ODE, and the steady state is necessary for the energy extremal,

$$\frac{\partial X}{\partial t} = 0 \quad \Rightarrow \quad E'(X) = 0.$$

The auxiliary variable t can be seen as a time (or scale) parameter, and $X = X(x,t)$ can be seen as a flow of the PDE. Actually, for the initial mapping $X_0 = X : (x^1, \ldots, x^n) \to \left(X^1(x^1, \ldots, x^n), \ldots, X^m(x^1, \ldots, x^n)\right)$ and the initial produced submanifold $\Sigma_0 = \Sigma$, the PDE (1.68) defines an one-parameter family of mappings

$$X_t : (x^1, \ldots, x^n) \to \left(X_t^1(x^1, \ldots, x^n, t), \ldots, X_t^m(x^1, \ldots, x^n, t)\right), \tag{1.69}$$

and the corresponding family of submanifolds Σ_t (called layers in image processing). This process of deforming the initial map is also called the evolution of the submanifold.

Let us resume: when the integral submanifold of (1.67) cannot be obtained, one can start with the initial submanifold and evolve it during the time by the descent flow (1.68).

Theoretical background, as well as constrains of the flow technique, are comprehensively presented in [49, 50].

1.6 Frameworks for dynamical systems

A dynamical system is defined by a system of second order ordinary differential equations, or equivalently, by a second order vector field on a manifold representing a set of all possible states of the dynamical system.

1.6.1 Dynamical systems on a differentiable manifold

Preliminary concepts and definitions

The understanding of a real phenomenon includes the proper understanding and descriptions of its possible states, parameters which affect the outcome and its changes over time. Time dependency of a process is called an evolution and it is closely related to the notion of dynamical system.

Definition 1.6.1. A *dynamical system* is a semigroup G acting on a space M, as follows:

$$T : G \times M \to M, \quad (g,x) \mapsto T_g(x) := T(g,x), \quad T_g \circ T_h = T_{g \circ h}.$$

This definition is of general type (see [109]), and we are interested in the particular case of continuous dynamical systems, where M is an n-dimensional differentiable manifold, usually called *configuration space* or *state space* with the elements $x \in M$ representing all the possible states of the system, and the semigroup G, also called the time domain, the real additive semigroup $G = \mathbb{R}^+$ or even the group $G = \mathbb{R}$ (in the second case the system is said to be reversible). The action of G on M leads to the changes of the states during time $\dot{x} = \dfrac{dx}{dt}$. The action is given by a mapping called the flow.

We shall additionally assume the following:

1. the phenomenon represented by a dynamical system is deterministic in past and future;

2. dynamical systems are autonomous: the evolution rule does not explicitly depend on time. For any two values $t, t_0 \in \mathbb{R}$, (with $t > 0$), from the time domain, an effect of the evolution over the time interval $[t_0, t_0 + t]$ does not depend on t_0, but only on t;

3. dynamical systems are nonconservative: for any external force influencing the system, the work of the force along some path depends not only on the end points, but also on the path itself.

Such a dynamical system describes a process in the configuration space M that is evolving in time. The rule of change is defined by a system of ODE on M, called *the evolution equation*:

$$\dot{x} = f(x),$$

where the same notation x will be used for the coordinate representation $x = (x^i),\ i = \overline{1,n}$ of a point in M and for the point itself, $x \in M$. This is a usual ODE (where $f = (f^1, f^2, \ldots, f^n) : M \to \mathbb{R}^n$ is assumed to be smooth enough on M), but it originates from a dynamical system. The local behavior is represented by a Cauchy problem consisting of the evolution equation and the initial state $x(0) = x_0$.

The evolution equation can also be regarded as a smooth vector field $X_f \in \chi(M)$, which can be decomposed in terms of the tangent frame

$$X_f = f^i \frac{\partial}{\partial x^i}. \tag{1.70}$$

Hence, the solution is called a trajectory or an integral curve of the dynamical system.

Assigning the maximal integral curve to a point produces the flow (1.43) which defines the dynamical system T, and which determines the action of the group $G = \mathbb{R}$ on the configuration space M [109]. More precisely, the flow associated to a given vector field is a local group with a parameter, which acts on an open set, and whose action is induced by the field after getting the maximal solution of the SODE.

According to the above assumptions and notions, we introduce an adjusted definition of dynamical system.

Definition 1.6.2. A *dynamical system* is a pair (M, X), where M is a finite dimensional differentiable manifold, and X is a global vector field on M defining the evolution by

$$\dot{x} = X(x). \tag{1.71}$$

Remark. According to the relations (1.43) and (1.44), another equivalent definition of the autonomous dynamical system can be given by a manifold and a flow function (M, φ).

The nature of a given dynamical system (1.71) is locally determined by the function $f = (f^1, \ldots, f^n)$, which defines the components of the vector field on a given chart, $X = f^i \frac{\partial}{\partial x^i}$.

The theory of linear dynamical systems has exact analyzing and solving procedures (cf. [58, 88, 92, 109]), and the integration of the system gives a general solution and trajectories corresponding to initial conditions. On the other hand, the theory of nonlinear dynamical systems is complex, because real phenomena often exhibit nonlinear characteristics and their integral curves are generally not given by classical, analytical functions, but rather by transcendental ones. Therefore, a qualitative study of these solutions is necessary including critical points and poles, bifurcations of the system, chaotical behavior and stability of solutions (cf. [88, 92, 109]). The study of nonlinear dynamical systems mainly consists of qualitative, analytical and numerical methods. The qualitative study of a dynamical system focuses on the critical points: fixed points, poles and other singularities by considering their nature in the configuration space. Further, it explains the dependence of the system evolution on the varying parameters (bifurcation theory), and its chaotical behavior - sensitivity on the initial conditions. The (local) stability at a point and global stability are also a part of the qualitative study (cf. [92, 109]).

Definition 1.6.3. A point $x_0 \in M$ is called a *fixed point* of the dynamical system (M, X) if $X(x_0) = 0$. Otherwise, x_0 is a *regular* point (assuming that f is bounded).

In a certain neighborhood of a given regular point, the vector field can be locally straightened. Moreover, away from the fixed point the tangent vectors from the vector field $X_f(x)$ can be locally uniformed as shown in the following lemma ([109]).

1.6.1. Lemma *For $X_f(x) \neq 0$ there exists a local transition map on M, such that $\widetilde{x} = \phi(x)$ transforms the dynamical system (1.71) into*

$$\dot{\widetilde{x}} = (1, 0, \ldots, 0), \quad \widetilde{x}(0) = \widetilde{x}_0.$$

A nonlinear system can be linearly approximated near certain fixed points, which makes the theory of linear dynamical systems applicable, but not completely accurate. For example, the stability of the linearized system is called linear stability of the original nonlinear dynamical system [33].

Definition 1.6.4. A fixed point x_0 of the dynamical system (M, X) is *(Lyapunov) stable*, if for any neighborhood U of x_0 there exists another neighborhood of x_0, $V \subset U$, such that any integral curve starting at $x \in V$ remains in U for $t \in I_x \cap [0, \infty)$.

A fixed point x_0 is said to be asymptotically stable if it is stable and all the integral curves converge to x_0.

A fixed point which is not stable is called *unstable*.

Lyapunov stability along the whole trajectory is related with its perturbation (1.50) by a Jacobi vector field ξ^i (1.51).

1.6.2. Theorem *The trajectories of (1.71) are Jacobi stable if and only if the real parts of the eigenvalues of the deviation tensor P^i_j (1.65) are strictly negative everywhere. An analogous statement holds truth for the second KCC-invariant B^i_j (1.53).*

The proof of this theorem and more details on the subject can be found in [1, 3, 33].

The global stability of a dynamical system (M, X) is not an intrinsic property, but involves environmental characteristics [89]. A family of (semi)norms in the ambient space will enable a measurement of perturbations of the integral curves. This is an additional motivation to introduce Finsler manifolds, which we present in the following.

Dynamics of Lagrange mechanical systems

In general, a dynamical system my arise from a mechanical system and determine its evolution, see,e.g., [35, 109]. One can describe a mechanical system as a triple (M, E, σ) where M is a configuration space, E is an energy function - a globally defined scalar characteristic of the system - and σ is an external force action that can be described by one tensor field of the first order.

If the external force (and hence, the system) is autonomous and nonconservative, the most of dynamical systems model the mechanical system are of the Lagrange type.[3]

Definition 1.6.5. A nonconservative mechanical system is a triple $\Sigma_L = (M, E, \sigma)$, where (M, L) is a Lagrange space, E is the energy related to the Lagrangian by (1.36) and σ is a vertical vector field $\sigma = \sigma^i(x, y)\frac{\partial}{\partial y^i} \in \chi(TM)$ or a covertical 1-form, which means $\sigma(\frac{\partial}{\partial y^i}) = 0,\ i = \overline{1, n}$, or equivalently $\sigma = \sigma_i(x, y)dx^i \in \Lambda(TM)$.

Remark. An external force σ can act on the system influencing its scalar or vector properties regarding its nature. Nonconservativity is reflected in the dependency of $\sigma^i(x, y)$ on direction y. There exists a natural mapping $\sigma_i = g_{ij}\sigma^j$, which can change the character of the external force.

In general, any system tends to the state of its minimal energy, and therefore the evolution equation of the system arises from the Euler-Lagrange variational equation,

$$\frac{d}{dt}\left(\frac{\partial E}{\partial y^i}\right) - \frac{\partial E}{\partial x^i} = 0, \tag{1.72}$$

whose integral curves are geodesics.

Remark. In the absence of the homogeneity property, besides energy minimization, we shall separately consider Lagrangian minimization.

Any kind of an external force demands reaction. Therefore, the evolution equations arise from the following one

$$\frac{d}{dt}\left(\frac{\partial E}{\partial y^i}\right) - \frac{\partial E}{\partial x^i} = \sigma_i(x, y), \quad y^i = \frac{dx^i}{dt}. \tag{1.73}$$

1.6.3. Theorem *The evolution equations (1.73) of the Lagrange mechanical system Σ_L with the energy* (1.36)*, have the equivalent form*

$$\frac{d^2x^i}{dt^2} + 2G^i_{DS}\left(x, \frac{dx}{dt}\right) = 0, \quad 2G^i_{DS}(x, y) = \frac{1}{2}g^{is}\left(\frac{\partial^2 L}{\partial y^s \partial x^j}y^j - \frac{\partial L}{\partial x^s}\right) - \frac{1}{2}\sigma^i \tag{1.74}$$

[3]Considerations that follow in this section are mostly based on [35, 75].

Proof. The left-hand side of the Euler-Lagrange equation (1.73) can be calculated

$$\frac{d}{dt}\left(\frac{\partial L}{\partial y^i}\right)-\frac{\partial L}{\partial x^i}=\frac{\partial^2 L}{\partial x^j\partial y^i}\frac{dx^j}{dt}+\frac{\partial^2 L}{\partial y^j\partial y^i}\frac{dy^j}{dt}-\frac{\partial L}{\partial x^i}=\frac{\partial^2 L}{\partial x^j\partial y^i}y^j+2g_{ji}\frac{d^2x^j}{dt^2}-\frac{\partial L}{\partial x^i}.$$

Then, substitution into (1.73) and multiplication by $\frac{1}{2}g^{is}$, where the regularity of L ensures the existence of the inverse of g_{ji} defined by (1.35), leads to

$$\frac{d^2x^s}{dt^2}+\frac{1}{2}g^{is}\left(\frac{\partial^2 L}{\partial x^j\partial y^i}y^j-\frac{\partial L}{\partial x^i}\right)=\frac{1}{2}\sigma^s,$$

and the statement follows by renaming the indices. □

This theorem allows the Lagrangian variational theory to become applicable to dynamical systems.

The dynamics of the system Σ_L is determined by the evolution equation (1.74), which is locally given on $\widetilde{TM}$ by the SODE of evolution (1.74), and is equivalent with the first order ODE system

$$\begin{cases}\dot{x}=y\\ \dot{y}=-2G^i_{DS}(x,y),\end{cases}$$

and globally, by a vector field on TM, the semispray (1.57)

$$S_{DS}(x,y)=y^i\frac{\partial}{\partial x^i}\bigg|_{(x,y)}-2\,G^i_{DS}(x,y)\frac{\partial}{\partial y^i}\bigg|_{(x,y)}.$$

1.6.2 Finslerian framework for dynamical systems

Proposition 1.3.5 shows that the variational problem on a Finsler manifold is represented by the SODE (1.26), that further produces a semispray by Proposition 1.5.3. Homogeneity of the fundamental function and the relation (1.27) result the 2-homogeneity of the semispray S_F, hence it is called a *spray.* The spray related to the geodesic equations (1.26) in a Finsler manifold is called *geodesic spray*

$$S_F(x,y)=y^i\frac{\partial}{\partial x^i}-2G^i_F(x,y)\frac{\partial}{\partial y^i}.$$

The geodesic spray S_F of the Finsler manifold is a vector field on TM, and it is an element of $\Gamma(TTM)$. Because of homogeneity, it mutually induces the nonlinear connection N_{S_F} (1.58), that is, the canonical nonlinear connection of the Finsler manifold, also called the *Cartan nonlinear connection*:

$$(N_{S_F})^i_j=\frac{\partial G^i_F}{\partial y^j}.$$

This further produces the Whitney decomposition (1.6), and there exist four special, intensively studied, N_{S_F}-linear connections in TTM of the Finsler manifold [27, 35, 40]. One of them is the Berwald connection $B\Gamma_{S_F}$ (1.66) which plays an essential role in defining the KCC invariants of the Finsler structure [5, 35, 18]. This connection is responsible for the Jacobi stability of the second order associated geodesic system, measuring the "distance" of the Finslerian paths to the flat affine behavior of straight paths.

If the configuration space of a dynamical system is supplemented with an appropriate Finsler structure, then all five invariants can be expressed in terms of the fundamental function and all trajectories become geodesic curves.

Chapter 2

Example of the fitting Finslerian structures for a dynamical system

The previously exposed theory on the relationship between dynamical systems and Finsler structures was the motivation for the following statistical fitting process, in which a Finsler fundamental function is numerically interpolated, by the least squared method, over a configuration space of a dynamical system. The same technique was used in [10], where a Finsler structure supporting the HARDI analysis of medical images is constructed.

In this chapter, the Garner dynamical system of cancer cell population will be presented as well as the procedure of fitting appropriate Finsler structures. We shall determine, by statistical fitting, three Finsler norms over a certain 2-dimensional subdomain related to the model,of the Randers, Euclidean and 4-th root type, $F_R, F_E, F_Q : TM \to [0, \infty)$. The proposed Finsler functions will provide point-independent norms, which means that they are of locally Minkowski type, i.e., $F_R(x, y) = F_R(y)$, $F_E(x, y) = F_E(y)$ and $F_Q(x, y) = F_Q(y)$. In that way, many geometric objects related to the chosen structures considerably simplify: the geodesics are (pieces of) straight lines, the KCC invariants vanish, the Berwald linear connection is trivial [5, 35]. Each of the structures respectively provides the corresponding Finsler metric tensor fields: g_R, g_E and g_Q. Considering the metrics as elements of appropriate Hilbert space we can analyze their properties and the way these metrics relate.

For convenience, we shall use the following notations in this chapter:

- the elements of the manifold that represent the configuration space of the dynamical system will be denoted by (x, y),
- the elements of the corresponding tangent bundle will be denoted by $(x, y, \dot{x}, \dot{y})$.

Actually, the configuration space of the dynamical system is a subspace of $\mathbb{R}^2$ and only one, trivial, chart is enough to consider. Tangent vectors represent changes of he current state of the dynamical system.

This chapter contains original results published in [23, 24].

2.1 The Garner cancer cell population dynamical system

It is a known fact that the subpopulations of abnormal cells responsible for the cancer disease contain the so called *cancer stem cells* (CSCs), [91]. In this context, it is very important

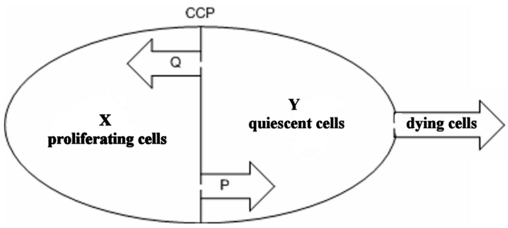

Figure 2.1: Transitions between cell classes in the Solyanik and Garner cancer evolution models

to describe changes in the cancer population, which contains three types of cells, [51, 68]: proliferating, quiescent (resting) and dead ones, their abundance being determinant in the prognostic of the cancerous disease.

The evolution of the cancer cells population was firstly modeled in 1995 by means of Solyanik's dynamical system, which is based on the following assumptions: cancer population consists of proliferating and quiescent cells, proliferating cells can lose the division feature and transit to the quiescent ones, and quiescent cells can become proliferating or die. The states of Solyanik's model were described by the amount $\tilde{x}$ of proliferating cells and the amount $\tilde{y}$ of quiescent cells, which satisfy the differential system

$$\begin{cases} \dot{\tilde{x}} = b\tilde{x} - P\tilde{x} + Q\tilde{y} \\ \dot{\tilde{y}} = -d\tilde{y} + P\tilde{x} - Q\tilde{y}, \end{cases}$$

where

- b is the rate of cell division of the proliferating cells;
- d is the rate of cell death of the quiescent cells;
- Q and P describe the intensity of cell transition from the quiescent to proliferating cells and converse,

with all the involved parameters reconsidered on a daily basis (see Fig. 2.1). Solyanik's model [106] was further improved by Garner et al. in [53] by regarding the parameters P, Q as dependent on $\tilde{x}$ and $\tilde{y}$, via $P = c(\tilde{x} + a\tilde{y})$ and $Q = \bar{A}\tilde{x}/(1 + \bar{B}\tilde{x}^2)$, where

- a measures the relative nutrient uptake by resting vs. proliferating cancerous cells;
- c gives the magnitude of the rate of cell transition from the proliferating to the resting state;
- $\bar{A}$ is the initial rate of Q increase at small $\tilde{x}$;
- $\bar{A}/\bar{B}$ is the rate of Q decrease for large $\tilde{x}$.

The Garner model describes the evolution of the scaled cell populations $x = \frac{c}{b}\tilde{x}$, $y = \frac{ca}{b}\tilde{y}$ by means of the dynamical system:

$$\begin{cases} \dot{x} = x - x(x+y) + \dfrac{hxy}{1+kx^2} \\ \dot{y} = -ry + ax(x+y) - \dfrac{hxy}{1+kx^2}, \end{cases} \tag{2.1}$$

where

- $r = d/b$ is the ratio between the death rate of quiescent cells and the birth rate of proliferating cells;
- $h = \bar{A}/(ac)$ represents a growth factor that preferentially shifts cells from quiescent to proliferating state;
- $k = \bar{B} \cdot (b/c)^2$ represents a mild moderating effect.

The associated nullclines, equilibrium points, the appropriate versal deformation and the static bifurcation diagram of the Garner's system were studied in [19, 20].

The set of all possible states of the GS is a bounded subset D of the first quadrant in $\mathbb{R}^2$,

$$K_+ = \{p = (x, y) \mid x > 0, y > 0\},$$

which contains the information on the scaled amount of proliferating and of quiescent cells.

We shall further consider the Garner dynamical system for the case of the fixed parameters ([53])

$$a = 1.998958904 \quad \text{and} \quad r = 0.03. \tag{A1}$$

The reduced Garner system

We observe that the original Garner dynamical system (2.1) - denoted further as GS - is the extended version of the reduced dynamical system (denoted as RS)[1]:

$$\begin{cases} \dot{x} = x - x(x + y) \\ \dot{y} = -ry + ax(x + y). \end{cases} \tag{2.2}$$

In the original system GS, for h being significant one notices a malignant evolution of the illness; this happens when:

- the parameter a significantly decreases, becoming negligible (i.e., there is a small ratio of nutrient uptake of resting vs. proliferating cells, which shows that the resources are absorbed mostly by the proliferating cells in detriment of quiescent cells);
- the parameter c is negligible (i.e., the rate of cell transition from cancerous to the resting state is negligible, hence the evolution of the disease is either stationary, or worsening);
- the parameter $\bar{A}$ significantly increases (the rate of increase of Q is abruptly big at small x, i.e., the cell transition from the quiescent to cancerous cells is intense).

When these conditions are far from being achieved (this might happen, e.g., under treatment, which may significantly modify the intake of nutrient ratio in disfavor of cancerous cells), the GS (2.1) can be approximated by RS (2.2).

We will assume that under mild (controlled) evolution of the disease (for $0 \leq |h| << 1$), the RS system (2.2) reasonably approximates the original system (2.1).

The change rate of cancer cell populations under changes of premises

The RS (2.2) attaches to any point $p = (x, y) \in D$ its related velocity $\dot{p} = (\dot{x}, \dot{y}) \in T_{(x,y)}(K_+)$ (see Fig. 2.2). Due to the polynomial form of its associated vector field, RS provides a reverse

[1]This happens when in the GS system (2.2) the constant $h = \bar{A}/(ac)$ is negligible ($0 < |h| \ll 1$), or vanishes.

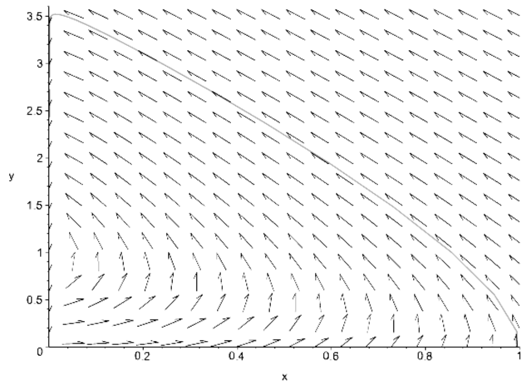

Figure 2.2: The field lines of the reduced Garner model RS, for $a = 1.998958904$ and $r = 0.03$.

association $\dot{p} = (\dot{x}, \dot{y}) \rightsquigarrow p(x, y)$, by solving the nonlinear algebraic system (2.2) in terms of $p = (x, y)$ for given $\dot{p} = (\dot{x}, \dot{y})$, but only in certain regions of K_+ and only for certain values of the parameters r, h, k,

We choose the domain D of the Finsler norm F as a set of tangent vectors, where $D = \varphi(I_\rho \times I_\theta) \subset T_p K_+$, with $I_\rho \times I_\theta = [0.329915, 0.888939] \times [1.0988, 1.51452] \subset [0, \infty) \times [0, 2\pi)$ and φ is the mapping which changes polar coordinates to Cartesian ones,

$$\varphi : [0, \infty) \times [0, 2\pi) \to \mathbb{R}^2, \quad \varphi(\rho, \theta) = (\rho \cos\theta, \rho \sin\theta).$$

Under an appropriate choice of I_1 and I_2, one can uniquely solve the quadratic system (2.2) in terms of $p = (x, y)$, with P located on a field line from K_+, with related tangent direction of the emerging velocity $\dot{p} \in D$.

By using the inverse function theorem for the feasible directions of the reduced dynamical system, one may solve the pair of algebraic nonlinear equations of the system, to locally find the associated point p.

The status of the cancerous disease changes from mild to severe status due to a multitude of factors which corresponds to a change of parameters in the GS Garner system (2.1).

Such a case occurs when h becomes significant; this transforms RS into GS and then (2.1) associates to the solutions p from the nonlinear system, the new rates of change $\dot{p}_e = (\dot{x}_e, \dot{x}_e)$ valid for the new circumstances of the illness. Namely, the point coordinates $p = (x, y)$ determined under mild conditions (by the inverse of the RS), plugging in (2.1), produce the new change rate $\dot{p}_e$ of the cancer cell populations (see Fig. 2.3).

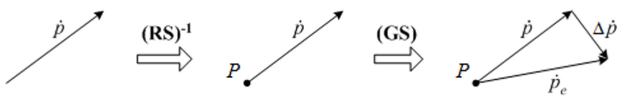

Figure 2.3: The transition $\dot{p} \rightsquigarrow \dot{p}_e$ between the RS and the GS change rates.

2.2 Statistical fitting of Finsler norms

The Euclidean norm $||\dot{p_e}||_E$ of the obtained rate-vector $\dot{p}_e = (\dot{x}_e, \dot{y}_e)$ can be used to evaluate the severeness of the disease evolution. This choice, however, has the drawback of being symmetric in the two components of $\dot{p}_e$, especially in the case $\dot{x} > 0$, since equal credit is given to the two rates of the increase.

One alternative choice is to design a tool which emphasizes the cancer cell population increase, by means of a *Finsler norm*, which is likely to emphasize a tuned fair evaluation of the illness evolution.

To this aim we note that $||\dot{p_e}||$ can provide a locally Minkowski (i.e., depending on directional variables only) Finsler norms $F_R(\dot{x}, \dot{y})$, $F_E(\dot{x}, \dot{y})$ and $F_Q(\dot{x}, \dot{y})$ by statistical fitting[2]. The proposed approximation, which provides the fit of the Finsler norm F is given by:

$$F(\dot{x}, \dot{y}) \sim ||\dot{p_e}||_E, \tag{2.3}$$

where $\|\cdot\|_E$ is the Euclidean norm. We note that the triangle inequality for norms shows that the rate-jump entailed by the change of status $RS \to GS$ due to the increase of $|h|$, does not exceed $||\dot{p_e} - \dot{p}||_E$.

We shall consider the following choices which follow the main requirements of a Finsler norm, and which are fundamental functions of locally Minkowski type[3]:

$$\begin{aligned} F_R(\dot{x}, \dot{y}) &= \sqrt{\dot{x}^2 + \dot{y}^2} + b_1\dot{x} + b_2\dot{y} && (2.4)\\ F_E(\dot{x}, \dot{y}) &= \sqrt{c_1\dot{x}^2 + c_2\dot{x}\dot{y} + c_3\dot{y}^2} && (2.5)\\ F_Q(\dot{x}, \dot{y}) &= \sqrt[4]{a(\dot{x})^4 + b(\dot{x})^3(\dot{y}) + c(\dot{x})^2(\dot{y})^2 + d(\dot{x})(\dot{y})^3 + e(\dot{y})^4} && (2.6) \end{aligned}$$

where $b_{1,2}$ and $c_{1,2,3}$ and $(a, b, c, d, e) = (q_1, q_2, q_3, q_4, q_5)$ are coefficients to be evaluated by statistic fitting. In our research, we use the values assumed in $(A1)$ for the systems RS (2.2) and GS (2.1). For the statistical fitting of $F(\dot{p})$ from (2.3) to $||\dot{p_e}||$, where $\dot{p} = (\dot{x}, \dot{y})$, and $p = (x, y)$, $\dot{p_e} = (\dot{x}_e, \dot{y}_e)$ are respectively obtained by tracing the process described in Fig. 2.3, we use for the Randers, Euclidean and 4-th root cases the following equalities ($k \in \overline{1, N}$)

$$\begin{aligned} &b_1\dot{x}_k + b_2\dot{y}_k = \sqrt{(\dot{x}_e)_k^2 + (\dot{y}_e)_k^2} - \sqrt{\dot{x}_k^2 + \dot{y}_k^2}, && (2.7)\\ &c_1\dot{x}_k^2 + c_2\dot{x}_k\dot{y}_k + c_3\dot{y}_k^2 = (\dot{x}_e)_k^2 + (\dot{y}_e)_k^2, && (2.8)\\ &a(\dot{x})_k^4 + b(\dot{x})_k^3(\dot{y})_k + c(\dot{x})_k^2(\dot{y})_k^2 + d(\dot{x})_k(\dot{y})_k^3 + e(\dot{y})_k^4 = \left((\dot{x}_e)_k^2 + (\dot{y}_e)_k^2\right)^2, && (2.9) \end{aligned}$$

which allows us to determine the statistical fit for the values $b_{1,2}$, $c_{1,2,3}$ and a, b, c, d, e by the method of least squares.

For finding $\dot{p}_e$ from $\dot{p}$ via RS and further GS, we use in (2.1) the parameter values ([19, 53]):

$$h = 1.236 \text{ and } k = 0.236. \tag{A2}$$

[2]Generally, when considering one of the three structures, we shall simply write $F(\dot{x}, \dot{y})$

[3]For brevity, we denote $(a, b, c, d, e) := (q_1, q_2, q_3, q_4, q_5)$.

The constructing process of the measuring Finslerian tool is presented in the following scheme:

$$\begin{tikzcd}
 & D \arrow[rr, "||\cdot||_F"] \arrow[dl, shift left, "\pi_1"] \arrow[dr, shift left, "\pi_2"] & & \mathbb{R} & \\
K_1 \arrow[ur, shift left, "\sigma_1 = X_R|_{K_1}"] \arrow[dr, hook] & & K_2 \arrow[ul, shift left, "\sigma_2"] \arrow[rr, "X_G"'] \arrow[dl, hook] & & V \arrow[ul, "||\cdot||_E"'] \\
 & K & & &
\end{tikzcd}$$

The field lines of the reduced system (2.2) yield a vector subset D of the tangent space TK_+, containing related feasible directions $\dot{p} \in T_pK_+$. By using the theorem of inverse function, the polynomial form of the reduced system RS (2.2) enables a reverse association $\dot{p} = (\dot{x}, \dot{y}) \rightsquigarrow p = (x, y)$, given by the second of the possible reverse mappings σ_1 and σ_2. Precisely, the second degree of the polynomials yields two p-domains, the subsets $K_{1,2} \subset K_+$, of which we choose just one in the statistical fitting.

Further, by using the Garner vector field X_G, corresponding to (2.1), we associate to the detected point $p = (x, y)$ (and hence, to the initial vector $\dot{p} \in D$), the corresponding shifted vector $\dot{p}_e \in V$.

The discretization is achieved by a grid spanned over the coordinates of the feasible directions over the p-domain K_2 and V:

$$\begin{tikzcd}
Gr(D) \arrow[r, "||\cdot||_F"] \arrow[d, "\pi_2"'] & \mathbb{R} \\
Gr(K_2) \arrow[r, "\sigma"'] & Gr(V) \arrow[u, "||\cdot||_E"']
\end{tikzcd}$$

The grid defines a discrete sample volume N, and leads to the approximation problem

$$||\dot{p}||_F = ||\dot{p}_e||_E,$$

which produces the system of linear equations in the unknown parameters of the Finsler structure. The influence of the grid dense on the fitting process is considered in [26].

We note that the uniform grid over the domain of the feasible directions provides the needed inputs for the fitting process. Maple computation produces the corresponding polar (ρ, θ)-domain of the field lines of the Garner system,

$$I_\rho \times I_\theta = [0.329915, 0.888939] \times [1.0988, 1.51452],$$

a grid with $N = (n_\rho + 1)(n_\theta + 1)$ knots

$$(\rho_i, \theta_j) \in I_\rho \times I_\theta, \; (i, j) \in \overline{0, n_\rho} \times \overline{0, n_\theta}.$$

The Cartesian domain of the feasible directions is $\varphi(I_\rho \times I_\theta) = I_1 \times I_2 = [0.05, 0.1596] \times [0.293844, 0.887532]$, and the used grid consists of scaled spherical harmonics regarded as tangent vectors

$$\dot{p}_k = (\dot{x}_k, \dot{y}_k) = (\rho_i \cos\theta_j, \rho_i \cos\theta_j) \in D = I_1 \times I_2, \quad k \in \overline{1, N}$$

where $k = (i - 1)n_\rho + j \in \overline{1, N}$.

Let us resume: the right hand side of the RS (2.2) contains quadratic polynomials, and that for given input $\dot{p} = \dot{p}_1$, $(RS)^{-1}$ provides a twofold point-solution, p', p'', of which one solution p_1 is chosen. For each next plugged-in scaled spherical harmonic $\dot{p}_{k+1}$, RS similarly provides two other point-solutions, and the right choice p_{k+1} is determined by both the non-negativity of its components and by the Euclidean proximity to the previous selected point p_k $(k \in \overline{1, N-1})$.

Finally, one gets the set of points $p_k = (x_k, y_k)$ and (via GS) the corresponding change rates $(\dot{p_e})_k$, $k \in \overline{1, N}$, which are further plugged in (2.7)-(2.9). The N samples $\dot{p}_k$ and the new rates $(\dot{p_e})_k$ $(k = \overline{1, N})$, plugged in the N relations from (2.7)-(2.9), provide in each case N linear equations with parameters as unknowns - which fix the Finsler function (2.4)-(2.6).

2.2.1 The Randers fitting

The system (2.7) is linear relative to b_1 and b_2, over-determined ($N >> 2$), and has the form $AS = B$, where $A = (\dot{x}_k, \dot{y}_k)_{k=\overline{1,N}} \in M_{N\times 2}(\mathbb{R})$, $S = (b_1, b_2)^t \in M_{2\times 1}(\mathbb{R})$ is the the unknown vector, and $B \in M_{N\times 1}(\mathbb{R})$ is given by the r.h.s. of (2.7) for $k = \overline{1, N}$. Computer Maple 17 simulation for $N = 36$, provides by the least square method the pseudosolution $(b_1, b_2)^t = (A^t A)^{-1} A^t B$, and under the assumptions $(A1)$ and $(A2)$, the exact fit-values of the parameters are

$$b_1 \approx .628481987778205518, \quad b_2 \approx -.269476980932055964. \tag{2.10}$$

Hence the fit Randers structure related to the dynamical system of the Garner cancer cells population model (2.1) becomes (for the obtained (2.10) fit values of the parameters)

$$F_R(\dot{x}, \dot{y}) \approx \sqrt{\dot{x}^2 + \dot{y}^2} + 0.63 \cdot \dot{x} - 0.27 \cdot \dot{y} \tag{2.11}$$

where the dot marks denote time derivatives, which describe the rates of increase for the scaled cancer cell populations[4].

2.2.2 The Euclidean fitting

For the Euclidean case, for fixing the Finsler function (2.5), the same N samples $\dot{p}_k$ and new rates $(\dot{p_e})_k$ $(k = \overline{1, N})$, are plugged in the N relations (2.8). The obtained system is linear in terms of c_1, c_2 and c_3, superdetermined ($N >> 3$), and has the form $AS = B$, where $A \in M_{N\times 3}(\mathbb{R})$, $S \in M_{3\times 1}(\mathbb{R})$, and $B \in M_{N\times 1}(\mathbb{R})$, with the unknown vector $S = (c_1, c_2, c_3)^t$. Analogous computer simulation provides the parameter solutions

$$\begin{cases} c_1 \approx 0.940805450748692151 \\ c_2 \approx 1.16189809024084268 \\ c_3 \approx 0.496069555231253400, \end{cases}$$

hence the fit Euclidean type fundamental function of the structure related to (2.1) is

$$F_E(\dot{x}, \dot{y}) \approx \sqrt{0.94\dot{x}^2 + 1.16\dot{x}\dot{y} + 0.50\dot{y}^2}. \tag{2.12}$$

[4] For display convenience, truncated values of the coefficients have been used, in this, but also in the next two structures

2.2.3 The 4-th root fitting

The 4-th root type Finsler function (2.6) (the third case) is determined by use of the same method as in the previous two cases with the differences: $A \in M_{N\times 5}(\mathbb{R})$, $S \in M_{5\times 1}(\mathbb{R})$, and $S = (a, b, c, d, e)^t$. The same computer simulation provides the parameter solutions[5]:

$$\begin{array}{ll} a \approx -0.320013354328217758; & b \approx 2.69642032805366582; \\ c \approx 2.42492765757201711; & d \approx 1.07381846633249766; \\ e \approx 0.254991915496320776, & \end{array} \tag{2.13}$$

hence the fit 4-th root Finsler fundamental function locally related to the GS (2.1) is

$$F_Q(\dot{x}, \dot{y}) \approx \sqrt[4]{-0.32\dot{x}^4 + 2.70\dot{x}^3\dot{y} + 2.42\dot{x}^2\dot{y}^2 + 1.07\dot{x}\dot{y}^3 + 0.25\dot{y}^4}. \tag{2.14}$$

2.3 The properties of the constructed Finsler metric structures

The constructed Finsler norms produce corresponding metrics g_R, g_E and g_Q, belonging to the Hilbert space of bounded and continuous d-tensor fields of the $(0, 2)$-type [35, 76]. Further, the Cartan tensors of the constructed structures are elements of the analogous Hilbert space of the $(0, 3)$-type. Hence, for the comparisons of the constructed metrics we need a metrical structure is the Hilbert spaces.

The scalar product which provides the Hilbert structure generally acts on a pair of two $(0, m)$-tensors $\mathcal{A}$ and $\mathcal{B}$ by means of the formula:

$$\langle \mathcal{A}, \mathcal{B} \rangle_g = \mathcal{A}_{i_1 \dots i_m} g^{i_1 j_1} \dots g^{i_m j_m} \mathcal{B}_{i_1 \dots i_m}.$$

This naturally induces the norm, the *projection* of $\mathcal{A}$ onto $\mathcal{B}$, and the *angle* between the two tensors as follows:

$$||\mathcal{A}||_g = \sqrt{\langle \mathcal{A}, \mathcal{A} \rangle}, \quad pr_{\mathcal{B}}\mathcal{A} = \frac{\langle \mathcal{A}, \mathcal{B} \rangle}{\langle \mathcal{B}, \mathcal{B} \rangle}\mathcal{B}, \quad \sphericalangle(\mathcal{A}, \mathcal{B}) = \arccos \frac{\langle \mathcal{A}, \mathcal{B} \rangle}{||\mathcal{A}|| \cdot ||\mathcal{B}||}.$$

The statistically fitted metrics are denoted by g_R, g_E and g_Q. We shall analyze the way these structures relate by examining their Cartan tensors, and by estimating their shift from the associated conformally Euclidean projection.

Except for the Euclidean case, where the Cartan tensor is identically zero, the Randers and the 4-th root cases provide a nontrivial Cartan tensor, whose squared *Frobenius norm* is a direction-dependent scalar function provided by the transvection[6]:

$$||C||_g^2 = C_{ijk} g^{ir} g^{js} g^{kt} C_{rst}.$$

The metric tensor fields are represented by square matrices A and B respectively, and for $g_{ij} = \delta_{ij}$ (i.e. Finsler space of Euclidean type), we have

$$\langle A, B \rangle_\delta = Trace(A \cdot B^t), \tag{2.15}$$

where $(\ )^t$ is the transposition operator.

[5]For brevity, we denote $(a, b, c, d, e) := (q_1, q_2, q_3, q_4, q_5)$.

[6]In [40] is presented an alternative of norm for the Cartan tensor, which results in a numerical value.

2.3.1. Proposition *The following assertions hold*[7]*:*

(1) The Finsler metric produced by (2.4) has the following conformally Euclidean projection

$$pr_\delta g_R = \frac{1}{2}\left(2 + \frac{3(b_1\dot{x} + b_2\dot{y})}{\sqrt{\dot{x}^2 + \dot{y}^2}} + b_1^2 + b_2^2\right)\delta. \tag{2.16}$$

(2) The Finsler metric produced by (2.5) has constant conformally Euclidean factor, i.e., conformally flat projection is

$$pr_\delta g_E = \frac{1}{2}(c_1 + c_3)\delta. \tag{2.17}$$

(3) The Finsler metric produced by (2.6) has the following conformally Euclidean projection

$$pr_\delta g_Q = \frac{p}{16F_Q^6}\delta, \tag{2.18}$$

where p is the following polynomial in the components of the tangent vector $y = (y^1, y^2) = (\dot{x}, \dot{y})$:

$$\begin{aligned} p = \; & (8q_1^2 + 4q_1q_3 - q_2^2)\dot{x}^6 + (12q_1q_4 + 12q_1q_2)\dot{x}^5\dot{y} \\ & +(12q_1q_3 + 6q_2q_4 + 24q_1q_5 + 3q_2^2)\dot{x}^4\dot{y}^2 \\ & +(16q_1q_4 + 4q_2q_3 + 16q_2q_5 + 4q_3q_4)\dot{x}^3\dot{y}^3 \\ & +(12q_3q_5 + 3q_4^2 + 24q_1q_5 + 6q_2q_4)\dot{x}^2\dot{y}^4 \\ & +(12q_4q_5 + 12q_2q_5)\dot{x}\dot{y}^5 + (4q_3q_5 + 8q_5^2 - q_4^2)\dot{y}^6. \end{aligned}$$

Proof. A straightforward calculation produces the components of Finsler metric tensor fields in the all three cases:

$$\begin{cases} g_{R11} = -\dfrac{\beta}{\alpha^3}\dot{x}^2 + \dfrac{2}{\alpha}b_1\dot{x} + \dfrac{F}{\alpha} + b_1^2, \\ g_{R12} = -\dfrac{\beta}{\alpha^3}\dot{x}\dot{y} + \dfrac{b_2}{\alpha}\dot{x} + \dfrac{b_1}{\alpha}\dot{y} + b_1b_2, \\ g_{R22} = -\dfrac{\beta}{\alpha^3}\dot{y}^2 + \dfrac{2}{\alpha}b_2\dot{y} + \dfrac{F}{\alpha} + b_2^2; \end{cases} \tag{2.19}$$

$$g_{E11} = c_1, \quad g_{E12} = \tfrac{1}{2}c_2, \quad g_{E22} = c_3;$$

[7] Hereby we denote by δ the canonic metric for the Euclidean 2-dimensional case, and use the notation $y = (y^1, y^2) = (\dot{x}, \dot{y})$.

$$\begin{cases} g_{Q11} = & \frac{1}{8F^6}\left(8q_1^2\dot{x}^6 + 12q_1q_2\dot{x}^5\dot{y} + (3q_2^2 + 12q_1q_3)\dot{x}^4\dot{y}^2\right. \\ & +(4q_2q_3 + 16q_1q_4)\dot{x}^3\dot{y}^3 + (24q_1q_5 + 6q_2q_4)\dot{x}^2\dot{y}^4 \\ & \left.+12q_2q_5\dot{x}\dot{y}^5 + (4q_3q_5 - q_4^2)\dot{y}^6\right) \\ g_{Q12} = & \frac{1}{8F^6}\left(2q_1q_2\dot{x}^6 + 3q_2^2\dot{x}^5\dot{y} + 6(q_2q_3 - q_1q_4)\dot{x}^4\dot{y}^2\right. \\ & \left.+(2q_2q_4 + 4q_3^2 - 16q_1q_5)\dot{x}^3\dot{y}^3 + 6(q_3q_4 - q_2q_5)\dot{x}^2\dot{y}^4 + 3q_4^2\dot{x}\dot{y}^5 + 2q_4q_5\dot{y}^6\right) \\ g_{Q22} = & \frac{1}{8F^6}\left((4q_1q_3 - q_2^2)\dot{x}^6 + 12q_1q_4\dot{x}^5\dot{y} + (24q_1q_5 + 6q_2q_4)\dot{x}^4\dot{y}^2\right. \\ & \left.+(16q_2q_5 + 4q_3q_4)\dot{x}^3\dot{y}^3 + (12q_3q_5 + 3q_4^2)\dot{x}^2\dot{y}^4 + 12q_4q_5\dot{x}\dot{y}^5 + 8q_5^2\dot{y}^6\right). \end{cases}$$

The inner product (2.15) of g and δ reduces to the trace and $\langle\delta,\delta\rangle = 2$, hence summation $\frac{1}{2}(g_{11}+g_{22})$ gives the conformal factors in (2.16), (2.17) and (2.18). □

2.3.2. Proposition *In the Hilbert space of $(0,2)$-type Finsler tensors, the following deviation angles occur:*

(1) The Finsler-Randers metric produced by (2.4) deviates from its conformally Euclidean approximation by the angle

$$\theta_R = \arccos\sqrt{\frac{1}{2} + \frac{(A+1)(A^2-4A+1)}{(2+3A+B)^2 - 2(A+1)(A^2-4A+1)}}, \tag{2.20}$$

where the following abbreviations are used: $A = (b_1\dot{x} + b_2\dot{y})/\sqrt{\dot{x}^2+\dot{y}^2}$ and $B = b_1^2 + b_2^2$.

(2) The Finsler metric produced by (2.5) and its conformally flat approximation determine the constant deviation angle

$$\theta_E = \arccos\frac{c_1 + c_3}{\sqrt{2c_1^2 + c_2^2 + 2c_3^2}}.$$

(3) The deviation function expressing the angle between the Finsler metric produced by (2.6) and its conformally Euclidean approximation is

$$\theta_Q = \arccos\frac{p}{\sqrt{2s}}, \tag{2.21}$$

where p is the polynomial from (2.3.1), and s is the following polynomial in $\dot{x}, \dot{y}$:

$$s = \pi + \sigma(\pi)$$

with

$$\begin{aligned}
\pi = \; & \Big(64q_1^4 + 8q_1^2q_2^2 - 8q_1q_2^2q_3 + 16q_1^2q_3^2 + q_2^4\Big)\dot{x}^{12} \\
& +\Big(192q_1^3q_2 + 96q_1^2q_3q_4 - 24q_1q_2^2q_4 + 24q_1q_2^3\Big)\dot{x}^{11}\dot{y} \\
& +\Big(192q_1^3q_3 + +192q_1^2q_2^2 + 144q_1^2q_4^2 - 48q_1^2q_2q_4 + 192q_1^2q_3q_5 \\
& \quad +48q_1q_2q_3q_4 + 48q_1q_2^2q_3 - 48q_1q_2^2q_5 - 12q_2^3q_4 + 18q_2^4\Big)\dot{x}^{10}\dot{y}^2 \\
& +\Big(256q_1^3q_4 + 352q_1^2q_2q_3 - 128q_1^2q_2q_5 + 576q_1^2q_4q_5 + 128q_1q_2q_3q_5 \\
& \quad -56q_1q_2^2q_4 + 32q_1q_2q_3^2 + 144q_1q_2q_4^2 - 8q_2^2q_4q_3 \\
& \quad +32q_1q_4q_3^2 + 72q_1q_2^3 + 72q_2^3q_3 - 32q_2^3q_5\Big)\dot{x}^9\dot{y}^3 \\
& +\Big(384q_1^3q_5 + 144q_1^2q_3^2 + 72q_1^2q_4^2 + 576q_1^2q_5^2 + 480q_1^2q_2q_4 - 96q_1q_2q_4q_3 \\
& \quad +672q_1q_2q_4q_5 + 168q_1q_2^2q_3 + 96q_1q_3^2q_5 + 120q_1q_3q_4^2 \\
& \quad +30q_2^2q_4^2 - 240q_1q_2^2q_5 - 24q_2^2q_3q_5 + 120q_2^2q_3^2 + 24q_2^3q_4 + 9q_2^4\Big)\dot{x}^8\dot{y}^4 \\
& +\Big(768q_1^2q_2q_5 + 384q_1^2q_3q_4 + 384q_1^2q_4q_5 - 96q_1q_3^2q_4 + 768q_1q_2q_5^2 - 384q_1q_2q_3q_5 \\
& \quad +576q_1q_3q_4q_5 + 48q_2q_3q_4^2 - 72q_2^3q_5 + 168q_2^2q_4q_5 + 120q_2^2q_3q_4 + 240q_1q_2^2q_4 \\
& \quad -24q_1q_2q_4^2 + 96q_1q_2q_3^2 + 72q_1q_4^3 + 24q_2^3q_3 + 96q_2q_3^3\Big)\dot{x}^7\dot{y}^5 \\
& +\Big(512q_1^2q_5^2 + 640q_1^2q_3q_5 + 272q_1q_2q_3q_4 + 32q_1q_2q_4q_5 + 272q_2q_3q_4q_5 \\
& \quad +432q_1q_2^2q_5 - 144q_1q_3q_4^2 - 144q_2^2q_3q_5 - 256q_1q_3^2q_5 + 432q_1q_4^2q_5 + 44q_2^2q_4^2 \\
& \quad +640q_1q_3q_5^2 + 176q_2q_3^2q_4 + 240q_1^2q_4^2 + 16q_2^2q_3^2 \\
& \quad +16q_3^2q_4^2 + 240q_2^2q_5^2 + 36q_2^3q_4 + 36q_2q_4^3 + 32q_3^4\Big)\dot{x}^6\dot{y}^6 \cdot \frac{1}{2},
\end{aligned}$$

and $\sigma(\pi)$ produced from π after interchanging $(q_1, q_2, q_3, q_4, q_5, \dot{x}, \dot{y}) \leftrightarrow (q_5, q_4, q_3, q_2, q_1, \dot{y}, \dot{x})$.

Proof. Let f be the conformal Euclidean factor of the projection in the equations (2.16)-(2.18), and let $\theta = \sphericalangle(g, pr_\delta g)$ be the angle between the corresponding metric and its projection to δ. Then, due to the homogeneity of the inner product, we infer:

$$\cos\theta = \frac{\langle g, f\delta\rangle}{\sqrt{\langle g, g\rangle}\sqrt{f^2\langle\delta,\delta\rangle}} = \mathrm{sign}(f)\cdot\frac{\langle g,\delta\rangle}{\sqrt{\langle g, g\rangle}\sqrt{\langle\delta,\delta\rangle}} = \mathrm{sign}(f)\cdot\cos\sphericalangle(g,\delta).$$

By use of (2.15), we have the following expressions[8]

$$\cos\theta = \frac{g_{11} + g_{22}}{\sqrt{2(g_{11}^2 + 2g_{12}^2 + g_{22}^2)}}, \qquad \sphericalangle(g,\delta) = \arccos\sqrt{\frac{(g_{11}+g_{22})^2}{2(g_{11}^2 + 2g_{12}^2 + g_{22}^2)}}. \tag{2.22}$$

By plugging into (2.22) the appropriate metric components, one gets (2.20)-(2.21). □

Moreover, by plugging in the fitted coefficients of the three structures into the appropriate equations from Propositions 2.3.1 and 2.3.2 one infers the characterization of each type structure.

[8]We shall further consider the absolute value of the factor, reducing thus the angle to the first quadrant.

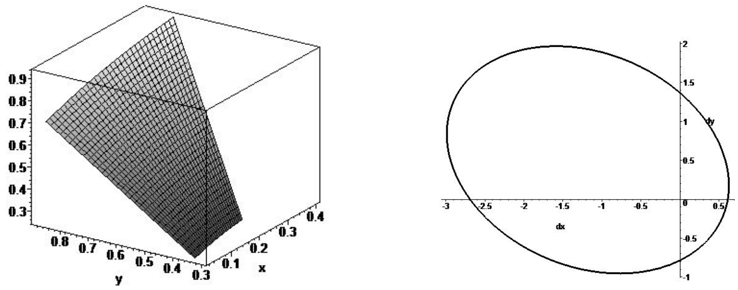

Figure 2.4: Plot of the squared locally Minkowski Finsler Randers norm $z = F^2(\dot{x}, \dot{y})$ and of the indicatrix $F(\dot{x}, \dot{y}) = 1$

2.3.1 The Randers type structure

The Randers metric g_R arised from the fitted structure (2.11) has the following norm[9]

$$||g_R|| \approx \sqrt{\frac{(-0.22\dot{x}^3 + 0.60\dot{x}^2\dot{y} + 0.97\alpha\dot{x}^2 - 1.02\alpha\dot{x}\dot{y} + 5.28\alpha^2\dot{x} - 2.34\alpha^2\dot{y} + 4.32\alpha^3}{\alpha^3}} \qquad (2.23)$$

with respect to the standard Hilbert structure (2.15).

2.3.3. Corollary *The conformally Euclidean projection of the metric produced by the Randers type Finsler structure (2.11) is*

$$pr_\delta g_R \approx \left(\frac{0.945\dot{x} - 0.405\dot{y}}{\sqrt{\dot{x}^2 + \dot{y}^2}} + 1.235 \right) \delta,$$

and the deviation between these two metrics is given by

$$\theta_R \approx \arccos \frac{1.89\alpha\dot{x} - 0.81\alpha\dot{y} + 2.47\alpha^2}{\sqrt{r}},$$

where $\alpha = \sqrt{\dot{x}^2 + \dot{y}^2}$ *and*

$$r = -4.68\alpha^3\dot{y} + 1.20\alpha\dot{x}^2\dot{y} - 0.44\alpha\dot{x}^3 + 10.56\alpha^3\dot{x} + 8.64\alpha^4 + 1.94\alpha^2\dot{x}^2 - 2.04\alpha^2\dot{x}\dot{y}.$$

The graphical representation of the values of the Finsler-Randers norm along the z-axis in terms of the inputs $(\dot{x}, \dot{y}) \in D = [0.05, 0.1596] \times [0.293844, 0.887532]$, and of the Finsler indicatrix are provided in Fig. 2.4. These clearly exhibit convexity and compactness the Randers indicatrix of (2.11).

By Maple symbolic programming one can easily test that the signature of the metric g is $(+, +)$, hence (D, F) with $D \subset K_+$ is a Randers geometric structure of locally-Minkowski type [76]. To illustrate the signature of the point-independent metric tensor g, one can see that, within a fiber of $T_{\dot{p}}\mathbb{R}^2$, its associated quadratic form[10]

$$Q^g_y(v) = g_{ij}|_y \, v^i v^j, \quad v = (v^i, v^j) \in \mathbb{R}^2 \equiv T_{\dot{p}}\mathbb{R}^2$$

[9]The "$\approx$" symbol expresses the truncation of numeric coefficients in the r.h.s. expressions.

[10]The quadratic form Q acts on the vertical fibre of velocities provided by the identification $T_{\dot{p}}\mathbb{R}^2 \equiv \mathbb{R}^2$, assuming the flagpole fixed, $\dot{p} = (.2, 1)$.

has its graph an elliptic paraboloid patch (see Fig. 2.5), which gives account of the positive signature of g, signalled by the inequality $||b||^2 \equiv b_1^2 + b_2^2 \approx (.63)^2 + (-.27)^2 < 1$.

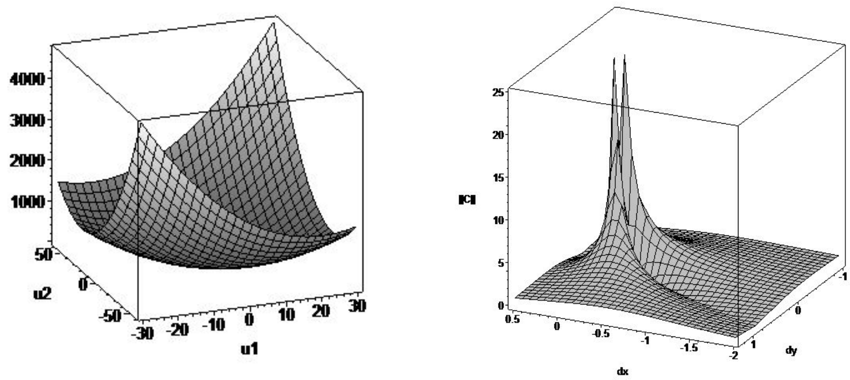

Figure 2.5: Graphs of the quadratic form $Q^g_{\mathbf{y}}$ and of $Q^C_{\mathbf{y}} = ||C||^2_{\mathbf{y}}$ for $\dot{p} \in [-1, 0.5] \times [-0.5, 1]$.

We note as well that the Cartan tensor (1.3.4) measures the "distance" between the constructed Finslerian F norm and the space of flat Euclidean-type norms. The distance can be locally estimated in terms of $\mathbf{y} = (y^1, y^2) = (\dot{x}, \dot{y})$ by the square of the Frobenius norm $Q^C_{\mathbf{y}} = ||C||^2_{\mathbf{y}}$ (see Fig. 2.5), where

$$||C||_y = \sqrt{C_{ijk} g^{ir} g^{js} g^{kt} C_{rst}}.$$

The plot of the energy $Q^C_{\mathbf{y}}$ of C_{ijk} emphasizes a special region inside $[-1, 0.5] \times [-0.5, 1]$, at which the difference between the fitted Randers norm and the canonic Euclidean norm significantly matter. This region (a small neighborhood of the origin) corresponds to slight variations of the cancer cell population, while for strong variations the Randers structure asymptotically approaches the canonic Euclidean one.

Regarding the Randers structure, it is remarkable that for $||b||_g < 1$, which is our case, one has (g_{ij}) positive definite, and there exists a vertical non-holonomic frame

$$\mathcal{F}_H = \left\{ X_j \;\middle|\; X_j = X^i_j \frac{\partial}{\partial y^i}, \;\; j = \overline{1,2} \right\},$$

called *the Holland frame* of the Randers structure [35],

$$X^i_j = \sqrt{\frac{\alpha}{F}} \left(\delta^i_j - \frac{y^i(\alpha_j + b_j)}{F} + \sqrt{\frac{\alpha}{F}} \cdot \frac{y^i \alpha_j}{\alpha} \right), \;\; j = \overline{1,2},$$

in which the Randers metric tensor field g_{ij} becomes the α-subjacent Riemannian one and $\alpha_i = \frac{\partial \alpha}{\partial y^i} = \frac{y^i}{\alpha}$. In this respect, we get the following results:

2.3.4. Proposition *The following assertions hold true:*
a) The associated Finsler metric tensor field $g = g_{ij}(\dot{p})dx^i \otimes dx^j$ of the Randers structure F_R has the components

$$g_{ij}(y) = \frac{\alpha+\beta}{\alpha}\left(\delta_{ij} - \frac{y^i y^j}{\alpha^2}\right) + \frac{y^i y^j + \alpha(b_i y^j + b_j y^i) + b_i b_j \alpha^2}{\alpha^2}, \tag{2.24}$$

where $(y^1, y^2) = (\dot{x}, \dot{y})$, $b_1 \approx 0.63, b_2 \approx -0.27$ and [11]

$$\alpha = \sqrt{\delta_{ij} y^i y^j} = \sqrt{\dot{x}^2 + \dot{y}^2}, \quad \beta = b_i y^i = b_1 \dot{x} + b_2 \dot{y}.$$

b) For the Finsler structure (2.4)*, the components of the fields of the Holland frame are given by:*

$$X^i_j = \frac{\alpha F \delta^i_j - y^i(y^j + \alpha b_j)}{\sqrt{\alpha F^3}} + \frac{y^i y^j}{\alpha F}, \quad j = \overline{1,2}.$$

Proof. a) By direct computation, one subsequently obtains:

$$\begin{aligned} g_{ij}(y) &= \frac{F}{\alpha}(\delta_{ij} - \alpha_i \alpha_j) + (\alpha_i + b_i)(\alpha_j + b_j) \\ &= \frac{\alpha+\beta}{\alpha}\left(\delta_{ij} - \tfrac{1}{\alpha^2} y^i y^j\right) + \left(\tfrac{y^i}{\alpha} + b_i\right)\left(\tfrac{y^j}{\alpha} + b_j\right), \end{aligned}$$

whence the result (2.24) follows. For b), one notices that using the definition of the Holland frame [35] and, by performing the calculations for our locally-Minkowski particular norm, one infers the claimed result. □

2.3.2 The Euclidean structure

The fitted Euclidean structure yields constant components of the corresponding Finslerian metric tensor,

$$g_{E11} = 0.94, \quad g_{E12} = 0.58, \quad g_{E22} = 0.50,$$

and with respect to the standard Hilbert structure (2.15), the metric has norm

$$||g_E|| = 1.34. \tag{2.25}$$

The Euclidean case δ is canonic, hence the corresponding equations from the Propositions 2.3.1 and 2.3.2 produce the constant conformally flat factor and the constant deviation angle,

$$pr_\delta g_E \approx 0.72\delta, \quad \theta_E \approx 0.71.$$

2.3.3 The 4-th root type structure

For the 4-th root Finsler metric, the substitution of the fit truncated parameters (2.13) into the corresponding equations of the Propositions 2.3.1 and 2.3.2 produce the following

[11]For display convenience, truncated values of the coefficients have been used, of the more accurate statistically determined values $b_1 = .628481987778205518 \cdot r \cdot cos(t)$ and $b_2 = -.269476980932055964 \cdot r \cdot sin(t)$.

2.3.5. Corollary *The conformally Euclidean projection of the metric produced by the 4-root type Finsler structure (2.14) and the deviation angle between the metric and its δ-projection respectively are*

$$pr_\delta g = \frac{1}{16F_Q^6} p\ \delta, \quad \theta_Q = \arccos\frac{p}{\sqrt{2s}},$$

where

$$\begin{cases} p \approx 9.61\dot{x}^6 + 14.93\dot{x}^5\dot{y} - 27.64\dot{x}^4\dot{y}^2 - 41.64\dot{x}^3\dot{y}^3 - 26.05\dot{x}^2\dot{y}^4 - 11.31\dot{x}\dot{y}^5 - 1.78\dot{y}^6, \\ s \approx \ +1.83\dot{x}^{12} - 1.34\dot{x}^{11}\dot{y} + 7.72\dot{x}^{10}\dot{y}^2 + 40.57\dot{x}^9\dot{y}^3 + 87.11\dot{x}^8\dot{y}^4 \\ \quad +104.79\dot{x}^7\dot{y}^5 + 84.73\dot{x}^6\dot{y}^6 + 52.57\dot{x}^5\dot{y}^7 + 25.57\dot{x}^4\dot{y}^8 \\ \quad +9.59\dot{x}^3\dot{y}^9 + 2.72\dot{x}^2\dot{y}^{10} + 0.49\dot{x}\dot{y}^{11} + 0.04\dot{y}^{12}. \end{cases}$$

The parameters of both type structures, F_R and F_Q have similar graphs, though the structures strongly differ, and the indicatrix of F_Q is non-convex. As well, the nature of F_Q causes

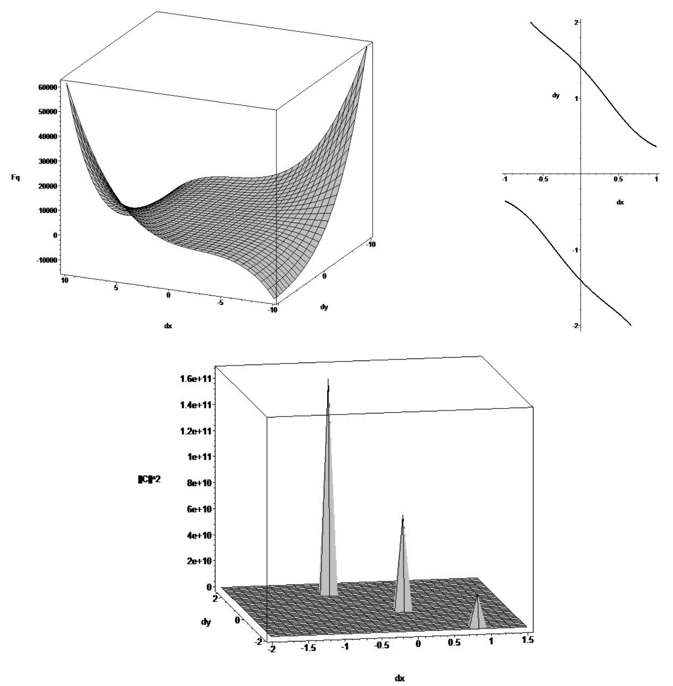

Figure 2.6: Graph of the energy $z = F^2(\dot{x}, \dot{y})$, indicatrix $F_Q(\dot{x}, \dot{y}) = 1$ and squared Cartan norm $z = Q^C_{\mathbf{y}}$ of the 4-th root Finsler structure.

much stronger dependency of the metric tensor on the directional argument, particularly in the neighborhood of $(0, 0)$ (see Fig. 2.6).

2.3.4 Comparison of the Randers and the Euclidean structures

Beside projections of the fitted structures onto the canonical Euclidean one, in [24] is developed the projection of the fitted Randers structure onto the fitted Euclidean one and the deviation angle between them.

2.3.6. Corollary

a) The projection of the metric tensor g_R associated to (2.11) onto the metric tensor g_E associated to (2.12) is

$$pr_{g_E} g_R = \frac{1}{\alpha^3}\left(-0.33\dot{x}^2 - 0.34\dot{x}^2\dot{y} + 0.98\alpha^2\dot{x} + 0.11\alpha^2\dot{y} + 0.91\alpha^3\right) g_E.$$

b) The deviation function expressing the angle between the Finsler metrics g_R and g_E is

$$\theta_{RE} = \arccos\left(\frac{-0.44\dot{x}^3 - 0.45\dot{x}^2\dot{y} + 1.32\alpha^2\dot{x} + 0.15\alpha^2\dot{y} + 1.23\alpha^3}{\alpha^{\frac{3}{2}}\sqrt{p}}\right),$$

where $\quad p = \begin{array}{l} -0.22\dot{x}^3 + 0.60\dot{x}^2\dot{y} + 0.97\alpha\dot{x}^2 - 1.02\alpha\dot{x}\dot{y} + 5.28\alpha^2\dot{x} \\ -2.34\alpha^2\dot{y} + 4.32\alpha^3. \end{array}$

Proof. *a*) The scalar product of the two metric tensors is

$$\langle g_R, g_E\rangle = 0.94 g_{R11} + 2\cdot 0.58 g_{R12} + 0.50 g_{R22},$$

and the squared norm of g_E is

$$\langle g_E, g_E\rangle = 1.8064 \approx 1.81.$$

By using the exact values of the Randers metric tensor components (2.19) and the definition of the projection, one directly obtains the claimed result.

b) Using the definition of angle for standard Hilbert structures (2.3.2), the angle between the fitted Randers and Euclidean metrics of the Finsler type $\theta_{RE} = \sphericalangle(g_R, g_E)$ is given by:

$$\cos\theta = \frac{Trace(g_R\cdot g_E^t)}{||g_R||\cdot||g_E||}.$$

The Maple calculation produces the numerator, i.e., the scalar product of the metrics

$$\langle g_R, g_E\rangle \approx \frac{1}{\alpha^3}\left(-0.59\dot{x}^3 - 0.61\dot{x}^2\dot{y} + 1.78\alpha^2\dot{x} + 0.21\alpha^2\dot{y} + 1.65\alpha^3\right).$$

By using the norms (2.23) and (2.25), we obtain (2.26). □

Another comparison of the two statistically fitted Finsler structures can be observed as well by considering certain relevant first order tensors. Namely, the 1-form $b = (b_1, b_2) = (0.63, -0.27)$ characterizes the fitted Randers structure through the linear deformation β, while the Euclidean fitted one has the major semiaxis oriented along the constant vector field v of the elliptic indicatrices space with fibers $I_{\dot{x}} = \{\dot{y} \mid F_E(\dot{x}, \dot{y}) = 1\}$[12]. For the fitted Euclidean structure, the semiaxis vector field is $v = (v^1, v^2) = (-0.71, -0.49)$.

Since the two objects are of the opposite tensor types, we consider the corresponding vector field related to b, with indices lifted by the canonical Euclidean scalar dual metric, $\widetilde{b} = (b_i\delta^{1i}, b_i\delta^{2i})$. Simple calculation gives us their canonical Euclidean norms and the angle - expressed in radians,

$$||\widetilde{b}|| = 0.68, \quad ||v|| = 0.86, \quad \sphericalangle(\widetilde{b}, v) = 2.13.$$

[12]Here, the vector v is the normalized principal eigenvector of the $\dot{y}-$ dependent quadratic form induced by the Euclidean structure.

2.3.5 The relevance of the Finsler structures for the Garner model

We note that the fit Randers Finsler norm (2.4) arises from the evaluation of the GS evolution-rate in terms of the reduced RS, and provides a mediated information on the prognosis of the disease after the state worsening signaled by the increase of the parameter h. The additive term $\beta = .63\dot{x} + -.27\dot{y}$ from the Randers norm evaluates the impact of the change in the parameter h and the rate of increase. The statistically determined coefficients $(b_1, b_2) \approx (.63, -.27)$ emphasize the dominant role of the proliferating cells in the dynamical system (2.1).

The Finsler norm (2.4) provides an evaluation of the severity of the rate of cancer cell evolution immediately after a significant change of the Garner parameter h, which can be experimentally measured or estimated in terms of the cause which determined the change. The benefit of the Randers structure relies on the fact that the vector input $y = \dot{p}$ of F (the growth rates of the cancerous cells) does not require knowledge of the amount of the total cell populations p. These inputs can be experimentally determined when the cancer evolution is controlled ("steady", for $h \approx 0$), and can be estimated by measuring the population increase/decrease of the cancerous cells by using only two subsequent laboratory samples. Moreover, the deformation term $\beta = .63\dot{x} + -.27\dot{y} \approx ||\dot{p_e}|| - ||\dot{p}||$ represents the *drift*[13] [28], which affects the straight paths of the Euclidean norm α, producing the new, curved paths of our Randers structure $F_R = \alpha + \beta$.

The Euclidean and the 4-th root fit Finsler norms exhibit different properties of the variation of cell populations. While F_E gives account via g_E on the anisotropic evolution of the illness process in the 2-dimensional $\dot{p}$ plane through its PCA spectral data, the 4-th root norm $F_Q(\mathbf{y}) = \sqrt[4]{P_4(y)}$ is much more dense in information, through the larger spectral data of its $(0, 4)$ tensor induced by halvings by the 4-homogeneous in the components of y quadratic polynomial $P_4(\mathbf{y})$. The qualitative advantage over the Euclidean case is sensed within the space of 4-th root Finsler norms by the difference $\Delta(y) = \sqrt[4]{P_4(y)} - F_E(y)$.

[13] In general, in terms of Zermelo navigation [38], the Randers structure represents the most appropriate model for exhibiting through its geodesics the influence of the β-force field on the geodesic trajectories of the Riemannian structure given by α.

Chapter 3

Anisotropic extensions of the Beltrami framework

The Beltrami framework is a general differential geometric framework that proved its usefulness for studding problems in image processing and computer vision. It contains two differentiable manifolds of different finite dimensions and an embedding. The main problem studied within the Beltrami framework is the problem of minimizing an energy functional depending on the embedding map and on the metric structures on both manifolds. However, direct methods of the variational calculus are not applicable in general. In such cases, flow techniques may bring the embedded surfaces to the state of minimal energy. The flow is a vector valued function on the embedded surface, and its components are given by partial differential equations, called the evolution equations of the embedded surface.

The Beltrami framework has been first introduced in [103] for the purpose of low level vision. Our goal is to extend the original construction in order to encompass also the directional dependency, and to appropriately generalize extend the evolution flow function in order to be defined on the tangent bundle of the embedded surface. Such new framework will be called the *anisotropic Beltrami framework*. The original results presented in this chapter are published in [22, 25].

The construction of the Beltrami framework is closely related to theory of submanifolds, calculus of variations and partial differential equations on manifolds.

3.1 The Beltrami framework and descent flow

Eugenio Beltrami provided models of the non-Euclidean geometry in Euclidean space. He published original papers in the second half of the 19th century. His theory particularly considers the definition of surface and the establishing of metric. A comprehensive overview of his research on the subject can be found in [8].

The first applications in image processing of the Beltrami framework were first considered by Sochen et al. in [103] and generalized by Bresson et al. in [36].

Although its intensive development is motivated by its applications in image processing, we will present a more general framework, in accordance with the theory of submanifolds and harmonic maps.

Let D denote an open connected subset in an n-dimensional manifold (in the sequel, D will be referred as a domain) and let (M, h) be an m-dimensional Riemannian manifold ($n < m$).

The embedding $X : D \to M$ is given by m smooth scalar functions of n variables,

$$X : (x^1, \dots, x^n) \to \left(X^1(x^1, \dots, x^n), \dots, X^m(x^1, \dots, x^n)\right), \tag{3.1}$$

and it produces an n-dimensional submanifold $\Sigma = X(D) \subset M$ embedded in M, called the image manifold or the image surface. A Riemannian metric tensor field g on Σ is not necessarily induced from h, so the couple (Σ, g) represents the Riemannian image surface. The Beltrami framework will be shortly denoted as the triple (X, M, Σ), or $(X, (M, h), (\Sigma, g))$ when it is necessary to emphasize metrics on manifolds M and Σ.

Throughout this chapter we shall employ the following notation: Greek indices will run from 1 to n, and indicate objects on the image surface, while Latin indices running from 1 to m will be reserved for the embedding space, e.g., $g = g_{\mu\nu} dx^\mu \otimes dx^\nu$ and $h = h_{ij} dx^i \otimes dx^j$. We shall also shorten the standard notation for partial differentials and write

$$X^i_\alpha = \frac{\partial X^i}{\partial x^\alpha}, \qquad X^i_{\alpha\beta} = \frac{\partial^2 X^i}{\partial x^\alpha \partial x^\beta},$$

not only for the embedding map, but for any smooth function dependent on the same parameters $x^1, \dots, x^n$.

The Beltrami framework uses the local intrinsic description of manifolds Σ and M and considers the metrics g and h as dynamic variables. It minimizes the weighted Polyakov action functional that depends on both the image surface Σ (through the embedding and chosen metric) and the Riemannian manifold M.

Definition 3.1.1. The weighted Polyakov action associated to the Beltrami framework (X, M, Σ) is given by the functional

$$S(X, g_{\sigma\mu}, h_{ij}) = \int f \cdot \langle \operatorname{grad} X^i, \operatorname{grad} X^j \rangle_g \cdot h_{ij} \, dV = \int f g^{\sigma\mu} X^i_\sigma X^j_\mu h_{ij} \sqrt{g} \, dx^1 \dots dx^n, \tag{3.2}$$

where $f = f(X^i, X^i_\alpha, g, h)$ is a smooth function depending on the embedding X and on the chosen metrics h and g, and is called the weight function.

Notice that in (3.2), the term $\langle \operatorname{grad} X^i, \operatorname{grad} X^j \rangle_g$ is the scalar product of the gradient vector field of X by itself (with respect to the metric g), $g = \det(g_{\sigma\mu})$ is the determinant of the metric tensor, and $dV = \sqrt{g}\, dx^1 dx^2 \dots dx^n$ is the volume element on Σ. Putting $f \equiv 1$ reduces the influence of the weighted Polyakov action (Bresson case) to the initial nonweighted one (Sochen case).

The standard methods of variational calculus lead to the minimization of the Polyakov action by considering the Lagrangian density

$$L(X(x^\alpha), f, g_{\sigma\mu}(x^\alpha), h_{ij}(x^\alpha)) = f \sqrt{g} g^{\sigma\mu} X^i_\sigma X^j_\mu h_{ij},$$

with respect to all variables. The Euler-Lagrange equations provide a necessary condition for an extremal for the corresponding variational problem.

It is shown in [102] that if minimization is considered with respect to the embedded metric g, then the optimal choice for the image metric is the induced one:

$$g_{\sigma\mu} = h_{ij} X^i_\sigma X^j_\mu. \tag{3.3}$$

By varying the weighted Polyakov action in terms of the embedding, one infers the Euler-Lagrange equations

$$\frac{\partial L}{\partial X^i} - \frac{\partial}{\partial x^\alpha}\left(\frac{\partial L}{\partial X^i_\alpha}\right) = 0.$$

Due to the complex dependencies within L, we use the following brief notation: for a given function Φ, we shall denote

$$\Phi_{;\alpha} := \frac{\partial \Phi}{\partial x^\alpha} \qquad \Phi_{,i} := \frac{\partial \Phi}{\partial X^i} \qquad \Phi_{,\binom{i}{\alpha}} := \frac{\partial \Phi}{\partial X^i_\alpha}.$$

Hence, the Euler-Lagrange equations can be written in the following condensed form:

$$L_{,i} - L_{,\binom{i}{\alpha};\alpha} = 0. \tag{3.4}$$

Similar to (1.68), the PDE (3.4) yields the flow that leads to the descent of the Polyakov action.

Definition 3.1.2. Let (Σ, g) be a Riemannian image surface of the Beltrami framework (X, M, Σ), and let L be the Lagrangian density of the corresponding Polyakov action. The descent flow which shifts the image surface to the state of minimal Polyakov action, is called the *Beltrami flow*: $\partial_t X = \big(\partial_t X^1, \ldots, \partial_t X^m\big)$, with

$$\partial_t X^r = -\frac{1}{2}\frac{1}{\sqrt{g}} h^{ir}\left(L_{,i} - L_{,\binom{i}{\alpha};\alpha}\right). \tag{3.5}$$

The multiplier $-\frac{1}{2}\frac{1}{\sqrt{g}}h^{ir}$ plays the role of making the flow invariant with respect to reparametrizations, hence to provide to the Beltrami flow geometric meaning. For fixed t, the flow (3.5) defines the flow vector field over the image manifold. Different choices of the metrics g and h produce various descent flows. Some particular examples are presented in the next two sections. For instance, if h and g are the fixed metrics, they can be viewed as parameters of the minimization. Moreover, if the weight is trivial ($f = const$), the process minimizes the area of the submanifold and it is closely related to the notion of harmonic maps. The equivalence between the intrinsic Beltrami framework approach with the induced metric g and the implicit harmonic map approach is considered in [105], and proved for the case of 2-dimensional hypersurfaces. The main difference between these two approaches is in the focus of interest: the Beltrami framework considers the image surface, while the harmonic map theory considers the maps themselves, which are not necessarily embeddings.

3.2 Riemannian submanifolds in a Riemannian space

Let X be the Beltrami embedding (3.1) into a Riemannian manifold (M, h), and let g be a metric of Riemannian type associated to the embedded submanifold Σ. The intrinsic properties of the manifold (Σ, g) and the comparison of the two geometries are studied by submanifold theory [2, 83].

The minimization of the submanifold area/volume can also be considered by the theory of harmonic maps. The theory focuses on the minimization of an energy functional E defined over the space of all smooth functions from D to M, $\mathcal{C}^\infty(D, M)$, aiming to deform a given embedding X into an extremal of E. At the same time, the embedded surface Σ evolves towards the extreme state of minimal energy E. The harmonic energy functional is the mapping

$$E : \mathcal{C}^\infty(D, M) \to \mathbb{R}, \quad E(X) = \frac{1}{2} \int g^{\sigma\mu} X^i_\sigma X^j_\mu h_{ij} \sqrt{g}\, dx^1 dx^2 \dots dx^n. \tag{3.6}$$

For a fixed embedding $X \in \mathcal{C}^\infty(D, M)$, the energy $E(X)$ coincides with the Polyakov action (3.2) with constant weight function $f = \frac{1}{2}$ and fixed metrics g and h.

The minimization of the harmonic energy functional E is achieved by variational vector field associated to the mapping in accordance with variational calculus principles and depends on the Christoffel symbols of the embedding space M and of the submanifold Σ:

$$\Gamma^r_{kl} = \frac{1}{2} h^{ri} \left(h_{il,k} + h_{ki,l} - h_{kl,i} \right),$$
$$\Gamma^\sigma_{\rho\theta} = \frac{1}{2} g^{\alpha\sigma} \left(g_{\rho\alpha;\theta} + g_{\alpha\theta;\rho} - g_{\rho\theta;\alpha} \right).$$

Definition 3.2.1. For a map $X \in \mathcal{C}^\infty(D, M)$, the *tension field* is the vector field $\tau(X) = \big(\tau^1(X), \dots, \tau^m(X)\big)$ defined by

$$\tau^r(X) = g^{\sigma\mu} X^r_{\sigma\mu} - g^{\rho\theta} \Gamma^\sigma_{\rho\theta} X^r_\sigma + g^{\sigma\mu} \Gamma^r_{kl} X^k_\sigma X^l_\mu. \tag{3.7}$$

If $\tau(X) \equiv 0$, the map X is said to be a *harmonic map*.

The tension field is a generalization of the Laplace-Beltrami operator Δ_g on Σ associated to the chosen metric g, applied to the field X. The components of the tension field are

$$\tau^r(X) = \Delta_g(X^r) + g^{\sigma\mu} \Gamma^r_{kl} X^k_\sigma X^l_\mu.$$

The Beltrami-Laplace operator is given by

$$\Delta_g(X^r) = \frac{1}{\sqrt{g}} \partial_\alpha \left(\sqrt{g} g^{\alpha\sigma} X^r_\sigma \right) = g^{\alpha\sigma} X^r_{\alpha\sigma} - g^{\rho\theta} \Gamma^\sigma_{\rho\theta} X^r_\sigma, \tag{3.8}$$

and $\Delta_g(X) = \big(\Delta_g(X^1), \dots, \Delta_g(X^m)\big)$ produced by (3.8) is a vector field over the submanifold Σ, $H : \Sigma \to (T\Sigma)^\perp \subset TM$, $H(x) = \Delta_g(X(x))$, called the *mean curvature* vector field.

The vanishing of the tension field is the necessary condition for the map X to be an extremal of the energy functional (3.6). In other words, the harmonic maps produce the minimal energy. Otherwise, i.e., for $\tau(X) \neq 0$, the tension field can be employed by (1.68) to deform X to a harmonic map. The corresponding flow is called the *tension flow*,

$$\frac{\partial X^r}{\partial t} = \tau^r(X).$$

The Eells-Sampson theorem gives the existence result for harmonic maps and justifies the flow technique (see [48]).

3.2.1. Theorem *Let D and M be compact Riemannian manifolds with M of non-positive sectional curvature. Then for any map $X \in \mathcal{C}^\infty(D, M)$ there is a unique function $X_t : D \times [0, \infty) \to M$, with $X_t = f(\cdot, t)$ continuous in t, which is a solution of the PDE*

$$\frac{\partial X_t}{\partial t} = \tau(X_t), \quad X_0 = X.$$

If the metric on the submanifold Σ is chosen to be induced from M, and the weight function to be $f = \frac{1}{n}$ (to absorb the surface dimension), then the harmonic energy functional reduces to

$$E(X) = \frac{n}{2} \int \sqrt{g}\, dx^1 dx^2 \dots dx^n,$$

and becomes proportional to the area functional $\int \sqrt{g}\, dx^1 dx^2 \dots dx^n$ considered in the minimal surfaces theory. In this case, the corresponding Beltrami (and the tension) vector field is proportional to the mean curvature vector field, $\tau(X) = \frac{n}{2} \cdot H(X)$. The corresponding *mean curvature flow* $\frac{\partial X^r}{\partial t} = H^r(X)$ deforms the embedded surface Σ to the state of minimal area/volume.

More details on the harmonic maps theory can be found in [48].

Remark. The Polyakov action, the harmonic energy functional and the area functional differ initially by multiplicative scalar terms (beside the weight function in the first case). This fact causes differences between corresponding flows. Even flows of the same type differ by some proportional coefficient, since the functionals might have different initial scalar multiplicative terms.

3.3 Riemannian submanifolds in a Euclidean space

Let us now consider a Beltrami embedding X into a Euclidean space ($M = \mathbb{R}^m, h_{ij} = \text{const}$) with the embedded submanifold of arbitrarily chosen Riemannian type (Σ, g). In this case, the Christoffel symbols Γ^i_{jk} of the ambient space are identically equal to zero, hence the tension vector field of the embedding coincides with the Laplace-Beltrami operator,

$$\tau^r(X) = g^{\sigma\mu} \left(X^r_{\sigma\mu} - \Gamma^{\nu}_{\sigma\mu} X^r_{\nu} \right) = \Delta_g(X^r).$$

Furthermore, a suitably chosen local chart will provide the vanishing of the Christoffel symbols of Σ, hence, the tension vector field will locally coincide with the Laplacian,

$$\tau^r(X) = \text{Trace}\big(\text{Hess}(X^r)\big) = g^{\sigma\mu} \left(\frac{\partial^2 X^r}{\partial x^\sigma \partial x^\mu} \right).$$

An example of the Beltrami framework, commonly used in image processing (cf. ([36, 64, 114])), will be presented for $m = 3$ and $n = 2$. The image Σ is a Monge surface in the Euclidean space $\mathbb{R}^3$ with the metric $h_{ij} = \text{diag}(1, 1, \beta^2)$. The embedding that produces the image surface is

$$X : (x^1, x^2) \to (x^1, x^2, I(x^1, x^2)). \tag{3.9}$$

Let Σ be endowed with the induced metric g, whose components are then

$$(g_{\sigma\mu}) = \begin{pmatrix} 1 + \beta^2 I^2_{x^1} & \beta^2 I_{x^1} I_{x^2} \\ \beta^2 I_{x^1} I_{x^2} & 1 + \beta^2 I^2_{x^2} \end{pmatrix}. \tag{3.10}$$

The (weighted) Polyakov action is given by

$$S(X) = 2fE(X) = \int f \sqrt{1 + \beta^2 I^2_{x^1} + \beta^2 I^2_{x^2}}\, dx^1 dx^2.$$

The corresponding Beltrami flow that evolves the Monge-image surface (into another Monge surface) has nontrivial only the third component,

$$\partial_t X = \left(\partial_t X^1, \partial_t X^2, \partial_t X^3\right) = (0, 0, \partial_t I)\,,$$

that coincides with the weighted mean curvature flow,

$$\partial_t I = f H^3 + \partial_k f g^{\mu\nu} \partial_\mu X^k \partial_\nu I - \frac{1}{\beta^2}\partial_3 f, \tag{3.11}$$

where H^3 is the third component of the mean curvature vector

$$H^3 = \frac{1}{g^2}(g_{11} I_{x^2x^2} + g_{22} I_{x^1x^1} - 2g_{12} I_{x^1x^2}). \tag{3.12}$$

3.4 The anisotropic Beltrami framework and deformation of the flow

In order to develop the anisotropic Beltrami framework we consider the embedding (3.1), and fix a Riemannian metric of the embedding space (M, h_{ij}). Initially, we will study the most general case of directionally dependent embedded metric structures, actually, a generalized Lagrange metric, which makes the framework anisotropic.

Anisotropic extensions of harmonic mappings have been considered in [80, 98, 108], where directions are involved in the variational processes. In [80, 98], the focus is on the energy of mappings from Finsler to Riemannian and Finslerian manifolds, with an anisotropic energy functional obtained by considering the Holmes-Thompson volume form on a Finsler type embedded surface. The corresponding Euler-Lagrange operator and the tension field, are introduced. In [108], anisotropy is achieved by considering the energy functional of mappings from Riemannian and Finslerian, to Finslerian manifolds.

The directional dependence of the structural tensor on the embedded space in the Beltrami framework appears firstly in [74], where the anisotropic curve length is considered, and in [52], where the Euclidean metric is complemented by the structural tensor, which depends on the surface gradient. Both cases consider geodesic active objects in the one-dimensional case. In other words, they evolve curves by anisotropic flows.

In [22], a non-weighted anisotropic evolution of the embedded surface is proposed, based on a 0-homogeneous direction-dependent metric tensor of the surface instead of the weight function dwelling inside the minimized functional.

In the following, we will study an anisotropic metric γ on the surface produced by the Beltrami embedding (3.1). In other words, γ is required to be a smooth metric d-tensor field on the tangent space $T\Sigma$. (In order to distinguish anisotropic metric from the Riemannian type metrics, we use the notation with Greek letters.) The tension field of the anisotropic Beltrami embedding is defined analogously with (3.7), and has the following components

$$\tau^r(X) = \gamma^{\sigma\mu}\left(X^r_{\sigma\mu} - \Gamma^\nu_{\sigma\mu} X^r_\nu + \Gamma^r_{kl} X^k_\sigma X^l_\mu\right), \tag{3.13}$$

where connection coefficients on the embedded surface are also anisotropic

$$\Gamma^\nu_{\sigma\mu} = \frac{1}{2}\gamma^{\nu\rho}\left(\gamma_{\sigma\rho;\mu} + \gamma_{\rho\mu;\sigma} - \gamma_{\sigma\mu;\rho}\right).$$

If the metric γ is symmetric, regular and of constant signature, then (Σ, γ) is a generalized Lagrange manifold [35], and the anisotropic Beltrami flow ensures the minimal Polyakov action.

The Polyakov action to be minimized has the same form, but depends on tangent vectors through the embedded metric γ,

$$S(X, \gamma_{\sigma\mu}, h_{jk}) = \int f \gamma^{\sigma\mu} X^i_\sigma X^j_\mu h_{ij} \sqrt{\gamma}\, dx^1 \dots dx^n.$$

According to the terms involved in the Lagrangian density $L = f\sqrt{\gamma}\gamma^{\sigma\mu} h_{kl} X^k_\sigma X^l_\mu$, it is important to simultaneously consider two metrics on the embedded surface: the arbitrarily chosen one, $\gamma = \gamma_{\sigma\mu}(x,v)\ dx^\sigma \otimes dx^\mu$, and the induced one $g = g_{\sigma\mu}(x)\ dx^\sigma \otimes dx^\mu$, where $g_{\sigma\mu} = h_{kl} X^k_\sigma X^l_\mu$. Without loss of generality, we will extend in additive manner the induced metric g to the new deformed anisotropic metric γ:

$$\gamma_{\sigma\mu}(x,v) = g_{\sigma\mu}(x) + a \cdot \varphi_{\sigma\mu}(x,v), \tag{3.14}$$

where $a \in \mathbb{R}$ and $\varphi_{\sigma\mu}$ are components of a d-tensor field on $T\Sigma$ that will be regarded to as the *additional tensor*, and obviously, for $a = 0$ this becomes the classical Beltrami framework. For the simplicity we will assume $a = 1$. The Lagrangian density can be written as

$$L(x,v) = f\sqrt{\gamma}\gamma^{\sigma\mu} g_{\sigma\mu},$$

where $\gamma^{\sigma\mu}$ are components of the contravariant metric, and γ is the determinant of the matrix $(\gamma_{\sigma\mu})$.

The Euler-Lagrange equations, which produce the anisotropic flow is derived in accordance with the Hilbert-Palatini variational principle [9].

3.4.1. Theorem *(The anisotropic weighted Beltrami flow) The PDE of the anisotropic Beltrami flow, which provides the minimality of the weighted Polyakov action on the surface (Σ, γ)- which is embedded into the Riemannian manifold (M, h) by the mapping (3.1), is*

$$\begin{aligned}
\partial_t X^r = {} & \frac{1}{2} f_{,\binom{i}{\alpha};\alpha} \gamma^{\sigma\mu} g_{\sigma\mu} h^{ir} - \frac{1}{2} f_{,i} \gamma^{\sigma\mu} g_{\sigma\mu} h^{ir} \\
& + \frac{1}{2} f_{,\binom{i}{\alpha}} h^{ir} \left[(\gamma^{\sigma\mu})_{;\alpha} g_{\sigma\mu} + \gamma^{\sigma\mu} g_{\sigma\mu;\alpha} + \gamma^{\sigma\mu} g_{\sigma\mu} (\ln\sqrt{\gamma})_{;\alpha} \right] \\
& + \frac{1}{2} f_{;\alpha} h^{ir} \left[(\gamma^{\sigma\mu})_{,\binom{i}{\alpha}} g_{\sigma\mu} + \gamma^{\sigma\mu} g_{\sigma\mu,\binom{i}{\alpha}} + \gamma^{\sigma\mu} g_{\sigma\mu} (\ln\sqrt{\gamma})_{,\binom{i}{\alpha}} \right] \\
& + f \tau^r(X) \\
& + \frac{1}{2} h^{ir} f \Big\{ g_{\sigma\mu;\alpha} \left[(\gamma^{\sigma\mu})_{,\binom{i}{\alpha}} + \gamma^{\sigma\mu} (\ln\sqrt{\gamma})_{,\binom{i}{\alpha}} \right] \\
& \qquad + g_{\sigma\mu} \Big[(\gamma^{\sigma\mu})_{,\binom{i}{\alpha};\alpha} + (\gamma^{\sigma\mu})_{,\binom{i}{\alpha}} (\ln\sqrt{\gamma})_{;\alpha} + (\gamma^{\sigma\mu})_{;\alpha} (\ln\sqrt{\gamma})_{,\binom{i}{\alpha}} \\
& \qquad\quad + \gamma^{\sigma\mu} \tfrac{1}{\sqrt{\gamma}} (\sqrt{\gamma})_{,\binom{i}{\alpha};\alpha} - (\gamma^{\sigma\mu})_{,i} - \gamma^{\sigma\mu} (\ln\sqrt{\gamma})_{,i} \Big] \Big\},
\end{aligned} \tag{3.15}$$

where $\tau(X)$ is the tension field of the embedding X (3.13), and $g_{\sigma\mu} = h_{kl} X^k_\sigma X^l_\mu$ is the induced metric tensor field on the embedded surface Σ.

Proof. A straightforward calculation expresses the partial derivatives of the Lagrangian density by the partial derivatives of both metrics, the embedding and the weight function, as follows:

$$
\begin{aligned}
L_{,i} &= f_{,i}\, \gamma^{\sigma\mu} g_{\sigma\mu}\sqrt{\gamma} + f(\gamma^{\sigma\mu})_{,i}\; g_{\sigma\mu}\sqrt{\gamma} + \gamma^{\sigma\mu} g_{\sigma\mu,i}\sqrt{\gamma} + \gamma^{\sigma\mu} g_{\sigma\mu}(\sqrt{\gamma})_{,i}, \\
L_{,\binom{i}{\alpha}} &= f_{,\binom{i}{\alpha}}\, \gamma^{\sigma\mu} g_{\sigma\mu}\sqrt{\gamma} \\
&\quad + f\left((\gamma^{\sigma\mu})_{,\binom{i}{\alpha}} g_{\sigma\mu}\sqrt{\gamma} + \gamma^{\sigma\mu} g_{\sigma\mu,\binom{i}{\alpha}}\sqrt{\gamma} + \gamma^{\sigma\mu} g_{\sigma\mu}(\sqrt{\gamma})_{,\binom{i}{\alpha}}\right),
\end{aligned}
\tag{3.16}
$$

$$
\begin{aligned}
L_{,\binom{i}{\alpha};\alpha} &= f_{,\binom{i}{\alpha};\alpha}\gamma^{\sigma\mu} g_{\sigma\mu}\sqrt{\gamma} \\
&\quad + f_{,\binom{i}{\alpha}}\left[(\gamma^{\sigma\mu})_{;\alpha} g_{\sigma\mu}\sqrt{\gamma} + \gamma^{\sigma\mu} g_{\sigma\mu;\alpha}\sqrt{\gamma} + \gamma^{\sigma\mu} g_{\sigma\mu}(\sqrt{\gamma})_{;\alpha}\right] \\
&\quad + f_{;\alpha}\left[(\gamma^{\sigma\mu})_{,\binom{i}{\alpha}} g_{\sigma\mu}\sqrt{\gamma} + \gamma^{\sigma\mu} g_{\sigma\mu,\binom{i}{\alpha}}\sqrt{\gamma} + \gamma^{\sigma\mu} g_{\sigma\mu}(\sqrt{\gamma})_{,\binom{i}{\alpha}}\right] \\
&\quad + f\Big\{(\gamma^{\sigma\mu})_{,\binom{i}{\alpha};\alpha} g_{\sigma\mu}\sqrt{\gamma} + (\gamma^{\sigma\mu})_{,\binom{i}{\alpha}} g_{\sigma\mu;\alpha}\sqrt{\gamma} + (\gamma^{\sigma\mu})_{,\binom{i}{\alpha}} g_{\sigma\mu}(\sqrt{\gamma})_{;\alpha} \\
&\qquad + (\gamma^{\sigma\mu})_{;\alpha} g_{\sigma\mu,\binom{i}{\alpha}}\sqrt{\gamma} + \gamma^{\sigma\mu} g_{\sigma\mu,\binom{i}{\alpha};\alpha}\sqrt{\gamma} + \gamma^{\sigma\mu} g_{\sigma\mu,\binom{i}{\alpha}}(\sqrt{\gamma})_{;\alpha} \\
&\qquad + (\gamma^{\sigma\mu})_{;\alpha} g_{\sigma\mu}(\sqrt{\gamma})_{,\binom{i}{\alpha}} + \gamma^{\sigma\mu} g_{\sigma\mu;\alpha}(\sqrt{\gamma})_{,\binom{i}{\alpha}} + \gamma^{\sigma\mu} g_{\sigma\mu}(\sqrt{\gamma})_{,\binom{i}{\alpha};\alpha}\Big\}.
\end{aligned}
\tag{3.17}
$$

By plugging (3.16) and (3.17) into (3.5), and using abbreviate notation

$$\frac{1}{\sqrt{\gamma}}(\sqrt{\gamma})_\star = (\ln\sqrt{\gamma})_\star$$

for all kind of derivatives $\star :\ {}_{;\alpha},\ {}_{,i},\ {}_{,\binom{i}{\alpha}}$, we obtain the gradient descent flow for the surface embedded in the Riemannian space in the form (3.15). □

Theorem 3.4.1 is a generalization of the Beltrami framework presented in [36, 103, 114], where the considered embedding goes into a Euclidean space ($h_{ij} = const$), and the metric on the surface is the induced one. In our approach, the present generalization relies on three aspects: the metric of the embedding space is of Riemannian type, the metric of the embedded space is generalized Lagrange one (regular and symmetric d-tensor on $T\Sigma$), and the weight function depends not only on the embedding itself, but also on its derivatives.

The weighted Polyakov action of the anisotropic Beltrami framework based on the embedding X (3.1), is influenced by tangent vectors through the weight function and through the anisotropic metric. Thus, we consider that the double directional influence is unnecessary, and in the following, we propose the absence of the weight function inside Polyakov action. Hence, by using $f \equiv 1$, one proves immediately the following result.

3.4.2. Theorem *(The anisotropic Beltrami flow) The explicit form of the anisotropic Beltrami flow minimizing non-weighted Polyakov action with generalized Lagrange image metric γ is*

$$
\begin{aligned}
\partial_t X^r = {} & \tau^r(X) \\
& + \frac{1}{2}h^{ir}\Big\{g_{\sigma\mu;\alpha}\left[(\gamma^{\sigma\mu})_{,\binom{i}{\alpha}} + \gamma^{\sigma\mu}(\ln\sqrt{\gamma})_{,\binom{i}{\alpha}}\right] \\
& \quad + g_{\sigma\mu}\Big[(\gamma^{\sigma\mu})_{,\binom{i}{\alpha};\alpha} + (\gamma^{\sigma\mu})_{,\binom{i}{\alpha}}(\ln\sqrt{\gamma})_{;\alpha} + (\gamma^{\sigma\mu})_{;\alpha}(\ln\sqrt{\gamma})_{,\binom{i}{\alpha}} \\
& \qquad + \gamma^{\sigma\mu}\frac{1}{\sqrt{\gamma}}(\sqrt{\gamma})_{,\binom{i}{\alpha};\alpha} - (\gamma^{\sigma\mu})_{,i} - \gamma^{\sigma\mu}(\ln\sqrt{\gamma})_{,i}\Big]\Big\}.
\end{aligned}
\tag{3.18}
$$

The process of determining the terms from the previous theorem is achieved by using the following auxiliary results, where the derivatives of the contravariant metric tensor and of the determinant are expressed in terms of the covariant metric components.

3.4.3. Lemma *The variations of the determinant and of the dual metric tensor for γ are described by the following expressions*

$$\gamma_* = \gamma\gamma^{\lambda\tau}\gamma_{\lambda\tau *}, \tag{3.19}$$

$$(\ln\sqrt{\gamma})_* = \frac{1}{2}\gamma^{\lambda\tau}\gamma_{\lambda\tau *} \tag{3.20}$$

$$(\gamma^{\sigma\mu})_* = -\gamma^{\sigma\lambda}\gamma^{\mu\tau}\gamma_{\lambda\tau *} \tag{3.21}$$

$$(\gamma^{\sigma\mu})_{,\binom{i}{\alpha};\alpha} = \left(\gamma^{\sigma\rho}\gamma^{\lambda\theta}\gamma^{\mu\tau} + \gamma^{\sigma\lambda}\gamma^{\mu\rho}\gamma^{\tau\theta}\right)\gamma_{\rho\theta;\alpha}\gamma_{\lambda\tau,\binom{i}{\alpha}} - \gamma^{\sigma\lambda}\gamma^{\mu\tau}\gamma_{\lambda\tau,\binom{i}{\alpha};\alpha} \tag{3.22}$$

$$\frac{1}{\sqrt{\gamma}}(\sqrt{\gamma})_{,\binom{i}{\alpha};\alpha} = \frac{1}{2}\left(\frac{1}{2}\gamma^{\rho\theta}\gamma^{\lambda\tau} - \gamma^{\lambda\rho}\gamma^{\tau\theta}\right)\gamma_{\rho\theta;\alpha}\gamma_{\lambda\tau,\binom{i}{\alpha}} + \frac{1}{2}\gamma^{\lambda\tau}\gamma_{\lambda\tau,\binom{i}{\alpha};\alpha} \tag{3.23}$$

where ϕ_* stands for $\phi_{;\alpha}$, $\phi_{,i}$ and $\phi_{,\binom{i}{\alpha}}$.

Proof. The assertions are obtained by straightforward calculations and by use of the following algebraic fact:
Let (s_{ij}) be a regular matrix, let (s^{ij}) be the corresponding inverse matrix and let s be its determinant. Then, the derivatives are related by

$$s^{ij}{}_\star = -s^{ik}s^{jl}s_{kl\,\star}, \qquad s_\star = s \cdot s^{ij}s_{ij\,\star}.$$

□

According to the assumed form of the anisotropic metric γ given by (3.14), its derivatives contain the derivatives of the induced metric components and of the additional tensor components, which are specific to certain cases.

The various derivatives of the induced metric tensor show its dependency of the embedding (3.1):

3.4.4. Proposition *Let X be an embedding (3.1) into the Riemannian space (M, h_{ij}), which produces the submanifold Σ, and let $g_{\sigma\mu}$ be the induced metric. Various derivatives of the metric components are*

$$g_{\sigma\mu;\alpha} = h_{kl,j}X^j_\alpha X^k_\sigma X^l_\mu + h_{kl}X^k_{\sigma\alpha}X^l_\mu + h_{kl}X^k_\sigma X^l_{\mu\alpha} \tag{3.24}$$

$$g_{\sigma\mu,i} = h_{kl,i}X^k_\sigma X^l_\mu \tag{3.25}$$

$$g_{\sigma\mu,\binom{i}{\alpha}} = h_{il}\delta^\alpha_\sigma X^l_\mu + h_{ik}X^k_\sigma\delta^\alpha_\mu \tag{3.26}$$

$$g_{\sigma\mu,\binom{i}{\alpha};\alpha} = h_{il,j}X^j_\sigma X^l_\mu + h_{ki,j}X^j_\mu X^k_\sigma + 2h_{ij}X^j_{\sigma\mu} \tag{3.27}$$

Proof. The properties of derivatives and the chain rule yield the assertions. □

The following result shows the impact of the anisotropic additional tensor onto the evolution, i.e., on the anisotropic Beltrami flow.

3.4.5. Theorem *The anisotropic Beltrami flow of an image surface with metric tensor* (3.14) *is described by the evolution PDE:*

$$\begin{aligned}\partial_t^{GL} X^r = {} & \tau^r(X) + \frac{1}{2}h^{ir}\left\{\frac{1}{2}\gamma^{\sigma\mu}\gamma^{\lambda\tau} - \gamma^{\sigma\lambda}\gamma^{\mu\tau}\right\} \cdot \\ & \left\{g_{\sigma\mu;\alpha}g_{\lambda\tau,\binom{i}{\alpha}} + g_{\sigma\mu}g_{\lambda\tau,\binom{i}{\alpha};\alpha} - g_{\sigma\mu}g_{\lambda\tau,i} + g_{\sigma\mu;\alpha}\varphi_{\lambda\tau,\binom{i}{\alpha}} + g_{\sigma\mu}\varphi_{\lambda\tau,\binom{i}{\alpha};\alpha} - g_{\sigma\mu}\varphi_{\lambda\tau,i}\right\} \\ & + \frac{1}{2}h^{ir}g_{\sigma\mu}\left\{g_{\rho\theta;\alpha}g_{\lambda\tau,\binom{i}{\alpha}} + g_{\rho\theta;\alpha}\varphi_{\lambda\tau,\binom{i}{\alpha}} + g_{\lambda\tau,\binom{i}{\alpha}}\varphi_{\rho\theta;\alpha} + \varphi_{\rho\theta;\alpha}\varphi_{\lambda\tau,\binom{i}{\alpha}}\right\} \cdot \\ & \left\{\gamma^{\sigma\rho}(\gamma^{\lambda\theta}\gamma^{\mu\tau} - \frac{1}{2}\gamma^{\mu\theta}\gamma^{\lambda\tau}) + \gamma^{\sigma\lambda}(\gamma^{\mu\rho}\gamma^{\tau\theta} - \frac{1}{2}\gamma^{\mu\tau}\gamma^{\rho\theta}) - \frac{1}{2}\gamma^{\sigma\mu}(\gamma^{\lambda\rho}\gamma^{\tau\theta} - \frac{1}{2}\gamma^{\rho\theta}\gamma^{\lambda\tau})\right\}.\end{aligned} \tag{3.28}$$

Proof. This proof is based on Theorem 3.4.2, relation (3.14) and derivative rules. Straightforward but lengthy calculations lead to

$$\left[(\gamma^{\sigma\mu})_{,\binom{i}{\alpha}} + \gamma^{\sigma\mu}(\ln\sqrt{\gamma})_{,\binom{i}{\alpha}}\right] = \left(\frac{1}{2}\gamma^{\sigma\mu}\gamma^{\lambda\tau} - \gamma^{\sigma\lambda}\gamma^{\mu\tau}\right)\left(g_{\lambda\tau,\binom{i}{\alpha}} + \varphi_{\lambda\tau,\binom{i}{\alpha}}\right), \tag{3.29}$$

$$[(\gamma^{\sigma\mu})_{,i} + \gamma^{\sigma\mu}(\ln\sqrt{\gamma})_{,i}] = \left(\frac{1}{2}\gamma^{\sigma\mu}\gamma^{\lambda\tau} - \gamma^{\sigma\lambda}\gamma^{\mu\tau}\right)(g_{\lambda\tau,i} + \varphi_{\lambda\tau,i}), \tag{3.30}$$

$$\begin{aligned}&\left[(\gamma^{\sigma\mu})_{,\binom{i}{\alpha}}(\ln\sqrt{\gamma})_{;\alpha} + (\gamma^{\sigma\mu})_{;\alpha}(\ln\sqrt{\gamma})_{,\binom{i}{\alpha}}\right] = \\ &-\frac{1}{2}\left(\gamma^{\sigma\lambda}\gamma^{\mu\tau}\gamma^{\rho\theta} + \gamma^{\sigma\rho}\gamma^{\mu\theta}\gamma^{\lambda\tau}\right)\left(g_{\rho\theta;\alpha}g_{\lambda\tau,\binom{i}{\alpha}} + g_{\rho\theta;\alpha}\varphi_{\lambda\tau,\binom{i}{\alpha}} + g_{\lambda\tau,\binom{i}{\alpha}}\varphi_{\rho\theta;\alpha} + \varphi_{\rho\theta;\alpha}\varphi_{\lambda\tau,\binom{i}{\alpha}}\right),\end{aligned} \tag{3.31}$$

$$\begin{aligned}&\left[(\gamma^{\sigma\mu})_{,\binom{i}{\alpha};\alpha} + \gamma^{\sigma\mu}\frac{1}{\sqrt{\gamma}}(\sqrt{\gamma})_{,\binom{i}{\alpha};\alpha}\right] = \\ &\left(\gamma^{\sigma\rho}\gamma^{\lambda\theta}\gamma^{\mu\tau} + \gamma^{\sigma\lambda}\gamma^{\mu\rho}\gamma^{\tau\theta} + \frac{1}{4}\gamma^{\sigma\mu}\gamma^{\rho\theta}\gamma^{\lambda\tau} - \frac{1}{2}\gamma^{\sigma\mu}\gamma^{\lambda\rho}\gamma^{\tau\theta}\right) \\ &\cdot\left(g_{\rho\theta;\alpha}g_{\lambda\tau,\binom{i}{\alpha}} + g_{\rho\theta;\alpha}\varphi_{\lambda\tau,\binom{i}{\alpha}} + g_{\lambda\tau,\binom{i}{\alpha}}\varphi_{\rho\theta;\alpha} + \varphi_{\rho\theta;\alpha}\varphi_{\lambda\tau,\binom{i}{\alpha}}\right) \\ &+\left(\frac{1}{2}\gamma^{\sigma\mu}\gamma^{\lambda\tau} - \gamma^{\sigma\lambda}\gamma^{\mu\tau}\right)\left(g_{\lambda\tau,\binom{i}{\alpha};\alpha} + \varphi_{\lambda\tau,\binom{i}{\alpha};\alpha}\right).\end{aligned} \tag{3.32}$$

By plugging the equations (3.29), (3.30), (3.31) and (3.32) into (3.18) and arranging the expression by the terms which contain the same contravariant metric components, one proves the assertion (3.28). □

The anisotropic Beltrami flow given in the previous theorem refers to a generalized Lagrange embedded surface (the most general case), hence it is also called generalized Lagrangian flow, or shortly, GL-flow.

Regarding the properties of the anisotropic metric γ, the structure on the embedded surface is classified as the one of the Finslerian, Lagrangian or generalized Lagrangian type.

If there is a fundamental function $F : T\Sigma \to \mathbb{R}$ satisfying the conditions from Definition 1.3.3, and which is related with the metric (3.14) by $\gamma = \frac{1}{2}\mathrm{Hess}(F^2)$[1], the embedded surface

[1] The Hessian is built by onsidering the directional argument.

$\Sigma_F = (\Sigma, \gamma)$ is said to be Finslerian. If there is a Lagrangian function $L : T\Sigma \to \mathbb{R}$ satisfying the conditions from Definition 1.4.3, and which is related with the metric (3.14) by $\gamma = \frac{1}{2}\mathrm{Hess}(L)$, the embedded surface $\Sigma_L = (\Sigma, \gamma)$ is said to be Lagrangian. Otherwise, the surface is of generalized Lagrangian type $\Sigma_{GL} = (\Sigma, \gamma)$.

In the following chapters we will develop anisotropic Beltrami flows for two particular cases. The Randers flow will be associated to the Finsler surface of Randers type, where the Finsler norm is the linearly deformed induced one (see Section 1.3.3.). It will be shown how the Synge-Beil flow evolves a generalized Lagrangian surface with induced metric deformed by the canonical vector field (see Section 1.4.2.).

3.5 The particular case of isometric embeddings

Isometric immersions are natural embeddings between two metric manifolds, which imply the induced metric on the embedded surface, and at the same time, they represent extremals of the Polyakov action with respect to embedded metric (see [102]). However, hey yield isotropic structures on the surface, and the directional impact in the Polyakov action can be achieved through a weight function. The corresponding Beltrami framework considers minimization of the weighted isotropic Polyakov action. Thus, the anisotropic metric structure reduces to the induced one $\gamma_{\sigma\mu} = g_{\sigma\mu}$, and the total contraction inside the Polyakov action gives the dimension of the submanifold, i.e.,

$$\gamma^{\sigma\mu} g_{\sigma\mu} = g^{\sigma\mu} g_{\sigma\mu} = n. \tag{3.33}$$

Hence, the Polyakov action has the following form

$$S(X) = n \int f \sqrt{g} dx^1 \dots dx^n.$$

By using the properties of the induced metric structure on the embedded surface, from Theorem 3.4.1 one gets the following result:

3.5.1. Proposition *Let the mapping X be the isometric immersion given by* (3.1) *into the Riemannian manifold (M, h), and let g be the induced metric structure. Then, the PDEs of the anisotropic Beltrami flow are*

$$\begin{aligned} \partial_t X^r = \; & \frac{n}{2} f_{,\binom{i}{\alpha};\alpha}\, h^{ir} + \frac{n}{2} f_{,\binom{i}{\alpha}} (\ln \sqrt{g})_{;\alpha}\, h^{ir} \\ & + \frac{n}{2} f_{;\alpha} (\ln \sqrt{g})_{,\binom{i}{\alpha}} h^{ir} - \frac{n}{2} f_{,i}\, h^{ir} + \frac{n}{2} f \tau^r(X). \end{aligned} \tag{3.34}$$

Proof. Taking the $\star$-derivative of (3.33), one can see that

$$(\gamma^{\sigma\mu})_\star\, g_{\sigma\mu} + \gamma^{\sigma\mu} g_{\sigma\mu\star} = 0.$$

Using this in (3.15) and employing Lemma 3.4.3 to simplify the factor which multiplies f, we obtain the formula (3.34). □

3.5.2. Corollary *If $f = f(X^i, h_{ij})$ is the weight function of the embedding (3.1) into a Euclidean space, with the induced metric on the surface, then the partial differential equations of the Beltrami flow become*[2]

$$\partial_t X^r = \frac{n}{2} f \tau^r(X) - \frac{n}{2} f_{,i}\, h^{ir} + \frac{n}{2} f_{,i}\, g^{\sigma\mu} X^i_\sigma X^r_\mu. \tag{3.35}$$

[2]The formula (3.35) is the corrected by the author version of the formula (13) from [114].

Proof. The reduction of the Beltrami framework to the isometric case means considering the Euclidean embedding space, the induced metric on the embedded surface and more freedom for the weight function, or, in other words

$$f_{,\binom{i}{\alpha}} = \frac{\partial f}{\partial X^i_\alpha} = 0, \qquad \frac{\partial f}{\partial g_{\sigma\mu}} = 0, \qquad \frac{\partial h_{ij}}{\partial x^\alpha} = 0,$$

which further, by the chain rule, lead to

$$f_{;\alpha} = \frac{\partial f}{\partial X^i}\frac{\partial X^i}{\partial x^\alpha} + \frac{\partial f}{\partial g_{\sigma\mu}}\frac{\partial g_{\sigma\mu}}{\partial x^\alpha} + \frac{\partial f}{\partial h_{ij}}\frac{\partial h_{ij}}{\partial x^\alpha} = f_{,i}X^i_\alpha.$$

The equality (3.26) yields

$$(\ln\sqrt{g})_{,\binom{i}{\alpha}}h^{ir} = \frac{1}{2}g^{\sigma\mu}(h_{il}\delta^\alpha_\sigma X^l_\mu + h_{ik}X^k_\sigma\delta^\alpha_\mu)h^{ir} = \frac{1}{2}(h_{il}X^l_\mu g^{\alpha\mu} + h_{ik}X^k_\sigma g^{\sigma\alpha})h^{ir} = g^{\alpha\mu}X^r_\mu.$$

Plugging these facts into (3.34) proves the statement. $\square$

Chapter 4

Particular cases of the evolution flow

So far we have introduced a geometric framework, namely the Beltrami framework, that is appropriate for the study of problems in image processing. The aim of this chapter is to develop anisotropic flows for Randers and Synge-Beil metric structures on the image surface in the Beltrami framework (X, M, Σ), for which we will assume that the embedding X as well as the Riemannian metric tensor field h on M are fixed, and only the anisotropic metric will be varied. Both Randers and Synge-Beil structures will be considered as deformations of the induced Riemannian metric g. Also, we will develop particular anisotropic flows of Randers, Ingarden and normalized Miron type for a Monge surface embedded into a 3-dimensional Riemannian space.

Throughout this chapter we shall use the following notation: x will refer to a point on the image surface Σ, and v to a tangent vector in $T_x\Sigma$. Then the induced g-quadratic form and the induced g-norm on $T_x\Sigma$ will be denoted by V and G, respectively:

$$V(x,v) = \|v\|_g^2 = g_{\sigma\mu}(x) v^\sigma v^\mu, \tag{4.1}$$

$$G(x,v) = \|v\|_g = \sqrt{g_{\sigma\mu}(x) v^\sigma v^\mu}. \tag{4.2}$$

In the sequel we shall omit the arguments and write just V and G, in order to simplify the expressions. The following lemma provides formulas for the derivatives of V and G.

4.0.3. Lemma *The derivatives of the induced g-quadratic form* (4.1) *and the induced g-norm* (4.2)*, are*

$$V_\star = g_{\sigma\mu\star} v^\sigma v^\mu, \qquad V_{,\binom{i}{\alpha};\alpha} = g_{\sigma\mu,\binom{i}{\alpha};\alpha}\, v^\sigma v^\mu, \tag{4.3}$$

$$G_\star = \frac{1}{2G} V_\star, \qquad G_{,\binom{i}{\alpha};\alpha} = \frac{1}{4G^3}\left(2V_{,\binom{i}{\alpha};\alpha} V - V_{,\binom{i}{\alpha}} V_{;\alpha}\right). \tag{4.4}$$

Proof. The expressions are obtained by the basic derivative rules. □

4.1 The general Randers case

Let us consider the embedded manifold of Finsler-Randers type $\Sigma_R = (\Sigma, \gamma)$, where γ arises from the Finsler fundamental function F that deforms the induced g-norm (4.2) by a linear (in v) function

$$\Omega(x, v) = b_\sigma(x) v^\sigma \tag{4.5}$$

given in all fibers $T_x\Sigma$

$$F(x, v) = \sqrt{g_{\sigma\mu} v^\sigma v^\mu} + b_\sigma v^\sigma = G + \Omega. \tag{4.6}$$

Coefficients b_σ of Ω are components of an 1-form over Σ, and depend on the embedding X, but also on the parameters (x^μ), i.e., $b_\sigma = b_\sigma(X^i(x^\mu), X^i_\alpha(x^\mu))$. Hence, we consider the following derivatives

$$b_{\sigma,i}, \quad b_{\sigma,\binom{i}{\alpha}}, \quad b_{\sigma;\alpha} = b_{\sigma\ ,i} X^i_\alpha + b_{\sigma,\binom{i}{\mu}} X^i_{\mu\alpha},$$

which define the derivatives of the scalar function Ω over $T\Sigma$,

$$\Omega_\star = b_{\sigma\star} v^\sigma, \quad \Omega_{,\binom{i}{\alpha};\alpha} = b_{\sigma,\binom{i}{\alpha};\alpha} v^\sigma. \tag{4.7}$$

The scalar functions on $T\Sigma$ produced by the induced g-norm G given by (4.2) and the linear function Ω given by (4.5), are

$$A = \frac{\Omega}{G}, \quad B = -\frac{\Omega}{G^3} = -\frac{\Omega}{GV}, \quad C = \frac{1}{G}.$$

The Randers fundamental function (4.6) produces by (1.30) the anisotropic metric tensor γ on Σ, whose covariant metric components are

$$\gamma_{\sigma\mu} = g_{\sigma\mu} + \varphi_{\sigma\mu}, \tag{4.8}$$

and the *Randers additional tensor* reads

$$\begin{aligned} \varphi_{\sigma\mu} &= A g_{\sigma\mu} + B g_{\sigma\rho} g_{\mu\theta} v^\rho v^\theta + C(g_{\sigma\rho} b_\mu + g_{\mu\rho} b_\sigma) v^\rho + b_\sigma b_\mu & (4.9) \\ &= A_{\sigma\mu} + B_{\sigma\mu\rho\theta} v^\rho v^\theta + C_{\sigma\mu\rho} v^\rho + b_\sigma b_\mu. & (4.10) \end{aligned}$$

The expression (4.9) contains the scalar functions, while the expression (4.10) involves the following d-tensor fields on $T\Sigma$ with the corresponding components:

$$\begin{aligned} &\widehat{A} = Ag, && A_{\sigma\mu} = A g_{\sigma\mu}, \\ &\widehat{B} = Bg \otimes g, && B_{\sigma\mu\rho\theta} = B g_{\sigma\rho} g_{\mu\theta}, \\ &\widehat{C} = C \cdot 2\mathrm{Sym}_{(13)}\left(g \otimes b\right), && C_{\sigma\mu\rho} = C(g_{\sigma\rho} b_\mu + g_{\mu\rho} b_\sigma), \end{aligned}$$

where the $\mathrm{Sym}_{(13)}$ operator means the symmetrization in the first and third indices. Notice that the functions $\varphi_{\alpha\beta}(x, v)$ are the components of a symmetric $(0, 2)$-type tensor field defined on the embedded surface Σ.

According to (1.31) we can express the components of the contravariant metric tensor $\gamma^{\sigma\mu}$ in terms of the inverse induced metric $g^{\sigma\mu}$

$$\gamma^{\sigma\mu} = g^{\sigma\mu} + \rho^{\sigma\mu}, \quad \rho^{\sigma\mu} = -\frac{\Omega}{F} g^{\sigma\mu} + \frac{\Omega + G\|b\|_g^2}{F^3} v^\sigma v^\mu - \frac{G}{F^2} g^{\sigma\alpha} b_\alpha v^\mu - \frac{G}{F^2} g^{\mu\alpha} b_\alpha v^\sigma,$$

where $\|b\|_g^2 = g^{\sigma\mu} b_\sigma b_\mu$ is the squared Frobenius norm of the 1-form $b_\sigma dx^\sigma$ in the Hilbert space of $(0, 1)$-type tensors on (Σ, g).

The Randers flow, which evolves the Randers embedded surface toward the state of the minimal Polyakov action, can be obtained by Theorem 3.4.2 or Theorem 3.4.5. Both of them require a detailed analysis of the derivatives of the metric tensor components. The first option implies consideration of the derivatives of the contravariant components of the metric tensor $\gamma^{\sigma\mu}$ and its determinant $\gamma = \left(\frac{F}{G}\right)^{n+1} g$. The second possibility involves Lemma 3.4.3, since the additive structure $\gamma_{\alpha\beta\star} = g_{\alpha\beta\star} + \varphi_{\alpha\beta\star}$ allows us to determine the derivatives of the additional Randers tensor:

$$\varphi_{\alpha\beta\star} = A_{\alpha\beta\star} + B_{\alpha\beta\mu\sigma\star} v^\mu v^\sigma + C_{\alpha\beta\sigma\star} v^\sigma + b_{\alpha\star} b_\beta + b_\alpha b_{\beta\star}.$$

Due to the complexity of the inverse metric tensor $\gamma^{\sigma\mu}$, we use Theorem 3.4.5, and the following auxiliary result.

4.1.1. Lemma *Let G and Ω be the scalar functions that characterize the Randers structure* (4.6)*, and let V be the g-induced quadratic form* (4.1)*. Then, we can express the $\star$-derivatives of the ratio $\frac{\Omega^p}{G^q}$ as follows*

$$\left(\frac{\Omega^p}{G^q}\right)_\star = \frac{\Omega^{p-1}}{G^{q+2}} \left(p\,\Omega_\star V - \frac{q}{2}\,\Omega\, V_\star\right), \quad p, q \in \mathbb{N}.$$

Proof. The derivative rules, the equation $V = G^2$, and the first expression from (4.4) yield

$$\begin{aligned}\left(\frac{\Omega^p}{G^q}\right)_\star &= \frac{1}{G^{2q}} \left(p\Omega^{p-1}\Omega_\star G^q - q\Omega^p G^{q-1} \frac{1}{2G} V_\star\right) \\ &= \frac{\Omega^{p-1} G^q}{G^{2q} G^2} \left(p\Omega_\star V - \frac{q}{2}\Omega V_\star\right),\end{aligned}$$

and hence the statement is proved. □

As a straightforward consequence of the previous lemma we have the following result that yields explicit forms of the derivatives of the scalar functions A, B and C, applicable for computing the derivatives of the Randers additional tensor, $\varphi_{\sigma\mu\star}$.

4.1.2. Lemma *The derivatives of the scalar functions A, B and C are*

$$A_\star = \frac{1}{GV}\left(\Omega_\star V - \frac{1}{2}\Omega V_\star\right), \tag{4.11}$$

$$B_\star = \frac{1}{GV^2}\left(\frac{3}{2}\Omega V_\star - \Omega_\star V\right), \tag{4.12}$$

$$C_\star = -\frac{1}{2GV} V_\star. \tag{4.13}$$

The mixed derivatives of the scalar functions A, B and C read

$$A_{,\binom{i}{\alpha};\alpha} = \frac{1}{G^5}\left(\Omega_{,\binom{i}{\alpha};\alpha} V^2 - \frac{1}{2}\Omega_{,\binom{i}{\alpha}} V_{;\alpha} V - \frac{1}{2}\Omega_{;\alpha} V_{,\binom{i}{\alpha}} V - \frac{1}{2}\Omega V_{,\binom{i}{\alpha};\alpha} V + \frac{3}{4}\Omega V_{,\binom{i}{\alpha}} V_{;\alpha}\right), \tag{4.14}$$

$$B_{,\binom{i}{\alpha};\alpha} = \frac{1}{G^7}\left(-\Omega_{,\binom{i}{\alpha};\alpha} V^2 + \frac{3}{2}\Omega_{,\binom{i}{\alpha}} V_{;\alpha} V + \frac{3}{2}\Omega_{;\alpha} V_{,\binom{i}{\alpha}} V + \frac{3}{2}\Omega V_{,\binom{i}{\alpha};\alpha} V - \frac{15}{4}\Omega V_{,\binom{i}{\alpha}} V_{;\alpha}\right), \tag{4.15}$$

$$C_{,\binom{i}{\alpha};\alpha} = \frac{1}{G^5}\left(\frac{3}{4} V_{;\alpha} V_{,\binom{i}{\alpha}} - \frac{1}{2} V V_{,\binom{i}{\alpha};\alpha}\right). \tag{4.16}$$

Proof. The first three relations follow from (4.3), (4.4), (4.7) and Lemma 4.1.1. Further, we calculate the derivative with respect to the parameters x^α of the equations (4.11), (4.12) and (4.13), with $\star =; \binom{i}{\alpha}$. Again, using the expression for $G_\star$ from Lemma 4.0.3, we obtain (4.14), (4.15) and (4.16). □

Now we can derive explicit expressions for the derivatives of the Randers additional tensor.

4.1.3. Proposition *The derivatives of the components of the additional tensor $\varphi_{\sigma\mu}$ in the Randers type metric on the induced surface Σ_R are given by*

$$\begin{aligned}
\varphi_{\sigma\mu\star} = & \frac{1}{G^3}\left[(\Omega_\star V - \frac{1}{2}\Omega V_\star)g_{\sigma\mu} + \Omega V g_{\sigma\mu\star}\right] + b_{\sigma\star}b_\mu + b_\sigma b_{\mu\star} \\
& + \frac{1}{G^5}\left[(\frac{3}{2}\Omega V_\star - \Omega_\star V)g_{\sigma\rho}g_{\mu\theta} - \Omega V(g_{\sigma\rho\star}g_{\mu\theta} + g_{\sigma\rho}g_{\mu\theta\star})\right] v^\rho v^\theta \\
& + \frac{1}{G^3}\left[V(g_{\sigma\rho\star}b_\mu + g_{\sigma\rho}b_{\mu\star} + g_{\mu\rho\star}b_\sigma + g_{\mu\rho}b_{\sigma\star}) - V_\star(g_{\sigma\rho}b_\mu + g_{\mu\rho}b_\sigma)\right] v^\rho.
\end{aligned} \tag{4.17}$$

The mixed derivatives of the additional tensor components $\varphi_{\sigma\mu}$ in the Randers type metric on the induced surface Σ_R are

$$\begin{aligned}
& \varphi_{\sigma\mu,\binom{i}{\alpha};\alpha} \\
= & \frac{1}{G^5}\Bigg[\left(\Omega_{,\binom{i}{\alpha};\alpha}V^2 - \frac{1}{2}\Omega_{,\binom{i}{\alpha}}V_{;\alpha}V - \frac{1}{2}\Omega_{;\alpha}V_{,\binom{i}{\alpha}}V - \frac{1}{2}\Omega V_{,\binom{i}{\alpha};\alpha}V + \frac{3}{4}\Omega V_{,\binom{i}{\alpha}}V_{;\alpha}\right)g_{\sigma\mu} \\
& \quad + V\left(\Omega_{,\binom{i}{\alpha}}V - \frac{1}{2}\Omega V_{,\binom{i}{\alpha}}\right)g_{\sigma\mu;\alpha} + V\left(\Omega_{;\alpha}V - \frac{1}{2}\Omega V_{;\alpha}\right)g_{\sigma\mu,\binom{i}{\alpha}} + \Omega V^2 g_{\sigma\mu,\binom{i}{\alpha};\alpha}\Bigg] \\
& + \frac{1}{G^7}\Bigg[\left(-\Omega_{,\binom{i}{\alpha};\alpha}V^2 + \frac{3}{2}\Omega_{,\binom{i}{\alpha}}V_{;\alpha}V + \frac{3}{2}\Omega_{;\alpha}V_{,\binom{i}{\alpha}}V + \frac{3}{2}\Omega V_{,\binom{i}{\alpha};\alpha}V - \frac{15}{4}\Omega V_{,\binom{i}{\alpha}}V_{;\alpha}\right)g_{\sigma\rho}g_{\mu\theta} \\
& \quad + V\left(\frac{3}{2}\Omega V_{,\binom{i}{\alpha}} - \Omega_{,\binom{i}{\alpha}}V\right)(g_{\sigma\rho;\alpha}g_{\mu\theta} + g_{\sigma\rho}g_{\mu\theta;\alpha}) \\
& \quad + V\left(\frac{3}{2}\Omega V_{;\alpha} - \Omega_{;\alpha}V\right)\left(g_{\sigma\rho,\binom{i}{\alpha}}g_{\mu\theta} + g_{\sigma\rho}g_{\mu\theta,\binom{i}{\alpha}}\right) \\
& \quad - \Omega V^2\left(g_{\sigma\rho,\binom{i}{\alpha};\alpha}g_{\mu\theta} + g_{\sigma\rho,\binom{i}{\alpha}}g_{\mu\theta;\alpha} + g_{\sigma\rho;\alpha}g_{\mu\theta,\binom{i}{\alpha}} + g_{\sigma\rho}g_{\mu\theta,\binom{i}{\alpha};\alpha}\right)\Bigg] v^\rho v^\theta \\
& + \frac{1}{G^5}\Bigg[\left(\frac{3}{4}V_{;\alpha}V_{,\binom{i}{\alpha}} - \frac{1}{2}VV_{,\binom{i}{\alpha};\alpha}\right)(g_{\sigma\rho}b_\mu + g_{\mu\rho}b_\sigma) \\
& \quad - VV_{,\binom{i}{\alpha}}(g_{\sigma\rho;\alpha}b_\mu + g_{\sigma\rho}b_{\mu;\alpha} + g_{\mu\rho;\alpha}b_\sigma + g_{\mu\rho}b_{\sigma;\alpha}) \\
& \quad - VV_{;\alpha}\left(g_{\sigma\rho,\binom{i}{\alpha}}b_\mu + g_{\sigma\rho}b_{\mu,\binom{i}{\alpha}} + g_{\mu\rho,\binom{i}{\alpha}}b_\sigma + g_{\mu\rho}b_{\sigma,\binom{i}{\alpha}}\right) \\
& \quad + V^2\Big(g_{\sigma\rho,\binom{i}{\alpha};\alpha}b_\mu + g_{\sigma\rho,\binom{i}{\alpha}}b_{\mu;\alpha} + g_{\sigma\rho;\alpha}b_{\mu,\binom{i}{\alpha}} + g_{\sigma\rho}b_{\mu,\binom{i}{\alpha};\alpha} \\
& \quad\quad + g_{\mu\rho,\binom{i}{\alpha};\alpha}b_\sigma + g_{\mu\rho,\binom{i}{\alpha}}b_{\sigma;\alpha} + g_{\mu\rho;\alpha}b_{\sigma,\binom{i}{\alpha}} + g_{\mu\rho}b_{\sigma,\binom{i}{\alpha};\alpha}\Big)\Bigg] v^\rho \\
& + b_{\sigma,\binom{i}{\alpha};\alpha}b_\mu + b_{\sigma,\binom{i}{\alpha}}b_{\mu;\alpha} + b_{\sigma;\alpha}b_{\mu,\binom{i}{\alpha}} + b_\sigma b_{\mu,\binom{i}{\alpha};\alpha}.
\end{aligned} \tag{4.18}$$

Proof. The Leibniz rule and the linearity of derivatives applied to the components of the tensors $\widehat{A}$, $\widehat{B}$ and $\widehat{C}$ yield

$$\begin{aligned}
A_{\alpha\beta\star} &= A_\star\, g_{\alpha\beta} + A g_{\alpha\beta\star} \\
B_{\alpha\beta\mu\sigma\star} &= B_\star\, g_{\alpha\mu} g_{\beta\sigma} + B g_{\alpha\mu\star}\, g_{\beta\sigma} + B g_{\alpha\mu}\, g_{\beta\sigma\star} \\
C_{\alpha\beta\sigma\star} &= C_\star\, (g_{\alpha\sigma} b_\beta + g_{\beta\sigma} b_\alpha) + C\,(g_{\alpha\sigma\star}\, b_\beta + g_{\beta\sigma}\, b_{\alpha\star} + g_{\alpha\sigma\star}\, b_\beta + g_{\beta\sigma}\, b_{\alpha\star})\,.
\end{aligned}$$

It then follows that the derivative of the additional Randers term (4.10), can be calculated as

$$\begin{aligned}
\varphi_{\sigma\mu\star} = {} & A_\star g_{\sigma\mu} + A g_{\sigma\mu\star} \\
& + [B_\star g_{\sigma\rho} g_{\mu\theta} + B g_{\sigma\rho\star} g_{\mu\theta} + B g_{\sigma\rho} g_{\mu\theta\star}]\, v^\rho v^\theta \\
& + [C_\star (g_{\sigma\rho} b_\mu + g_{\mu\rho} b_\sigma) + C(g_{\sigma\rho\star} b_\mu + g_{\sigma\rho} b_{\mu\star} + g_{\mu\rho\star} b_\sigma + g_{\mu\rho} b_{\sigma\star})]\, v^\rho \\
& + b_{\sigma\star} b_\mu + b_\sigma b_{\mu\star}.
\end{aligned}$$

Then, the substitution of the scalar functions derivatives (4.11)-(4.16) leads to (4.17).

By fixing the previous equation for $\star =, \binom{i}{\alpha}$ and by computing its derivative with respect to the parameter x^α, we yield

$$\begin{aligned}
\varphi_{\sigma\mu,\binom{i}{\alpha};\alpha} = {} & A_{,\binom{i}{\alpha};\alpha} g_{\sigma\mu} + A_{,\binom{i}{\alpha}} g_{\sigma\mu;\alpha} + A_{;\alpha} g_{\sigma\mu,\binom{i}{\alpha}} + A g_{\sigma\mu,\binom{i}{\alpha};\alpha} \\
& + \Big[B_{,\binom{i}{\alpha};\alpha} g_{\sigma\rho} g_{\mu\theta} + B_{,\binom{i}{\alpha}} (g_{\sigma\rho;\alpha} g_{\mu\theta} + g_{\sigma\rho} g_{\mu\theta;\alpha}) + B_{;\alpha} \Big(g_{\sigma\rho,\binom{i}{\alpha}} g_{\mu\theta} + g_{\sigma\rho} g_{\mu\theta,\binom{i}{\alpha}} \Big) \\
& \quad + B \Big(g_{\sigma\rho,\binom{i}{\alpha};\alpha} g_{\mu\theta} + g_{\sigma\rho,\binom{i}{\alpha}} g_{\mu\theta;\alpha} + g_{\sigma\rho;\alpha} g_{\mu\theta,\binom{i}{\alpha}} + g_{\sigma\rho} g_{\mu\theta,\binom{i}{\alpha};\alpha} \Big) \Big]\, v^\rho v^\theta \\
& + \Big[C_{,\binom{i}{\alpha};\alpha} (g_{\sigma\rho} b_\mu + g_{\mu\rho} b_\sigma) + C_{,\binom{i}{\alpha}} (g_{\sigma\rho;\alpha} b_\mu + g_{\sigma\rho} b_{\mu;\alpha} + g_{\mu\rho;\alpha} b_\sigma + g_{\mu\rho} b_{\sigma;\alpha}) \\
& \quad + C_{;\alpha} \Big(g_{\sigma\rho,\binom{i}{\alpha}} b_\mu + g_{\sigma\rho} b_{\mu,\binom{i}{\alpha}} + g_{\mu\rho,\binom{i}{\alpha}} b_\sigma + g_{\mu\rho} b_{\sigma,\binom{i}{\alpha}} \Big) \\
& \quad + C \Big(g_{\sigma\rho,\binom{i}{\alpha};\alpha} b_\mu + g_{\sigma\rho,\binom{i}{\alpha}} b_{\mu;\alpha} + g_{\sigma\rho;\alpha} b_{\mu,\binom{i}{\alpha}} + g_{\sigma\rho} b_{\mu,\binom{i}{\alpha};\alpha} \\
& \qquad + g_{\mu\rho,\binom{i}{\alpha};\alpha} b_\sigma + g_{\mu\rho,\binom{i}{\alpha}} b_{\sigma;\alpha} + g_{\mu\rho;\alpha} b_{\sigma,\binom{i}{\alpha}} + g_{\mu\rho} b_{\sigma,\binom{i}{\alpha};\alpha} \Big) \Big]\, v^\rho \\
& + b_{\sigma,\binom{i}{\alpha};\alpha} b_\mu + b_{\sigma,\binom{i}{\alpha}} b_{\mu;\alpha} + b_{\sigma;\alpha} b_{\mu,\binom{i}{\alpha}} + b_\sigma b_{\mu,\binom{i}{\alpha};\alpha}.
\end{aligned}$$

Then, by using the expressions (4.11)-(4.16), one obtains (4.18). □

Finally, the Randers embedded surface evolution can be expressed by the use of Theorem 3.4.5. We shall denote by $\Sigma_R = (\Sigma, \gamma)$ the Randers manifold embedded into the Riemannian manifold (M, h) by the mapping (3.1), with the anisotropic metric structure given by (4.8) and (4.9). The general Randers flow PDEs, which provide minimality of the Polyakov action on the Randers surface Σ_R, are given by

$$\begin{aligned}
\partial_t^{GR} X^r = {} & \tau^r(X) \\
& + \frac{1}{2} h^{ir} \Big[g_{\sigma\mu;\alpha} g_{\lambda\tau,\binom{i}{\alpha}} + g_{\sigma\mu} g_{\lambda\tau,\binom{i}{\alpha};\alpha} - g_{\sigma\mu} g_{\lambda\tau,i} + g_{\sigma\mu;\alpha} \varphi_{\lambda\tau,\binom{i}{\alpha}} + g_{\sigma\mu} \varphi_{\lambda\tau,\binom{i}{\alpha};\alpha} - g_{\sigma\mu} \varphi_{\lambda\tau,i} \Big] \\
& \quad \cdot \left\{ \tfrac{1}{2} \gamma^{\sigma\mu} \gamma^{\lambda\tau} - \gamma^{\sigma\lambda} \gamma^{\mu\tau} \right\} \\
& + \frac{1}{2} h^{ir} g_{\sigma\mu} \Big[g_{\rho\theta;\alpha} g_{\lambda\tau,\binom{i}{\alpha}} + g_{\rho\theta;\alpha} \varphi_{\lambda\tau,\binom{i}{\alpha}} + g_{\lambda\tau,\binom{i}{\alpha}} \varphi_{\rho\theta;\alpha} + \varphi_{\rho\theta;\alpha} \varphi_{\lambda\tau,\binom{i}{\alpha}} \Big] \\
& \quad \cdot \left\{ \gamma^{\sigma\rho} (\gamma^{\lambda\theta} \gamma^{\mu\tau} - \tfrac{1}{2} \gamma^{\mu\theta} \gamma^{\lambda\tau}) + \gamma^{\sigma\lambda} (\gamma^{\mu\rho} \gamma^{\tau\theta} - \tfrac{1}{2} \gamma^{\mu\tau} \gamma^{\rho\theta}) - \tfrac{1}{2} \gamma^{\sigma\mu} (\gamma^{\lambda\rho} \gamma^{\tau\theta} - \tfrac{1}{2} \gamma^{\rho\theta} \gamma^{\lambda\tau}) \right\},
\end{aligned} \tag{4.19}$$

where $\tau(X)$ is the tension of the embedding X (cf. (3.13)), $g_{\sigma\mu}$ is the induced metric tensor field and $\varphi_{\sigma\mu}$ is the Randers additional term (4.9) whose derivatives are given by (4.17) and (4.18).

4.1.1 The Randers case

In this section we shall consider the Beltrami framework with 2-dimensional domain embedded into a 3-dimensional Riemannian space $(\mathbb{R}^3, h)$. The corresponding image surface Σ is obtained as a Monge surface

$$X : (x^1, x^2) \to (x^1, x^2, I(x^1, x^2))$$

and endowed with the induced Riemannian metric $g_{\sigma\mu} = h_{ij} X^i_\sigma X^j_\mu$.

The gradient of the image surface, $\operatorname{grad} I = (g^{1\alpha} I_{x^\alpha}, g^{2\alpha} I_{x^\alpha})$, is the tangent vector that points in the direction of the greatest rate of increase of the feature $I(x^1, x^2)$. It naturally provides a deformation of the Riemannian norm into a Finslerian norm of Randers type

$$F_R(x, v) = \sqrt{g_{\sigma\mu} v^\sigma v^\mu} + \mathrm{pr}_{\operatorname{grad} I} v.$$

The term $\mathrm{pr}_{\operatorname{grad} I} v$ is the algebraic projection of an arbitrary tangent vector onto the gradient one, and a straightforward calculation expresses it in terms of components

$$\mathrm{pr}_{\operatorname{grad} I} v = \frac{\langle v, \operatorname{grad} I \rangle_g}{\langle \operatorname{grad} I, \operatorname{grad} I \rangle_g} = \frac{1}{P} I_{x^\sigma} v^\sigma,$$

where we use the brief notation P for the induced squared norm of the gradient vector

$$P = \|\operatorname{grad} I\|_g^2 = g^{\sigma\mu} I_{x^\sigma} I_{x^\mu} = \frac{1}{g}(I_{x^1}^2 + I_{x^2}^2).$$

If we consider the canonical Euclidean norm and denote its square of the gradient vector by $Z = I_{x^1}^2 + I_{x^2}^2$, we can write $P = \frac{1}{g} Z$. Further, the particular Finsler-Randers norm has the following form

$$F_R(x, v) = \sqrt{g_{\sigma\mu} v^\sigma v^\mu} + b_\sigma v^\sigma = G + \Omega_R, \tag{4.20}$$

where the particular linear deformation Ω_R has the following coefficients

$$b_\sigma = \frac{1}{P} I_{x^\sigma} = \frac{g}{Z} I_{x^\sigma}. \tag{4.21}$$

The anisotropic metric tensor of the particular Randers structure is $\gamma_{\sigma\mu} = g_{\sigma\mu} + \varphi_{\sigma\mu}$, and the particular Randers additional tensor has the following components:

$$\varphi_{\sigma\mu} = \frac{\Omega_R}{G} g_{\sigma\mu} - \frac{\Omega_R}{G^3} g_{\sigma\rho} g_{\mu\theta} v^\rho v^\theta + \frac{g}{GZ}(g_{\sigma\theta} I_{x^\mu} + g_{\mu\theta} I_{x^\sigma}) v^\theta + \frac{g^2}{Z^2} I_{x^\sigma} I_{x^\mu}. \tag{4.22}$$

4.1.4. Proposition *The particular linear function Ω_R, characterizing the Randers type embedded surface Σ_R with the fundamental function* (4.20), *has the derivatives* (4.7) *with*

$$
\begin{aligned}
b_{\sigma\,,i} &= 0; \\
b_{\sigma\,;\alpha} &= \frac{g}{Z} I_{x^\sigma x^\alpha} - \frac{1}{Z^2} Z_{;\alpha} I_{x^\sigma}; \\
b_{\sigma,\binom{3}{\alpha}} &= \frac{g}{Z}\delta^\alpha_\sigma - \frac{2}{Z^2} I_{x^\sigma} I_{x^\alpha}; \\
b_{\sigma,\binom{3}{\alpha};\alpha} &= \frac{1}{Z^3}\left(4Z_{;\alpha} I_{x^\sigma} I_{x^\alpha} - 2Z(I_{x^\alpha x^\alpha} I_{x^\sigma} + I_{x^\alpha} I_{x^\sigma x^\alpha}) - ZZ_{;\alpha}\delta^\alpha_\sigma\right);
\end{aligned}
$$

where $Z_{;\alpha} = 2I_{x^1} I_{x^1 x^\alpha} + 2I_{x^2} I_{x^2 x^\alpha}$.

Proof. By taking the derivatives of (4.21) one proves the assertions. In particular, $b_{\sigma,\binom{1}{\alpha}}$ and $b_{\sigma,\binom{2}{\alpha}}$ vanish, which follows from the form of the embedding. □

Properties of the particular Randers case, presented in Proposition 4.1.4, and Proposition 4.1.3 can be used in computing the derivatives of the additional Randers tensor. Hence, the Randers flow can be achieved by (4.19).

4.1.2 The Ingarden case

Another Randers type metric on the 2-dimensional surface Σ embedded into the Beltrami framework with Riemannian embedding space $(\mathbb{R}^3, h)$ as the Monge surface, can be obtained by the use of the gradient vector field grad I. Deforming the induced norm on the embedded surface by the Euclidean scalar product of an arbitrary tangent vector with grad I, one obtains

$$F(x,v) = \sqrt{g_{\sigma\mu} v^\sigma v^\mu} + I_{x^\sigma} v^\sigma. \tag{4.23}$$

According to the considerations presented in Subsections 1.3.2-1.3.4, the Finsler fundamental function (4.23) produces a Randers metric of special Ingarden type. The corresponding linear deformation of the induced norm is the following Ingarden linear function

$$\Omega_I = I_{x^\sigma} v^\sigma. \tag{4.24}$$

The anisotropic metric tensor of the particular Ingarden structure is $\gamma_{\sigma\mu} = g_{\sigma\mu} + \varphi_{\sigma\mu}$, and the particular Randers-Ingarden additional tensor has the following components:

$$\varphi_{\sigma\mu} = \frac{\Omega_I}{G} g_{\sigma\mu} - \frac{\Omega_I}{G^3} g_{\sigma\rho} g_{\mu\theta} v^\rho v^\theta + \frac{1}{G}(g_{\sigma\theta} I_{x^\mu} + g_{\mu\theta} I_{x^\sigma}) v^\theta + I_{x^\sigma} I_{x^\mu}. \tag{4.25}$$

The straightforward calculation leads to the following result:

4.1.5. Proposition *The linear function Ω_I which characterizes the particular Ingarden type embedded surface Σ_I with the fundamental function* (4.23), *has the derivatives* (4.7) *defined by*

$$
\begin{aligned}
& b_{\sigma\,,i} = 0; \\
& b_{\sigma\,;\alpha} = I_{x^\sigma x^\alpha}; \\
& b_{\sigma,\binom{1}{\alpha}} = 0, \quad b_{\sigma,\binom{2}{\alpha}} = 0, \quad b_{\sigma,\binom{3}{\alpha}} = \delta^\alpha_\sigma; \\
& b_{\sigma,\binom{i}{\alpha};\alpha} = 0.
\end{aligned}
$$

The particular Ingarden flow can be obtained by (4.19), where the derivatives of the additional Randers-Ingarden tensor can be evaluated by Propositions 4.1.3 and 4.1.5.

4.2 General-Lagrange evolution flow

Both Theorems 3.4.2 and 3.4.5 may produce the general-Lagrange flow, which evolves the embedded GL surface (Σ, γ) of the anisotropic Beltrami framework (X, M, Σ). While considering only Synge-Beil structures we employ Theorem 3.4.2.

The Synge-Beil type structure has simple components (covariant and contravariant ones) of the metric tensor, hence, the derivatives of both type metric components and the metric determinant can be directly computed by the algebraic Lemma 1.3.7, and further substituted in (3.18).

4.2.1 The Synge-Beil case

The Synge-Beil type metric on the embedded surface Σ has the following form

$$\gamma_{\sigma\mu} = g_{\sigma\mu} + c \cdot v_\sigma v_\mu, \tag{4.26}$$

where $g_{\sigma\mu}$ is the metric induced from the embedding space, $v_\sigma = g_{\sigma\mu} v^\mu$ is a covariant component of a vector tangent to the surface Σ and $c = c(X^i, X^i_\alpha)$ is a smooth scalar field over Σ with the following derivatives

$$c_{,i}; \quad c_{,\binom{i}{\alpha}}; \quad c_{;\alpha} = c_{,i} X^i_\alpha + c_{,\binom{i}{\sigma}} X^i_{\sigma\alpha}.$$

The algebraic Lemma 1.3.7 describes the determinant and the inverse metric tensor

$$\gamma = K g, \tag{4.27}$$

$$\gamma^{\sigma\mu} = g^{\sigma\mu} + S \cdot v^\sigma v^\mu, \tag{4.28}$$

where

$$K = 1 + cV, \tag{4.29}$$

$$S = \frac{-c}{1 + cV} = \frac{-c}{K}. \tag{4.30}$$

In order to apply Theorem 3.4.2 to this case, we need the following results.

4.2.1. Lemma *For the scalar functions K and S defined on $T\Sigma$ by (4.29) and (4.30), the $\star$-derivatives are*

$$\begin{aligned} K_\star &= c_\star V + c V_\star \\ S_\star &= \frac{1}{K^2}\left(c^2 V_\star - c_\star\right) \end{aligned}$$

and the mixed derivatives are

$$\begin{aligned} K_{,\binom{i}{\alpha};\alpha} &= c_{,\binom{i}{\alpha};\alpha} V + c_{,\binom{i}{\alpha}} V_{;\alpha} + c_{;\alpha} V_{,\binom{i}{\alpha}} + c V_{,\binom{i}{\alpha};\alpha} \\ S_{,\binom{i}{\alpha};\alpha} &= \frac{1}{K^3}\Big[c^3\left(V_{,\binom{i}{\alpha};\alpha} V - 2V_{,\binom{i}{\alpha}} V_{;\alpha}\right) - c_{,\binom{i}{\alpha};\alpha} \\ &\quad + 2c_{,\binom{i}{\alpha}} c V_{;\alpha} + 2c_{;\alpha} c V_{,\binom{i}{\alpha}} + c^2 V_{,\binom{i}{\alpha};\alpha} - V(c_{,\binom{i}{\alpha};\alpha} c - 2c_{,\binom{i}{\alpha}} c_{;\alpha})\Big]. \end{aligned}$$

Proof. The first equation is just the product rule for derivatives, and the second one follows from

$$
\begin{aligned}
S_\star &= \frac{1}{K^2}\left(cK_\star - c_\star K\right) \\
&= \frac{1}{K^2}\left(c(c_\star V + cV_\star) - c_\star(1 + cV)\right).
\end{aligned}
$$

Further, they respectively produce the third and fourth equations, by the use of relations (4.1), (4.29) and (4.30). □

In order to apply Theorem 3.4.2, it is also necessary to consider the derivatives of the determinant (4.27) and the inverse metric tensor (4.28) of the Synge-Beil metric (4.26).

4.2.2. Lemma *Let γ be a metric tensor of the Synge-Beil type with its components given by (4.26) on the embedded surface Σ. Then, the derivatives of the corresponding inverse tensor are given by*

$$
(\gamma^{\sigma\mu})_\star = (g^{\sigma\mu})_\star + S_\star v^\sigma v^\mu
$$

$$
(\gamma^{\sigma\mu})_{,\binom{i}{\alpha};\alpha} = (g^{\sigma\mu})_{,\binom{i}{\alpha};\alpha} + S_{,\binom{i}{\alpha};\alpha} v^\sigma v^\mu,
$$

where the first term on the right-hand side in both equations is explicitly related with the derivatives of the inverse induced metric components (3.21) *and* (3.22) *from Lemma 3.4.3 and Proposition 3.4.4.*

Proof. All the equations result from (4.28) and from the fact that v^σ are independent variables. □

4.2.3. Lemma *Let γ be a metric tensor of the Synge-Beil type with its components given by (4.26) on the embedded surface Σ. Then, the derivatives of the term $\ln\sqrt{\gamma}$ are*

$$
\begin{aligned}
(\ln\sqrt{\gamma})_\star &= \frac{1}{2\gamma}\left(K_\star g + K g_\star\right), \\
\frac{1}{\sqrt{\gamma}}(\sqrt{\gamma})_{,\binom{i}{\alpha};\alpha} &= \frac{1}{4K^2}\left(2KK_{,\binom{i}{\alpha};\alpha} - K_{,\binom{i}{\alpha}}K_{;\alpha}\right) \\
&\quad + \frac{1}{4g^2}\left(2gg_{,\binom{i}{\alpha};\alpha} - g_{,\binom{i}{\alpha}}g_{;\alpha}\right) + \frac{1}{4\gamma}\left(K_{,\binom{i}{\alpha}}g_{;\alpha} + K_{;\alpha}g_{,\binom{i}{\alpha}}\right),
\end{aligned}
$$

where g is the determinant of the induced metric.

Proof. The derivation rules and equation (4.27) yield (4.31), while another derivation of $\left(\ln\sqrt{\gamma}\right)_{,\binom{i}{\alpha}}$ produces (4.31). □

4.2.4. Theorem *The Synge-Beil evolution flow partial differential equations, which provide minimality of the Polyakov energy on the surface Σ_{SB} embedded into the Riemannian manifold*

(M,h) by the mapping (3.1), are given by

$$
\begin{aligned}
&\partial_t^{SB} X^r \\
&= \tau^r(X) + \frac{1}{2}h^{ir}\left[(g^{\sigma\mu})_{,\binom{i}{\alpha};\alpha} g_{\sigma\mu} + (g^{\sigma\mu})_{,\binom{i}{\alpha}} g_{\sigma\mu;\alpha} + g^{\sigma\mu} g_{\sigma\mu,i}\right] \\
&\quad + \frac{1}{2}h^{ir}\left[c\frac{1}{2\gamma}\left(g^{\sigma\mu}g_{\sigma\mu;\alpha}(V_{,\binom{i}{\alpha}}g + Vg_{,\binom{i}{\alpha}}) - n(V_{,i}g + Vg_{,i})\right) + c_{,\binom{i}{\alpha}}\frac{1}{2\gamma}Vg^{\sigma\mu}g_{\sigma\mu;\alpha}g\right. \\
&\qquad \left. - c_{,i}\frac{n}{2\gamma}Vg + + \frac{1}{2\gamma}\left(g^{\sigma\mu}g_{\sigma\mu;\alpha}g_{,\binom{i}{\alpha}} - ng_{,i}\right)\right] \\
&\quad + \frac{1}{2}h^{ir}\frac{1}{2K^2g}\left[c^2\left((V_{,\binom{i}{\alpha}}g - Vg_{,\binom{i}{\alpha}})g_{\sigma\mu;\alpha} + (Vg_{,i} - V_{,i}g)g_{\sigma\mu}\right) - cc_{,\binom{i}{\alpha}}Vg_{\sigma\mu;\alpha}g\right. \\
&\qquad \left. + cc_{,i}Vg_{\sigma\mu}g - 2c_{,\binom{i}{\alpha}}g_{\sigma\mu;\alpha}g + 2c_{,i}g_{\sigma\mu}g - cg_{\sigma\mu;\alpha}g_{,\binom{i}{\alpha}} + cg_{\sigma\mu}g_{,i}\right]v^\sigma v^\mu \\
&\quad + \frac{1}{2}h^{ir}\frac{1}{4\gamma^2}\left[c^2\left(2V\left\{V_{;\alpha}(g^{\sigma\mu})_{,\binom{i}{\alpha}} + V_{,\binom{i}{\alpha}}(g^{\sigma\mu})_{;\alpha}\right\}g_{\sigma\mu}g^2\right.\right. \\
&\qquad + 2V^2\left\{(g^{\sigma\mu})_{,\binom{i}{\alpha}}g_{;\alpha} + (g^{\sigma\mu})_{;\alpha}g_{,\binom{i}{\alpha}}\right\}g_{\sigma\mu}g + n\left\{2VV_{,\binom{i}{\alpha};\alpha} - V_{,\binom{i}{\alpha}}V_{;\alpha}\right\}g^2 \\
&\qquad \left. + nV^2\left\{2gg_{,\binom{i}{\alpha};\alpha} - g_{,\binom{i}{\alpha}}g_{;\alpha}\right\} + nV\left\{V_{,\binom{i}{\alpha}}g_{;\alpha} + V_{;\alpha}g_{,\binom{i}{\alpha}}\right\}g\right) \\
&\qquad + n\left(2cc_{,\binom{i}{\alpha};\alpha} - c_{,\binom{i}{\alpha}}c_{;\alpha}\right)V^2g^2 + cc_{,\binom{i}{\alpha}}V\left(2V(g^{\sigma\mu})_{;\alpha}g_{\sigma\mu}g + nV_{;\alpha}g + nVg_{;\alpha}\right)g \\
&\qquad + cc_{;\alpha}V\left(2V(g^{\sigma\mu})_{,\binom{i}{\alpha}}g_{\sigma\mu}g + nV_{,\binom{i}{\alpha}}g + nVg_{,\binom{i}{\alpha}}\right)g + 2nc_{,\binom{i}{\alpha};\alpha}Vg^2 \\
&\qquad + c_{,\binom{i}{\alpha}}\left(2V(g^{\sigma\mu})_{;\alpha}g_{\sigma\mu}g + 2nV_{;\alpha}g + nVg_{;\alpha}\right)g \\
&\qquad + c_{;\alpha}\left(2V(g^{\sigma\mu})_{,\binom{i}{\alpha}}g_{\sigma\mu}g + 2nV_{,\binom{i}{\alpha}}g + nVg_{,\binom{i}{\alpha}}\right)g \\
&\qquad + c\left(2\left\{V_{;\alpha}g + 2Vg_{;\alpha}\right\}(g^{\sigma\mu})_{,\binom{i}{\alpha}}g_{\sigma\mu}g + 2\left\{V_{,\binom{i}{\alpha}}g + 2Vg_{,\binom{i}{\alpha}}\right\}(g^{\sigma\mu})_{;\alpha}g_{\sigma\mu}g\right. \\
&\qquad \left. + 2nV_{,\binom{i}{\alpha};\alpha}g^2 + 2nV\{2gg_{,\binom{i}{\alpha};\alpha} - g_{,\binom{i}{\alpha}}g_{;\alpha}\} + n\{V_{,\binom{i}{\alpha}}g_{;\alpha} + V_{;\alpha}g_{,\binom{i}{\alpha}}\}g\right) \\
&\qquad \left. + 2\left((g^{\sigma\mu})_{,\binom{i}{\alpha}}g_{;\alpha} + (g^{\sigma\mu})_{;\alpha}g_{,\binom{i}{\alpha}}\right)g_{\sigma\mu}g + n(2gg_{,\binom{i}{\alpha};\alpha} - g_{,\binom{i}{\alpha}}g_{;\alpha})\right] \\
&\quad + \frac{1}{2}h^{ir}\frac{V}{K^3g}\left[c^3\left(\left\{2VV_{,\binom{i}{\alpha};\alpha} - V_{,\binom{i}{\alpha}}V_{;\alpha}\right\}g^2 - V^2\left\{2gg_{,\binom{i}{\alpha};\alpha} - g_{,\binom{i}{\alpha}}g_{;\alpha}\right\} - 2V_{,\binom{i}{\alpha}}V_{;\alpha}g^2\right.\right. \\
&\qquad \left. + V\left\{V_{,\binom{i}{\alpha}}g_{;\alpha} + V_{;\alpha}g_{,\binom{i}{\alpha}}\right\}g\right) + c^2c_{,\binom{i}{\alpha}}V(V_{;\alpha}g - Vg_{;\alpha})g + c^2c_{;\alpha}V\left(V_{,\binom{i}{\alpha}}g - Vg_{,\binom{i}{\alpha}}\right)g \\
&\qquad - c\left(2cc_{,\binom{i}{\alpha};\alpha} - c_{,\binom{i}{\alpha}}c_{;\alpha}\right)V^2g^2 + 2\left(2c_{,\binom{i}{\alpha}}c_{;\alpha} - 3cc_{,\binom{i}{\alpha};\alpha}\right)Vg^2 \\
&\qquad + c^2\left(V_{,\binom{i}{\alpha};\alpha}g^2 + \left\{V_{,\binom{i}{\alpha}}g_{;\alpha} + V_{;\alpha}g_{,\binom{i}{\alpha}}\right\}g - 2V\left\{2gg_{,\binom{i}{\alpha};\alpha} - g_{,\binom{i}{\alpha}}g_{;\alpha}\right\}\right) \\
&\qquad + cc_{,\binom{i}{\alpha}}(4V_{;\alpha}g - 3Vg_{;\alpha})g + cc_{;\alpha}\left(4V_{,\binom{i}{\alpha}}g - 3Vg_{,\binom{i}{\alpha}}\right)g - c\left(2gg_{,\binom{i}{\alpha};\alpha} - g_{,\binom{i}{\alpha}}g_{;\alpha}\right) \\
&\qquad \left. - 4c_{,\binom{i}{\alpha};\alpha}g^2 - 2c_{,\binom{i}{\alpha}}g_{;\alpha}g - 2c_{;\alpha}g_{,\binom{i}{\alpha}}g\right]
\end{aligned} \tag{4.31}
$$

where $\tau(X)$ is the tension (3.13) of the embedding X, $g_{\sigma\mu} = h_{kl}X^k_\sigma X^l_\mu$ is the induced metric tensor field and $c = c(X)$ is the scalar field which defines the Synge-Beil metric.

Proof. The substitution of the derivatives expressions obtained in Lemma 4.2.2, 4.2.3 and 4.2.1 into the anisotropic Beltrami flow (3.18), yields (4.31). □

4.2.2 The normalized Miron case

We will present one particular case of the Synge-Beil type metric structure on the Monge surface Σ. A Synge-Beil deformation (1.40) of the induced Riemannian metric g, with particularly chosen scalar function $c = \frac{1}{V}$ (see (4.1)), yields the normalized Miron metric

$$\gamma_{\sigma\mu} = g_{\sigma\mu} + \frac{1}{V} v_\sigma v_\mu, \tag{4.32}$$

where $v_\sigma = g_{\sigma\mu} v^\mu$ are covariant components of a tangent vector v.

Characteristic scalar functions of the NM-structure are

$$K = 2 \quad \text{and} \quad S = \frac{-1}{2V},$$

hence, the components of the inverse metric tensor and the determinant are

$$\gamma^{\sigma\mu} = g^{\sigma\mu} - \frac{1}{2V} v^\sigma v^\mu, \qquad \gamma = 2g. \tag{4.33}$$

In order to apply Theorem 3.4.2 to $\Sigma_{NM} = (\Sigma, \gamma)$ with the anisotropic NM-metric (4.32) one can use the adjusted flow for general Synge-Beil structures (4.31) by plugging therein derivatives obtained in Lemma 4.2.1 and evaluating derivatives of the scalar function c. However, due to the simplicity of the scalar functions c, K, S and γ one can evaluate the terms in (3.18) directly. Thus, the straightforward calculation gives the following result:

4.2.5. Proposition *The components of the inverse NM-metric and the determinant of the NM-metric* (4.33) *have the following derivatives*

$$\begin{aligned}
(\gamma^{\sigma\mu})_* \quad &= (g^{\sigma\mu})_* + \frac{1}{2V^2} V_* v^\sigma v^\mu \\
(\gamma^{\sigma\mu})_{,\binom{i}{\alpha};\alpha} \quad &= (g^{\sigma\mu})_{,\binom{i}{\alpha};\alpha} + \frac{1}{2V^3}\left(V V_{,\binom{i}{\alpha};\alpha} - 2V_{,\binom{i}{\alpha}} V_{;\alpha}\right) \\
(\ln\sqrt{\gamma})_* \quad &= \frac{1}{2g} g_* \\
\frac{1}{\sqrt{\gamma}}(\sqrt{\gamma})_{,\binom{i}{\alpha};\alpha} \quad &= \frac{1}{4g^2}\left(2g g_{,\binom{i}{\alpha};\alpha} - g_{,\binom{i}{\alpha}} g_{;\alpha}\right).
\end{aligned}$$

4.2.6. Proposition *Let Σ_{NM} be the image surface of the Beltrami framework $(X, (\mathbb{R}^3, h), \Sigma_{NM})$, endowed with the normalized Miron metric* (4.32). *The NM flow that minimizes the Polyakov* *action of the surface Σ_{NM}, has the following equations*

$$\begin{aligned}\partial_t^{NM} X^r = {} & \tau^r(X) \\ & +\frac{1}{2}h^{ir}\Big\{ g_{\sigma\mu;\alpha}\left[(g^{\sigma\mu})_{,\binom{i}{\alpha}} + \frac{1}{2g}g^{\sigma\mu}g_{,\binom{i}{\alpha}} + \left(\frac{1}{V^2}V_{,\binom{i}{\alpha}} - \frac{1}{4Vg}g_{,\binom{i}{\alpha}}\right)v^\sigma v^\mu \right] \\ & \quad + g_{\sigma\mu}\Bigg[(g^{\sigma\mu})_{,\binom{i}{\alpha};\alpha} + \frac{1}{2V^3}\left(VV_{,\binom{i}{\alpha};\alpha} - 2V_{,\binom{i}{\alpha}}V_{;\alpha}\right) \\ & \qquad + \frac{1}{2g}\left((g^{\sigma\mu})_{,\binom{i}{\alpha}}g_{;\alpha} + (g^{\sigma\mu})_{;\alpha}g_{,\binom{i}{\alpha}} - (g^{\sigma\mu})_{,i}\right)\Bigg] \\ & \quad + \frac{n}{4g^2}\left(2gg_{,\binom{i}{\alpha};\alpha} - g_{,\binom{i}{\alpha}}g_{;\alpha} - 2gg_{,i}\right) + \frac{1}{2V^2}\left(VV_{,\binom{i}{\alpha};\alpha} - 2V_{,\binom{i}{\alpha}}V_{;\alpha}\right) - \frac{1}{4Vg}V_{,i} \\ & \quad + \frac{1}{4Vg}\left(V_{,\binom{i}{\alpha}}g_{;\alpha} + V_{;\alpha}g_{,\binom{i}{\alpha}}\right) - \frac{1}{8g^2}\left(2gg_{,\binom{i}{\alpha};\alpha} - g_{,\binom{i}{\alpha}}g_{;\alpha}\right) - \frac{1}{2V}V_{,i} - \frac{1}{4g}g_{,i}\Big\}. \end{aligned} \tag{4.34}$$

Proof. The proof is obtained by plugging results of Proposition 4.2.5 into the general anisotropic Beltrami flow (3.18). □

Chapter 5

Applications in image processing

The last chapter is devoted to applying the geometric approach to image processing, that will be presented in accordance with [63, 64, 95, 103]. A comprehensive mathematical background of the theory can be found in [64, 95], while we refer to [59, 95] for image processing terminology.

The chapter is organized as follows. First, we present the Beltrami framework as a mathematical model of a digital image, and the discretization of theoretical results. In the second section several examples of classical (isotropic) Beltrami flows applications are outlined, while the last section considers possible applications of the new theoretical results obtained in Section 3.4 and Chapter 4.

5.1 Beltrami framework in image processing

Image processing commonly uses the Beltrami framework for modelling digital images as surfaces over a 2-dimensional bounded continuous domain, a subset of $\mathbb{R}^2_+$. The parameter coordinates are (x^1, x^2) and the embedding is given by

$$X : (x^1, x^2) \to (x^1, x^2, I(x^1, x^2))$$

where $I(x^1, x^2)$ is regarded as an image feature, and can be scalar, vector or even tensor valued. Monochrome (grayscale) images are described with scalar values of $I(x^1, x^2)$, while vector valued $I(x^1, x^2) = (I^R, I^G, I^B)$ refer to color images (see [63, 103]). Tensorial features are extremely useful in the so called diffusion tensor image regularization [56].

In this chapter we will focus on monochrome image surfaces Σ obtained as Monge surfaces in $\mathbb{R}^3$ endowed with the Euclidean metric, i.e., on the Beltrami framework $(X, \mathbb{R}^3, \Sigma)$ presented in Section 3.3.

Regardless of the chosen Polyakov action type that has to be minimized, the obtained Beltrami flow is a continuous function. Hence, the theoretical results should be discretized, in order to become applicable in image processing (see Fig. 5.1).

The discretization of an image surface from the Beltrami framework is induced by the discretization of the domain, hence the corresponding (monochrome) image is viewed as an image matrix $\Sigma = (I(i, j))$ whose elements $I(i, j)$ are in correspondence with the locations of the pixels of the image $(i, j) = (x^1, x^2) =: x$ and their values $I(i, j) \in \{0, 1, \dots, 255\}$ represent the level of their grey color intensity. The matrix dimensions are defined by the image resolution.

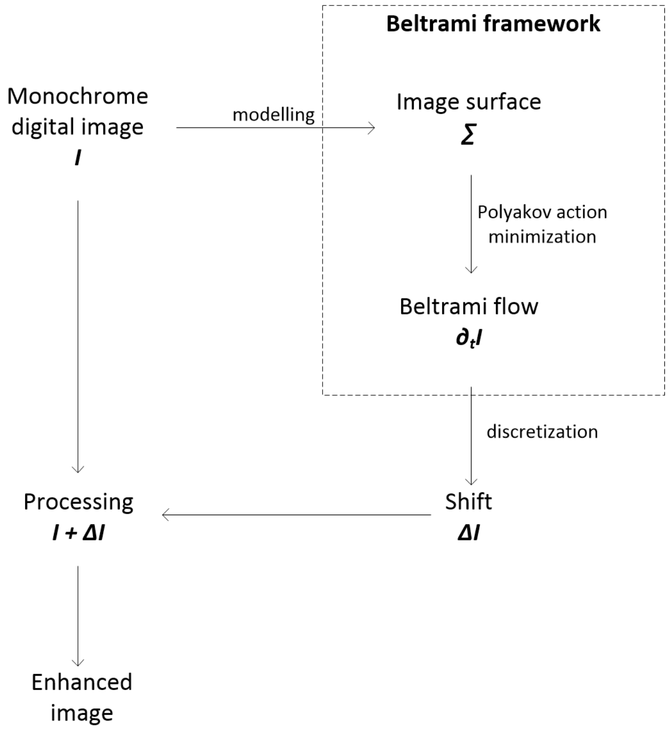

Figure 5.1: Image processing by the use of Beltrami framework

The partial derivatives of the feature are respectively determined by

$$
\begin{aligned}
&I_{x^1}(i,j) = I(i+1,j) - I(i,j),\\
&I_{x^2}(i,j) = I(i,j+1) - I(i,j),\\
&I_{x^1x^1}(i,j) = I(i+2,j) + I(i,j) - 2I(i+1,j),\\
&I_{x^1x^2}(i,j) = I(i+1,j+1) + I(i,j) - I(i+1,j) - I(i,j+1),\\
&I_{x^2x^2}(i,j) = I(i,j+2) + I(i,j) - 2I(i,j+1).
\end{aligned}
$$

Tangent vectors in a discrete model point to the neighboring pixels

$$v = (v^1, v^2) \in \{(-1,-1), (-1,0), (-1,1), (0,-1), (0,1), (1,-1), (1,0), (1,1)\}.$$

The gradient vector is discretized by the shift tangent vector computed as max-abs of the shifts towards the pixels of the eight neighbors of the current pixel. Namely, a direction of maximal difference between the feature values in the considered pixel (i,j) and its neighbors $|I(i,j) - I(i+v^1, j+v^2)|$ determines the gradient vector $v(i,j)$.

The image surface $I(x^1,x^2)$ evolves as a geometric active surface by the Beltrami flow PDE $\partial_t I$. The evolution is discretized in the frame of the level set formulation ([64]), and is gained by the successive shifting of the grayscale image

$$I(i,j) \to I(i,j) + \triangle I(i,j),$$

where $\triangle I(i,j)$ discretizes one of the Beltrami flows $\partial_t I$.

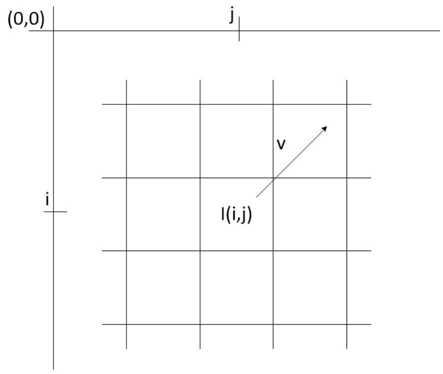

Figure 5.2: An element of image matrix and the tangent vector $v = (-1, 1)$.

5.2 Applications of isotropic flows

Classical Beltrami frameworks are widely used in image processing. Weighted and non-weighted Polyakov actions taken for various embedding metrics, commonly of Euclidean type, produce different flows and hence different processing effects. Offen, the induced embedded metric is of Riemannian type, and an anisotropic impact can be reached through the weight function. Produced Beltrami flows are referred to as the isotropic flows, and the corresponding theoretical background is presented in Sections 3.1-3.3.

The isotropic Beltrami evolution of the monochrome image $\Sigma = (I(i,j))$ is achieved by successive shifting, where each iteration implies the following steps:

- accessing pixel and its neighborhood-data (excluding the boundary of the image), in order to get the corresponding feature value I;
- determining weight function value (optionally) and the shift value $\triangle I(i,j)$;
- computing the modified feature value, $I \to I + \triangle I$.

An appropriate embedding space, an embedded metric, and a weight function are chosen by the purpose of the processing.

In the sequel we indicate some applications, while their comprehensive overview can be found in [95, 113].

Many linear and non-linear scale space methods of image processing can be expressed as an appropriate Beltrami flow corresponding to a certain embedding metric and a certain weight function [36, 63]. The main property of scale spaces is the embedding metric with the following components

$$(h_{ij}) = \operatorname{diag}\left(\frac{1}{c^2} I_n, \frac{1}{c^2 \rho^2}\right),$$

where n is the spatial dimension, I_n is the identity matrix, and c and ρ are conductance and density functions from a general model of heat diffusion transfer [46, 47].

The Euclidean embedding metric, through the induced metric, produces a Beltrami flow that evolves the image surface toward a minimal area, hence it is usually called mean curvature flow. This process is edge-preserving, or equivalently area-preserving, hence appropriate for various kinds of image enhancements, e.g., smoothing, denoising, contrast enhancement

[63, 95]. The image evolution for the purpose of smoothing is often called Gauss filtering, and for a monochrome image modelled in the Beltrami framework (3.9)-(3.10), it is gained by the Beltrami flow (3.12),

$$\triangle I = \frac{1}{g^2}\left(I_{x^1x^1}g_{22} + I_{x^2x^2}g_{11} - 2I_{x^1x^2}g_{12}\right). \tag{5.1}$$

Further applications of this type edge-preserving Beltrami flow are in segmentation, registration and object extraction. In image segmentation process presented in [97], the same Beltrami framework (3.9)-(3.10) is used, but the weighted Polyakov action is minimized. The weight function is taken as the edge-detector function

$$f(x^1,x^2) = \left(1 + \frac{1}{\beta^2}\|\nabla G(x^1,x^2) * I(x^1,x^2)\|^2\right)^{-1},$$

where ∇G is derivative of the Gaussian kernel and $*$ denotes the convolution. Hence, the Beltrami flow arises from (3.11), and the obtained evolution produces clear separation of the image segments. A generalization of this method is presented in [36], as the multiscale active contours method. An arbitrary weight function is taken, and the embedded surface is considered as a level-set-function (see [82]).

Image registration processes two images, one of them, I, is embedded into the Beltrami framework (3.9)-(3.10), and the other one is seen as the target image I_T. In [67, 110], the intensity mismatch $f(x^1,x^2) = I_T(x^1,x^2) - I(x^1,x^2)$ is taken as the weight function, and β^2 is related to the topology of objects on the images. The evolution of the image I toward the target one is gained by the flow (3.11). The geodesic active fields approach to image registration is proposed in [114, 113, 115], where the embedded surface does not represent an image, but the deformation field between two images to be registered. Three different weight functions are considered: squared error, local joint entropy and absolute error. The simplest image registration is a stereo vision, where two images differ only in lateral shift. Hence the deformation field consists of scalar values $u(x^1,x^2) = I_T(x^1,x^2) - I(x^1,x^2)$, and can be embedded into the Beltrami framework with the third component in the embedding (3.9) denoted by u (the notation in (3.10) has to be adjusted, too). One of the considered weight functions is the squared error $f(x^1,x^2,u) = \left((I(x^1,x^2) + u(x^1,x^2) - I_T(x^1,x^2))\right)^2$, and the Beltrami flow is obtained by (3.11).

Some enhancements of color images, processed by the use of Beltrami frameworks are presented in [93, 104]. Beltrami flow of the mean curvature type is also suitable for texture enhancement, but the embedding has to be from 4-dimensional to 6-dimensional space [63].

5.3 Anisotropic flows - tentative applications

In our developed approach, the concept of anisotropic Beltrami flow refers to the employment of anisotropic metrics on the image surface and non-weighted Polyakov action. We shall further implement the theoretical results obtained in Chapter 4 into the Beltrami framework presented in Section 3.3. In the application, the embedding (3.9) will be discretized by taking $x^1 = i,\ x^2 = j$, and the induced metric components (3.10) will be evaluated in each pixel.

Since the metric tensor $(h_{ij}) = \mathrm{diag}(1,1,\beta^2)$ is constant, by using Proposition 3.4.4 and Lemma 4.0.3, one can prove the following results, which are essential in the implementation process

5.3.1. Corollary *The induced metric tensor on the Monge surface in the Beltrami framework* (3.9)-(3.10) *has the following nonvanishing derivatives*

$$\begin{aligned} g_{\sigma\mu;\alpha} &= \beta^2 I_{\sigma\alpha} I_\mu + \beta^2 I_\sigma I_{\mu\alpha} && (5.2)\\ g_{\sigma\mu,\binom{3}{\alpha}} &= \beta^2 \delta^\alpha_\sigma I_\mu + \beta^2 I_\sigma \delta^\alpha_\mu && (5.3)\\ g_{\sigma\mu,\binom{3}{\alpha};\alpha} &= 2\beta^2 I_{\sigma\mu}. && (5.4) \end{aligned}$$

The induced g-quadratic norm V is

$$V = (v^1)^2 + (v^2)^2 + \beta^2 \left(I^2_{x^1}(v^1)^2 + 2I_{x^1}I_{x^2}v^1v^2 + I^2_{x^2}(v^2)^2 \right). \tag{5.5}$$

5.3.2. Corollary *The derivatives of the induced g-quadratic form $V = g_{\sigma\mu}v^\sigma v^\mu$ in the Beltrami framework* (3.9)-(3.10), *are*

$$\begin{aligned} V_{,i} &= 0,\\ V_{;\alpha} &= 2\beta^2 \left(I_{x^1}I_{x^1x^\alpha}(v^1)^2 + (I_{x^1x^\alpha}I_{x^2} + I_{x^1}I_{x^2x^\alpha})v^1v^2 + I_{x^2}I_{x^2x^\alpha}(v^2)^2 \right),\\ V_{,\binom{3}{1}} &= 2\beta^2 \left(I_{x^1}(v^1)^2 + I_{x^2}v^1v^2 \right),\\ V_{,\binom{3}{2}} &= 2\beta^2 \left(I_{x^1}v^1v^2 + I_{x^2}(v^2)^2 \right),\\ V_{,\binom{3}{\alpha};\alpha} &= 2\beta^2 \left(I_{x^1x^1}(v^1)^2 + 2I_{x^1x^2}v^1v^2 + I_{x^2x^2}(v^2)^2 \right). \end{aligned}$$

The aim here is to consider and analyze the following types of Beltrami flows: particular Randers, Ingarden, and normalized Miron. Therefore, we need the exact forms of the corresponding metric tensors components.

The particular Randers flow

The linear deformation Ω_R of the induced norm $G = \sqrt{V}$ in the particular Randers case (4.20)-(4.21), is given by

$$\Omega_R = b_{R\sigma}v^\sigma = \left(\frac{1}{Z} + \beta^2\right)(I_{x^1}v^1 + I_{x^2}v^2), \tag{5.6}$$

where $Z = I^2_{x^1} + I^2_{x^2}$. The particular Randers additional tensor components (4.22), can be evaluated as

$$\begin{aligned} \varphi_{R11} = \;& \frac{\Omega_R}{G}g_{11} - \frac{\Omega_R}{G^3}\left(g^2_{11}(v^1)^2 + 2g_{11}g_{12}v^1v^2 + g^2_{12}(v^2)^2\right)\\ &+\frac{2}{G}\left(\frac{1}{Z}+\beta^2\right)I_{x^1}(g_{11}v^1 + g_{12}v^2) + \left(\frac{1}{Z}+\beta^2\right)^2 I^2_{x^1},\\ \varphi_{R12} = \;& \varphi_{R21} = \frac{\Omega_R}{G}g_{12} - \frac{\Omega_R}{G^3}\left(g_{11}g_{12}(v^1)^2 + (g_{11}g_{22} + g^2_{12})v^1v^2 + g_{12}g_{22}(v^2)^2\right)\\ &+\frac{1}{G}\left(\frac{1}{Z}+\beta^2\right)(g_{11}I_{x^2}v^1 + g_{12}I_{x^2}v^2 + g_{12}I_{x^1}v^1 + g_{22}I_{x^1}v^2) + \left(\frac{1}{Z}+\beta^2\right)^2 I_{x^1}I_{x^2},\\ \varphi_{R22} = \;& \frac{\Omega_R}{G}g_{22} - \frac{\Omega_R}{G^3}\left(g^2_{21}(v^1)^2 + 2g_{12}g_{22}v^1v^2 + g^2_{22}(v^2)^2\right)\\ &+\frac{2}{G}\left(\frac{1}{Z}+\beta^2\right)I_{x^2}(g_{12}v^1 + g_{22}v^2) + \left(\frac{1}{Z}+\beta^2\right)^2 I^2_{x^2}. \end{aligned}$$

The derivatives of the $\varphi_{R\sigma\mu}$, which appear in the flow expression, can be obtained by Proposition 4.1.3, (4.7), and the derivatives of the components $b_{R\sigma}$ (see Proposition 4.1.4):

$$
\begin{aligned}
b_{R\sigma\,,i} &= 0;\\
b_{R\sigma\,;\alpha} &= \left(\frac{1}{Z}+\beta^2\right) I_{x^\sigma x^\alpha} - \frac{1}{Z^2} Z_{;\alpha} I_{x^\sigma};\\
b_{R\sigma,\binom{3}{\alpha}} &= \left(\frac{1}{Z}+\beta^2\right)\delta^\alpha_\sigma - \frac{2}{Z^2} I_{x^\sigma} I_{x^\alpha};\\
b_{R\sigma,\binom{3}{\alpha};\alpha} &= \frac{1}{Z^3}\left(4Z_{;\alpha} I_{x^\sigma} I_{x^\alpha} - 2Z(I_{x^\alpha x^\alpha} I_{x^\sigma} + I_{x^\alpha} I_{x^\sigma x^\alpha}) - ZZ_{;\alpha}\delta^\alpha_\sigma\right);
\end{aligned}
$$

where $Z_{;\alpha} = 2I_{x^1} I_{x^1 x^\alpha} + 2I_{x^2} I_{x^2 x^\alpha}$.

In the anisotropic Beltrami framework (3.9)-(3.10) the tension field coincides with the Laplace-Beltrami operator, and only the third component is significant for the application,

$$\triangle_\gamma(I) = \tau^3(X) = \gamma^{\sigma\mu}\left(I_{x^\sigma x^\mu} - \Gamma^\nu_{\sigma\mu} I_{x^\nu}\right). \tag{5.7}$$

Additional tensor components of the Randers metric γ, defined by (5.6), are involved in the connection coefficients $\Gamma^\nu_{\sigma\mu}$, hence they differ from the Cristoffel symbols of the induced metric. Anyway, the tension $\tau(I)$ is the generalization of the third component of the mean curvature vector (3.12). The particular Randers flow $\partial^R_t I$ can be evaluated by the use of (4.19) for $r = i = 3$ and $h^{33} = \beta^{-2}$,

$$\partial^R_t I = \triangle_\gamma(I) + \Phi(V, \Omega_R, b_{R\sigma}). \tag{5.8}$$

We omit here the explicit form of the flow, since its complete expression is computationally tedious.

The Ingarden flow

Another proposed linear deformation Ω_I of the induced norm $G = \sqrt{V}$ in (4.20)-(4.21) is of the Ingarden type, and is given by

$$\Omega_I = b_{I\sigma} v^\sigma = I_{x^1} v^1 + I_{x^2} v^2.$$

The Ingarden additional tensor components (4.25) have the explicit form

$$
\begin{aligned}
\varphi_{I11} =\ & \frac{\Omega_I}{G} g_{11} - \frac{\Omega_I}{G^3}\left(g_{11}^2 (v^1)^2 + 2g_{11}g_{12}v^1v^2 + g_{12}^2(v^2)^2\right)\\
& + \frac{2}{G} I_{x^1}(g_{11}v^1 + g_{12}v^2) + I_{x^1}^2,\\
\varphi_{I12} =\ & \varphi_{I21} = \frac{\Omega_I}{G} g_{12} - \frac{\Omega_I}{G^3}\left(g_{11}g_{12}(v^1)^2 + (g_{11}g_{22} + g_{12}^2)v^1v^2 + g_{12}g_{22}(v^2)^2\right)\\
& + \frac{1}{G}(g_{11}I_{x^2}v^1 + g_{12}I_{x^2}v^2 + g_{12}I_{x^1}v^1 + g_{22}I_{x^1}v^2) + I_{x^1}I_{x^2},\\
\varphi_{I22} =\ & \frac{\Omega_I}{G} g_{22} - \frac{\Omega_I}{G^3}\left(g_{21}^2 (v^1)^2 + 2g_{12}g_{22}v^1v^2 + g_{22}^2(v^2)^2\right)\\
& + \frac{2}{G} I_{x^2}(g_{12}v^1 + g_{22}v^2) + I_{x^2}^2.
\end{aligned}
$$

The derivatives of the $\varphi_{I\sigma\mu}$, required for the flow expression, can be obtained by Proposition 4.1.3. The derivatives of the Ingarden linear function Ω_I can be expressed by (4.7), and Proposition 4.1.5,

$$\Omega_{I,i} = 0; \qquad \Omega_{I;\alpha} = I_{x^\sigma x^\alpha} v^\sigma;$$
$$\Omega_{I,\binom{3}{\alpha}} = v^\alpha; \quad \Omega_{I,\binom{3}{\alpha};\alpha} = 0.$$

Similarly as in the previous case, the Ingarden flow $\partial_t^I I$ can be evaluated by the use of (4.19) for $r = i = 3$ and $h^{33} = \beta^{-2}$,

$$\partial_t^I I = \triangle_\gamma(I) + \Phi(V, \Omega_I, I_{x^\sigma}), \tag{5.9}$$

where $\triangle_\gamma(I)$ is given by (5.7), with the connection coefficients produced by the Ingarden metric.

The normalized Miron flow

As shown in Subsection 4.2.2., the NM flow is completely determined by metric components h_{ij} and $g_{\sigma\mu}$, and induced g-quadratic norm V. For the Beltrami framework $(X, \mathbb{R}^3, \Sigma)$ given by (3.9), the components of the metric g are presented in (3.10), and their derivatives in Corollary 5.3.1. The contravariant metric components are

$$(g^{\sigma\mu}) = \frac{1}{g}\begin{pmatrix} 1+\beta^2 I_{x^2}^2 & -\beta^2 I_{x^1} I_{x^2} \\ -\beta^2 I_{x^1} I_{x^2} & 1+\beta^2 I_{x^1}^2 \end{pmatrix}, \quad \text{where} \quad g = 1 + \beta^2 I_{x^1}^2 + \beta^2 I_{x^2}^2.$$

By the use of Lemma 3.4.3, their derivatives can be obtained in detail. Hence, the NM flow $\partial_t^{NM} I$ of the image surface in the Beltrami flow $(X, \mathbb{R}^3, \Sigma)$ can be evaluated according to (4.34), by taking $r = i = 3$ and $h^{33} = \beta^{-2}$,

$$\partial_t^{NM} I = \triangle_\gamma(I) + \Phi(V, g^{\sigma\mu}, g), \tag{5.10}$$

where $\triangle_\gamma(I)$ is given by (5.7), with the connection coefficients produced by the normalized Miron metric.

5.3.1 The implementation

The main difference in the implementation of isotropic and anisotropic flow types, lays the following fact: anisotropic flows $\triangle I$ produce eight shifting values in a pixel comparing to the only one obtained by isotropic flows. Therefore, at each pixel of the processed image, one has more possibilities for shifting. Immediately, the following question arises: how to choose only one for the shifting? In our tentative application we have decided to always take the shifting value in direction of the gradient.

The Beltrami induced successive evolutive shifting of the monochrome image $\Sigma = (I(i,j))$ is achieved by Matlab implementation, where each iteration implies the following steps:

- accessing pixel (excluding the boundary) to get the corresponding feature value I;
- determining the shift tangent vector;
- applying the flow expression on the feature value and the shift tangent vector to obtain the shift value $\triangle I(i,j)$;

- computing the modified feature value, $I \to I + \triangle I$.

The first observation is that the computing of the shift value $\triangle I$ takes remarkably more time. This was expected, because of the complexity of the flow expressions $\partial_t^R I$, $\partial_t^I I$ and $\partial_t^{NM} I$, comparing to $\partial_t^{MC} I$.

We present in [22] an approximate minimizing Beltrami flow, containing only the most important term from the scaled extremal equation. The output differs from the input by a slight increase of the contrast between the compact regions, which exhibits a significant difference between the mean levels. It is observed that the presence of the anisotropic metric in the expression of the modified mean curvature flow leads to region-growing and slight salt-and-pepper low granular denoising (see Fig. 5.3).

Figure 5.3: Original image and output provided by the approximate anisotropic evolution process.

Further, we use Matlab programming for implementing the whole Beltrami flow expression. We process the flower image of low resolution (60x60) for $\beta = 2$, with the aim of its enhancement. The flower image is shifted by the following four flows: mean curvature (5.1), Randers (5.8), Ingarden (5.9) and normalized Miron (5.10). Each shifting is tracked separately. A sample of tracking for the NM flow can be seen in Figure 5.4.

Also, simultaneous shifting is implemented, and the effects can be compared in Figure 5.5. The doorknob image was efficiently evolved by the isotropic MC flow, and by the anisotropic R, I and NM flows. In the image enhancement, produced effects display similar results, however, anisotropic flows offer more possibilities: at each pixel they produce eight values, and the shifting one could be chosen regarding some other criteria, not necessarily the gradient vector.

Moreover, it is also important to underline that the large number of iterations in the processing would result in a substantial enhancement.

Based on the implementation results, we are able to conclude that the anisotropic evolution process is substantially slower than the isotropic one - the mean curvature flow, but it is more

Figure 5.4: Original flower image, image evolved by NM flow with 15 iterations, shift no15.

Figure 5.5: Original doorknob image, image evolved with 15 iterations by MC,R,I, and NM flow, respectively.

sensitive. The later implies that the more comprehensive processing could be expected in the fiture. The anisotropic metric structure causes the dependence of the Finsler (Synge-Beil) metric coefficients on the shift vector, and emphasizes the action of the flow at noisy pixels.

The future research will address the following areas:

- selecting an appropriate adaptive anisotropic metric structure (possibly non-smooth);
- considering a weight function in order to accelerate the convergence speed of the evolution process;
- exploring the possibilities for application in image processing: feature detection, image enhancement, segmentation, image registration, etc.;
- considering criteria for the selection of the shift value among the eight values;
- considering two levels of neighboring pixels to further increase the sensitiveness of image enhancement;
- quantitative analysis of image matrices produced by the various evolutions.

Conclusions

After a theoretical introduction, the procedure of constructing several concrete Finsler fundamental functions for the Garner dynamical system was presented. It was shown that produced anisotropic norms correlate change rates of the dynamical system with significant increase of its growth factor parameter. The produced Finsler norms were compared with the Euclidean one, and mutually, by the corresponding elements of the Hilbert tensor spaces.

The next goal was to study surfaces embedded into a Riemannian space, endowed with an anisotropic metric of General Lagrange type, and the minimization of the energy of the embedding. It was shown that the variational problem provides the PDE of the surface evolution, defined by the evolution flow function on the tangent space (having as arguments both position and direction). The evolution flow PDE was explicitly determined for a Finsler surface of a general Randers type and several particular cases, as well as for a Synge-Beil surface and the particular normalized Miron case.

Eventually, theoretical results were adjusted and discretized for processing monochrome images, and tentatively applied for the image enhancement. Implementation results were analyzed, and further research directions were addressed.

Bibliography

[1] H. Abolghasem, *Jacobi stability of Hamiltonian systems*, International Journal of Pure and Applied Mathematics, **87**(1) (2013), 181-194.

[2] Yu. Aminov, *The Geometry of Submanifolds*, Gordon and Breach Science Publisher, 2001.

[3] P.L. Antonelli, *Equivalence Problem for Systems of Second Order Ordinary Differential Equations*, Encyclopedia of Mathematics, Kluwer Academic Publishers, 2000.

[4] P.L. Antonelli, R. Bradbury, *Volterra-Hamilton Models in Ecology and Evolution of Colonial Organisms*, World Scientific Press, 1994.

[5] P.L. Antonelli, I. Bucataru, *New results about the geometric invariants in KCC-theory*, An.St. Univ. "Al.I.Cuza" Iasi. Mat. N.S. **47** (2001), 405-420.

[6] P.L. Antonelli, R. Ingarden, M. Matsumoto, *The Theory of Sprays and Finsler Spaces with Applications in Physics and Biology*, Springer Netherlands, 1993.

[7] P.L. Antonelli, R. Miron eds., *Lagrange and Finsler Geometry Applications to Physics and Biology*, Kluwer Press, 1996.

[8] N. Arcozzi, *Beltrami's Models of Non-Euclidean Geometry*, In S. Coen (ed), Mathematicians in Bologna 1861-1960, Springer Basel, 2012, 1-30.

[9] G.S. Asanov, *Finsler Geometry, Relativity and Gauge Theories*, Springer Netherlands, 1985.

[10] L. Astola, L. Florack, *Finsler Geometry on higher order tensor fields and applications to high angular resolution diffusion imaging*, International Journal of Computer Vision, **92**(3) (2011), 325-336.

[11] V. Balan, M. Neagu, *Jet Single-Time Lagrange Geometry and Its Applications*, Wiley, 2011.

[12] V. Balan, M. Crasmareanu, *Euclidean geometry of Finsler wavefronts through Gaussian curvature*, U.P.B. Sci. Bull., Series A, **72**(2) (2010), 3-12.

[13] V. Balan, *Synge-Beil and Riemann-Jacobi jet structures with applications to physics*, International Journal of Mathematics and Mathematical Sciences, **2003**(27) (2003), 1693-1702.

[14] V. Balan, S. Lebedev, *On the Legendre transform and Hamiltonian formalism in Berwald-Moor geometry*, Differential Geometry - Dynamical Systems, **12** (2010), 4-11.

[15] V. Balan, *CMC and minimal surfaces in Finsler spaces*, Tensor N.S., **68** (2007), 23-29.

[16] V. Balan, *Euler-Lagrange characterization of area-minimizing graphs in Randers spaces with non-constant potential*, WSEAS Transactions on Mathematics, **7**(1) (2008), 1-5.

[17] V. Balan, *CMC and minimal surfaces in Berwald-Moor spaces*, Hypercomplex Numbers in Geometry and Physics, **2**(6)(3) (2006), 113-122.

[18] V. Balan, I.R. Nicola, *Berwald-Moor metrics and structural stability of conformally-deformed geodesic SODE*, Applied Sciences, **11** (2009), 19-34.

[19] V. Balan, I.R. Nicola, *Static bifurcation diagrams and the universal unfolding for cancer cell population model*, Proc. of The 9-th WSEAS International Conference on Mathematics and Computers in Biology and Chemistry (MCBC′08), Bucharest, Romania, June 24-26, 2008.

[20] V. Balan, I.R. Nicola, *Versal deformation and static bifurcation diagrams for the cancer cell population model*, Quarterly of Applied Mathematics, **67**(4) (2009), 755-770.

[21] V. Balan, P.C. Stavrinos, *On general Randers-Kropina Finslerian metrics*, Proc. of The International Workshop of Differential Geometry, June 25-28, Thessaloniki, Greece 1997, BSG Proc. 5, Geometry Balkan Press, Bucharest 2001, 16-26.

[22] V. Balan, J. Stojanov, *Finslerian extensions of geodesic active fields for digital image registration*, Proceedings in Applied Mathematics and Mechanics / PAMM, Special Issue, **13**(1) (2013), 493-494.

[23] V. Balan, J. Stojanov, *Finsler-type estimators for the cancer cell population dynamics*, Publications de l'Institut Mathématique, accepted 2014.

[24] V. Balan, J. Stojanov, *Statistical Finsler-Randers structures for the Garner cancer cell model*, Proceedings of RIGA 2014 (Riemannian Geometry and Applications to Engineering and Economics), May 19-21, 2014, Bucharest, Romania, Publishing House of the University of Bucharest 2015, 11-20.

[25] V. Balan, J. Stojanov, *Finslerian-type GAF extensions of the Riemannian framework in digital image processing*, Filomat, accepted 2014.

[26] V. Balan, J. Stojanov, *Anisotropic metric models in the Garner oncologic framework*, Proceedings CAIM 2014 (The 22nd Conference on Applied and Industrial Mathematics), September 18-21, 2014, Bacău, Romania, accepted 2014.

[27] D. Bao, S.S. Chern, Z. Shen, *An Introduction to Riemann-Finsler Geometry*, Volume 200, Graduate Texts in Mathematics, Springer-Verlag, 2000.

[28] D. Bao, C. Robles, Z. Shen, *Zermelo navigation on Riemannian manifolds*, Journal of Differential Geometry, **66**(3) (2004), 345-479.

[29] R.G. Beil, *Comparison of unified field theories*, Tensor N.S., **56** (1995), 175-183.

[30] R.G. Beil, *Equations of motion from Finsler geometric methods*, In: Antonelli, P.L. (ed), Finslerian Geometries. A meeting of minds., Kluwer Academic Publisher, FTPH 109 (2000), 95-111.

[31] A. Bejancu, *Tangent bundle and indicatrix bundle of a Finsler manifold*, Kodai Mathematical Journal, **31**(2) (2008), 272-306.

[32] N. Berglund, *Geometrical Theory of Dynamical Systems*, Lecture Notes, 2001, http://arxiv.org/pdf/math/0111177v1.pdf

[33] C.G. Boehmer, T. Harko, S.V. Sabau, *Jacobi stability analysis of dynamical systems: Applications in gravitation and cosmology*, Advances in Theoretical and Mathematical Physics, **16**(4) (2012), 1145-1196.

[34] W. M. Boothby, *An Introduction to Differentiable Manifolds and Riemannian Geometry*, Academic Press, 2003.

[35] I. Bucataru, R. Miron, *Finsler-Lagrange Geometry; Applications to Dynamical Systems*, Editura Academiei Romane, 2007.

[36] X. Bresson, P. Vanndergheynst, J.P. Thiran, *Multiscale active contours*, International Journal of Computer Vision, **70**(3) (2006), 197-211.

[37] I. Chavel, *Riemannian Geometry, A Modern Introduction*, Cambridge University Press, 2006.

[38] X. Cheng, Z. Shen, *Finsler Geometry: An Approach via Randers Spaces*, Science Press & Springer, 2012.

[39] S.S. Chern, W.H. Chen, K.S. Lam, *Lectures on Differential Geometry*, World Scientific Publishers, 2000.

[40] S.S. Chern, Z. Shen, *Riemann-Finsler Geometry*, World Scientific Publishers, 2005.

[41] M.P. do Carmo, *Riemannian Geometry*, Birkhauser, 1992.

[42] B.A. Dubrovin, A.T. Fomenko, S.P. Novikov, *Modern Geometry (Methods and Applications)*, Part I. GTM 93. Springer Verlag, 1985.

[43] M. Dahl, *A Brief Introduction to Finsler Geometry*, Lecture Notes, 2006, http://math.aalto.fi/ fdahl/finsler/finsler.pdf

[44] A. Deicke, *Über die Finsler-Räume mit* $A_i = 0$, Arch. Math. **4** (1953), 45-51.

[45] C. Duval, *Finsler spinoptics*, Communications in Mathematical Physics, **283**(3) (2008), 701-727.

[46] D. Eberly, *A Differential Geometric Approach to Anisotropic Diffusion*, In B.M. ter Haar Romeny (ed.) Geometry-Driven Diffusion in Computer Vision, series Computational Imaging and Vision, **1** (1994), 371–392, Springer Netherlands.

[47] D. Eberly, *Geometric Methods For Analysis Of Ridges In n- Dimensional Images*, Ph.D Thesis, University of North Carolina, 1994.

[48] J. Eells, J.H. Sampson, *Harmonic mappings of Riemannian manifolds*, American Journal of Mathematics, **86**(1) (1964), 109-160.

[49] L.C. Evans, *Partial Differential Equations*, volume 19 of Graduate Studies in Mathematics, American Mathematical Society, 1997.

[50] G.B. Folland, *Introduction to Partial Differential Equations*, Princeton Academic Press, 1995.

[51] J.P. Freyer, R.M. Sutherland, *Regulation of growth saturation and development of necrosis in EMT6/R0 multicellular spheroids by the glucose and oxygen supply*, Cancer Research, **46**(7) (1986), 3504-3512.

[52] G. Gallego, J.I. Ronda , A. Valdes, *Directional geodesic active contours*, 19th IEEE International Conference on Image Processing (ICIP), 2561–2564, September 30 - October 3, Orlando, FL, USA, 2012.

[53] A.L. Garner, Y.Y. Lau, D.W. Jordan, M.D. Uhler, R.M. Gilgenbach, *Implication of a simple mathematical model to cancer cell population dynamics*, Cell Proliferation, **39**(1) (2006), 15–28.

[54] M. Gheorghe, *The indicatrix in Finsler Geometry*, Analele Stiintifice ale Universitatii "Al.I.Cuza" din Iasi (S.N.) Matematica, Tomul LIII (2007), Supliment, 163–180.

[55] Y. Giga, *Surface Evolution Equations: A Level Set Approach*, Monographs in Mathematics 99, Birkhäuser, 2006.

[56] Y. Gur, O. Pasternak, N. Sochen, *Fast GL(n)-invariant framework for tensors regularization*, International Journal of Computer Vision, **85**(3) (2009), 211–222.

[57] N.J. Hicks, *Notes on Differential Geometry*, Van Nostrand, 1965.

[58] M.W. Hirsch, S. Smale, *Differential Equations, Dynamical Systems and Linear Algebra*, Academic Press, 1974.

[59] A.K. Jain, *Fundamentals of Digital Image Processing*, Prentice Hall, 1989.

[60] J. Jost, *Riemannian Geometry and Geometric Analysis*, Springer-Verlag, 2005.

[61] J. Kern, *Lagrange Geometry*, Archiv der Mathematik, **25**(1974), 438-443.

[62] S. Kikuchi, *Theory of Minkowski space and of non-linear connections in Finsler space*, Tensor N.S., **12** (1962), 47-60.

[63] R. Kimmel, R. Malladi, N. Sochen, *Images as embedded maps and minimal surfaces: movies, color, texture, and volumetric medical images*, International Journal of Computer Vision, **39**(2) (2000), 111-129.

[64] R. Kimmel, *Numerical Geometry of Images*, Springer-Verlag, 2004.

[65] M. Kunzinger, *Differential Geometry 1*, Lecture notes, 2008, http://www.mat.univie.ac.at/ mike/teaching/ss08/dg.pdf

[66] J.M. Lee, *Differential Geometry, Analysis and Physics*, Lecture notes, 2000, http://research.rmutp.ac.th/research/Differential%20Geometry,%20Analysis%20and%20Physics.pdf

[67] X. Li, X. Long, C.L. Wyatt, ADNI *Registration of images with topological change via Riemannian embedding*, In IEEE International Symposium on Biomedical Imaging: From Nano to Macro, 2011, 1247-1252. March 30 2011-April 2 2011, Chicago, IL.

[68] A.M. Luciani, A. Rosi, P. Matarrese, G. Arancia, L. Guidoni, V. Viti, *Changes in cell volume and internal sodium concentration in HrLa cells during exponential growth and following Ionidamine treatment*, European Journal of Cell Biology, **80**(2) (2001), 187-195.

[69] W.T. Loring, *An Introduction to Manifolds*, Springer-Verlag, 2011.

[70] J.E. Marsden, T. Ratiu, R. Abraham, *Manifolds, Tensor Analysis, and Applications*, Springer-Verlag, 2001.

[71] M. Matsumoto, S. Numata, *On Finsler spaces with cubic metric*, Tensor N. S., **33** (1979), 153–162.

[72] M. Matsumoto, H. Shimada, *On Finsler spaces with 1-form metric. II. Berwald-Moor's metric* $L = (y^1 y^2 \dots y^n)^{1/n}$, Tensor N. S., **32** (1978), 275–278.

[73] M. Matsumoto, *Foundations of Finsler Geometry and Special Finsler Spaces*, Kaiseisha Press, 1986.

[74] J. Melonakos, E. Pichon, S. Angenent, A. Tannenbaum, *Finsler active contours*, IEEE Transactions on Pattern Analysis and Machine Intelligence **30**(3) (2008), 412–423.

[75] R. Miron, M. Anastasiei, *The Geometry of Lagrange Space, Theory and Applications*, Kluwer Acad. Publ., FTPH 59, 1994.

[76] R. Miron, M. Anastasiei, *Vector Bundles and Lagrange Spaces with Applications to Relativity*, Geometry Balkan Press, Bucharest, 1997.

[77] R. Miron, *On the notion of Ingarden space, Lagrange and Hamiltonian geometries and their applications*, Radu Miron (Ed.), Handbooks. Treatises. Monographs, 49 (2004), 161-168.

[78] R. Miron, *The geometry of Ingarden spaces*, Reports on Mathematical Physics, **54**(2) (2004), 131–147.

[79] A.S. Mischchenko, A.T. Fomenko, *A Course on Differential Geometry and Topology* (in Russian), Moscow Univ., 1980.

[80] X.H. Mo, *Harmonic maps from Finsler manifolds*, Illinois Journal of Mathematics, **45**(4) (2001), 1331–1345.

[81] J. Nash, *The imbedding problem for Riemannian manifolds*, Annal of Mathematics **63**(1) (1956), 20–63.

[82] S. Osher, J.A. Sethian, *Fronts propagating with curvaturedependent speed: Algorithms based on Hamilton-Jacobi formulations*, Journal of Computational Physics, **79**(1) (1988), 12–49.

[83] R. Osserman, *A Survay of Minimal Surfaces*, Dover Phoenix Editions, 1986.

[84] T.N. Pandey, V.K. Chaubey, B.N. Prasad, *Scalar curvature of two-dimensional cubic Finsler spaces*, Journal of International Academy of Physical Sciences, **12** (2008), 127–137.

[85] A. Pandey, V.K. Chaubey, T.N. Pandey, *Antisotropic cosmological models of Finsler space with (α, β)-metric*, Mathematical Combinatorics, **2** (2014), 63–73.

[86] D.G. Pavlov, *Four-dimensional time*, Hypercomplex Numbers in Geometry and Physics, **1**(1) (2004), 31–39.

[87] D.G. Pavlov, *Generalization of scalar product axioms*. Hypercomplex Numbers in Geometry and Physics, **1**(1) (2004), 5–18.

[88] L. Perko, *Differential Equations and Dynamical Systems*, Springer-Verlag, 2001.

[89] R. Punzi, M.N.R. Wohlfarth, *Geometry and stability of dynamical systems*, Physical Review E, **79** (2009), (046606)1-11.

[90] P.K. Rashevski, *Riemannian Geometry and Tensor Analysis* (in Russian), Izd. Nauka, 1964.

[91] T. Reya, S.J. Morrison, M.F. Clarke, I.L. Weissman, *Stem cells, cancer, and cancer stem cells*, Nature **414** (2001), 105-111.

[92] C. Robinson, *Dynamical Systems Stability, Symbolic Dynamics and Chaos*, CRC Press, 1995.

[93] G. Rosman, X.C. Tai, L. Dascal, R. Kimmel, *Polyakov action minimization for efficient color image processing*, Trends and Topics in Computer Vision, Lecture Notes in Computer Science, **6554** (2012), 50–61.

[94] H. Rund, *The Differential Geometry of Finsler Spaces*, Springer-Verlag, 1959.

[95] G. Sapiro, *Geometric Partial Differential Equations and Image Analysis*, Cambridge University Press, 2006.

[96] D.J. Saunders, *The Geometry of Jet Bundles*, London Mathematical Society Lecture Note Series, 1989.

[97] A. Sarti, R. Malladi, J.A. Sethian, *Subjective Surfaces : A geometric model for boundary completion*, International Journal of Computer Vision, **46**(3) (2002), 201–221.

[98] Y.B. Shen, Y. Zhang, *Second variation of harmonic maps between Finsler manifolds*, Science in China Series A: Mathematics, **47**(1) (2004), 39–51.

[99] Z. Shen, *On Finsler geometry of submanifolds*, Mathematische Annalen, **311**(3) (1998), 549–576.

[100] Z. Shen, *Differential Geometry of Spray and Finsler Spaces*, Kluwer Academic Publishers, 2001.

[101] Z. Shen, *Lectures on Finsler Geometry*, World Scientific Publishers, 2001.

[102] N. Sochen, R. Kimmel, R. Malladi, *From high energy physics to low level vision*, Report LBNL 39243, LBNL, UC Berkeley, CA 94720, August 1996. Presented in ONR workshop, UCLA, Sept. 5, 1996.

[103] N. Sochen, R. Kimmel, R. Malladi, *A general framework for low level vision*, IEEE Transactions on Image Processing, **7**(3) (1998), 310-318.

[104] N. Sochen, Y.Y. Zeevi, *The Beltrami geometrical framework of color image processing*, In Proceedings of IEEE International Conference on Acoustics, Speech, and Signal Processing, **6** (1999), 3301–3304.

[105] N. Sochen, R. Deriche, L. Lopez-Perez, *The Beltrami flow over manifolds*, Technical Report TR-4897, INRIA Sophia-Antipolis, Sophia Antipolis, France, 2003.

[106] G.I. Solyanik, N.M. Berezetskaya, R.I. Bulkiewicz, G.I. Kulik, *Different growth patterns of a cancer cell population as a function of its starting growth characteristics: Analysis by mathematical modelling*, Cell Proliferation, **28**(5) (1995), 263–278.

[107] M. Spivak, *A Comprehensive Introduction to Differential Geometry*, vol. 2, Publish or Perish, 1970.

[108] A. Tachikawa, *Existence and regularity of weakly harmonic maps into a Finsler manifold with a special structure*, Bulletin of the London Mathematical Society, **44**(5) (2012), 1020–1033.

[109] G. Teschl, *Ordinary Differential Equations and Dynamical Systems*, American Mathematical Society, Graduate Studies in Mathematics 140, 2012.

[110] C. L. Wyatt, X. Li, X. Gong, *A Framework for Registration of Images with Varying Topology using Embedded Maps : Reimannian Embedding Spaces*, Technical Report, Virginia Polytechnic Institute and State University, 2009.

[111] T. Yajima, H. Nagahama, *Nonlinear Dynamical systems and KCC-theory*, Acta Mathematica Academiae Paedagogicae Nyiregyhaziensis, **24** (2008), 179-189.

[112] T. Yajima, H. Nagahama, *Finsler geometry of seismic ray path in anisotropic media*, Proceedings of the Royal Society A, **465**(2106) (2009), 1763-1777.

[113] D. Zosso, *Geodesic Active Fields: A Geometric Framework for Image Registration*, PhD Thesis, École Polytechnique Fédérale De Lausanne, 2011.

[114] D. Zosso, X. Bresson, J.-P. Thiran, *Geodesic active fields - a geometric framework for image registration*, IEEE Transactions on Image Processing, **20**(5) (2011), 1300-1312.

[115] D. Zosso, X. Bresson, J.-P. Thiran, *Fast geodesic active fields for image registration based on splitting and augmented Lagrangian approaches*, IEEE Transactions on Image Processing, **23**(2) (2014), 673–683.

Index

Biography

Jelena Stojanov was born on May 11th, 1974. in Sombor, Serbia.

She enrolled Faculty of Sciences, University of Novi Sad, in 1993, and finished studies at Department of Mathematics and Informatics in 1998. In the same year, she enrolled the master of science studies at Department of Mathematics and Informatics, Faculty of Sciences, University of Novi Sad. She defended the master of science thesis "Geometry of curves in higher-order osculator bundles" in 2005.

She works at Technical Faculty "Mihajlo Pupin", University of Novi Sad, since 1998.

She published several scientific papers in refereed journals and in conference proceedings. She participated in two projects (national and cross-border).

She speaks English, and has basic knowledge of German and Russian.

She lives in Zrenjanin, with her husband Željko and two children, Mina and Vlada.

Novi Sad, January 13, 2015

Jelena Stojanov

UNIVERZITET U NOVOM SADU
PRIRODNO-MATEMATIČKI FAKULTET
KLJUČNA DOKUMENTACIJSKA INFORMACIJA

Redni broj:
RBR
Identifikacioni broj:
IBR
Tip dokumentacije: Monografska dokumentacija
TD
Tip zapisa: Tekstualni štampani materijal
TZ
Vrsta rada: Doktorska disertacija
VR
Autor: Jelena Stojanov
AU
Mentori: Prof. dr Vladimir Balan, Doc. dr Sanja Konjik
MN

Naslov rada: Anizotropna radna okruženja za dinamičke sisteme i obradu slika
NR

Jezik publikacije: engleski
JP
Jezik izvoda: srpski/engleski
JI
Zemlja publikovanja: Srbija
ZP
Uže geografsko područje: Vojvodina
UGP
Godina: 2015.
GO
Izdavač: Autorski reprint
IZ

Mesto i adresa: Novi Sad, Prirodno-matematički fakultet, Trg Dositeja Obradovića 4
MA
Fizički opis rada: 5/107/115/0/11/0/0
(broj poglavlja/strana/lit. citata/tabela/slika/grafika/priloga)
FO
Naučna oblast: Matematika
NO
Naučna disciplina: Geometrija
ND
Predmetna odrednica/Ključne reči: diferencijabilna mnogostrukost, tangentni omotač, metrička struktura, Finslerovi prostori, Lagranžovi prostori, uopšteni Lagranžovi prostori, semisprej, KCC-teorija, dinamički sistem, Beltramijevo radno okruženje, evolucija površi, digitalna obrada slika.
PO

UDK:
Čuva se: u biblioteci Departmana za matematiku i informatiku, Novi Sad
ČU
Važna napomena:
VN
Izvod: Predmet istraživanja doktorske disertacije je uporedna analiza klasičnih i specifičnih geometrijskih radnih okruženja i njihovih anizotropnih proširenja; konstrukcija tri Finslerova radna okruženja različitog tipa koja su pogodna za analizu dinamičkog sistema populacije kanceroznih ćelija; razvoj teorije anizotropnog Beltramijevog radnog okruženja i formiranje jednačina evolutivnog toka za različite klase anizotropnih metrika, kao i mogućnost primene dobijenih teorijskih rezultata u digitalnoj obradi slika.
IZ

Datum prihvatanja teme od strane NN Veća: 18.07.2014.
DP
Datum odbrane:
DO
Članovi komisije:
Predsednik: Akademik dr Stevan Pilipović, redovni profesor, Prirodno-matematički fakultet, Univerzitet u Novom Sadu,

Član: dr Nevena Pušić, redovni profesor, Prirodno-matematički fakultet, Univerzitet u Novom Sadu,

Član: dr Mirjana Đorić, redovni profesor, Matematički fakultet, Univerzitet u Beogradu,

Član: dr Vladimir Balan, redovni profesor, Fakultet primenjenih nauka, Politehnika univerzitet u Bukureštu, Rumunija,

Član: dr Sanja Konjik, docent, Prirodno-matematički fakultet, Univerzitet u Novom Sadu.
KO

UNIVERSITY OF NOVI SAD
FACULTY OF SCIENCES
KEY WORDS DOCUMENTATION

Accession number:
ANO
Identification number:
INO
Document type: Monograph type
DT
Type of record: Printed text
TR
Contents code: PhD thesis
CC
Author: Jelena Stojanov
AU
Mentors: Vladimir Balan, PhD; Sanja Konjik, PhD
MN

Title: Anisotropic frameworks for dynamical systems and image processing
TI

Language of text: English
LT
Language of abstract: Serbian/English
LA
Country of publication: Serbia
CP
Locality of publication: Vojvodina
LP
Publication year: 2015.
PY
Publisher: Author's reprint
PU

Publication place: Novi Sad, Faculty of Sciences, Trg Dositeja Obradovića 4
PP
Physical description: 5/107/115/0/11/0/0
(chapters/pages/literature/tables/pictures/graphics/appendices)
PD
Scientific field: Mathematics
SF
Scientific discipline: Geometry
SD
Subject / Key words: differentiable manifold, tangent bundle, metric structure, Finsler spaces, Lagrange spaces, generalized Lagrange spaces, semispray, KCC-theory, dynamical system, Beltrami framework, surface evolution, image processing.
SKW
UC:
Holding data: library of the Department of Mathematics and Informatics, Novi Sad.
HD
Note:
N
Abstract: The research topic of this PhD thesis is a comparative analysis of classical specific geometric frameworks and of their anisotropic extensions; the construction of three different types of Finsler frameworks, which are suitable for the analysis of the cancer cells population dynamical system; the development of the anisotropic Beltrami framework theory with the derivation of the evolution flow equations corresponding to different classes of anisotropic metrics, and tentative applications in image processing.
AB

Accepted by Scientific Board on: July 18, 2014.
ASB
Defended:
DE
Thesis defend board:
President: Academician Stevan Pilipović, PhD, Full professor, Faculty of Sciences, University of Novi Sad,

Member: Nevena Pušić, PhD, Full professor, Faculty of Sciences, University of Novi Sad,

Member: Mirjana Đorić, PhD, Full professor, Faculty of Mathematics, University of Belgrade,

Member: Vladimir Balan, PhD, Full professor, Faculty of Applied Sciences, University Politehnica of Bucharest, Bucharest, Romania,

Member: Sanja Konjik, PhD, Assistant professor, Faculty of Sciences, University of Novi Sad.
DB